Z-SOURCE INVERTER (ZSI) BASED RECONFIGURABLE ARCHITECTURE FOR SOLAR PHOTO-VOLTAIC (PV) MICROGRID

Karavita Arachchige Himali Lakshika

178077T

Degree of Master of Science

Department of Electrical Engineering

University of Moratuwa

Sri Lanka

April 2021

Z-SOURCE INVERTER (ZSI) BASED RECONFIGURABLE ARCHITECTURE FOR SOLAR PHOTO-VOLTAIC (PV) MICROGRID

Karavita Arachchige Himali Lakshika

178077T

Thesis submitted in fulfilment of the requirements for the degree of Master of Science by Research

Department of Electrical Engineering

University of Moratuwa

Sri Lanka

April 2021

DECLARATION

I declare that this is my work and this thesis does not incorporate without acknowledgement any material previously submitted for a Degree or Diploma in any other University or institute of higher learning and to the best of my knowledge and belief it does not contain any material previously published or written by another person except where the acknowledgement is made in the text.

Also, I hereby grant to the University of Moratuwa the non-exclusive right to reproduce and distribute my thesis, in whole or part in print, electronic or another medium. I retain the right to use this content in whole or part in future works (such as articles or books).

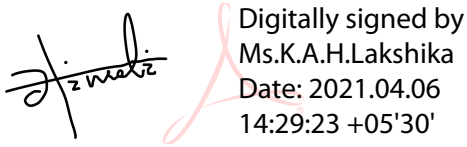

Signature: Date: 2021.04.06

The above candidate has carried out research for the Master's thesis under my supervision.

Signature of the supervisor: Date

ABSTRACT

The principal aim of this research is to identify and use the advantages of Z-source inverter and to develop a reconfigurable architecture for residential microgrid. The researcher has described the summary of the studies on Z-source inverter and reconfigurable systems. The distinctive feature of the proposed, reconfigurable, residential microgrid is the capability to reconfigure microgrid components to operate as a current source (current controlling mode) and a voltage source (voltage-frequency controlling mode) and a static synchronous compensator (STATCOM) (reactive power controlling mode) while replacing the traditional solar inverter from latest Z-source inverter. Where grid-connected, solar photovoltaic customers get uninterrupted power supply from their solar system even at a grid fault, and utility grids can use the same assets to improve the power quality and use their distribution network when it is idle at night. Then, it improves the utilization factor of solar photovoltaic system, power quality at the point of common coupling, and reliable power supply to the loads while increasing controllability of residential microgrid and taking part grid operations with utility grid request. Both the customer and the grid owner could get benefits. The proposed architecture is developed in MATLAB/Simulink platform and results are discussed to prove the proposed architecture.

Index Terms—*Reconfigurable architecture; Solar photovoltaic; Microgrids; Z-source inverte*r, STATCOM, *Power quality, Battery storage system*

ACKNOWLEDGMENTS

Foremost, I am deeply indebted to my supervisor Professor K.T.M.U. Hemapala and co-supervisor Dr. W.D. Prasad of the Department of Electrical Engineering, University of Moratuwa for their constant guidance, encouragement and support from the beginning to the end. It is my pleasure to acknowledge all the other academic staff members of the Department of Electrical Engineering of the University of Moratuwa for their valuable suggestions, comments and assistance which were beneficial to achieve the project objectives. I am grateful to the Department of Science and Technology (DST), Government of India and Ministry of Science, Technology and Research (MSTR), Government of Sri Lanka for the financial grants under Indo-Sri Lanka Joint Research program Grant (MSTR/TR/AGR/3/02/13) scheme and the Faculty of Graduate Studies for the given administrative support to conduct the research. I specially thank to our research team in university of Moratuwa Eng. Gayashan, Eng. Ranaweera, Eng. Lemasha, Eng. Bhagya, Eng. Sisitha, Eng. Malith, Eng. Kaushali, Eng. Yomal and all motivating and helping me to completer this successfully. I thank to the technical officers and other support staff for the assistance they have given to perform laboratory experiments. Moreover, I would like to extend my gratitude to my family for their encouragement, understanding and patience throughout my academic pursuit. Finally, I am grateful to my colleagues and friends for showing interest in my work and giving constructive ideas towards the success of the research.

TABLE OF CONTENTS

LIST OF TABLES

LIST OF TABLES

LIST OF ABBREVIATIONS

Abbreviation	Description
AR	Array Reconfiguration
BESS	Battery Energy Storage System
BL	Bridge-Linked
CSI	Current Source Inverters
DG	Distributed Generations
DN	Distribution Network
DOD	Depth of Discharge
DSO	Distribution System Operators
EV	Electrical Vehicle
FACTS	Flexible AC Transmission System
GWO	Grey Wolf Optimization
HC	Hill Climbing
INC	Incremental Conductance
LTC	Load Tap Changers
LV	Low Voltage
LVR	Line Voltage Regulators
MAS	Multi-agent system
MCBC	Maximum constant boost control
MG	Microgrid
MPP	Maximum Power Point
MPPT	Maximum Power Point Tracker
MSVMBC	Modified space vector modulation boost
MV	Medium Voltage
P&O	Perturb and Observe
PCC	Point of Common Coupling
PSO	Partial Swarm Optimization
PWM	Pulse Width Modulation
qZSSRC	Quasi-Z-Source Series Resonant DC/DC Converter
RMS	Root Mean Square
RSC	Reconfigurable Solar Converter
SPV	Solar Photovoltaic

Abbreviation	Description
SB	State Based
SBC	Simple boost control
SCC	Short Circuit Current
SIDO	Single-Input Dual-Output
SPWM	Sine PWM
SP	Series-Parallel
ST	Shoot-Through
STATCOM	Static Synchronous Compensator
STC	Standard Test Condition
SVPWM	Space-vector PWM
TCT	Total Cross-Tied
TDD	Total Demand Distortion
THD	Total Harmonic Distortion
TSI	Two-Stage Inverter
UC	Ultra-Capacitor
UOF	Under/Over Frequency
UOV	Under/Over Voltage
VDR	Voltage-Doubler Rectifier
VFOC	Virtual Flux-Oriented Control
VOC	Voltage-Oriented Control
VSI	Voltage Source Inverter
ZSI	Z-Source Inverter
MBC	Maximum boost control

LIST OF APPENDICES

1 INTRODUCTION

1.1 Problem identification

Solar photovoltaic (SPV) is the most attractive renewable source due to its long life with fewer maintenance requirements and reduced costs. Since its modular nature and lightweight, it has minimum site limitations, easy to transport and install (Can be implemented for an office building. M. Malinowski,2017) Hence, compared to other renewable energy sources, penetration of SPV systems into the utility grids for residential use are expected to be increased gradually.

With the government incentives and attractive feed in tariff shames, there is a trend for rooftop solar implementation by electricity and the customers are allowed to produce and store energy. As a result, a new category of participants namely "prosumers" came into the picture (Santiago Grijalva, 2011) and their expectations are further augmented. (Figure.1.1 portrays the concept of the prosumer.)

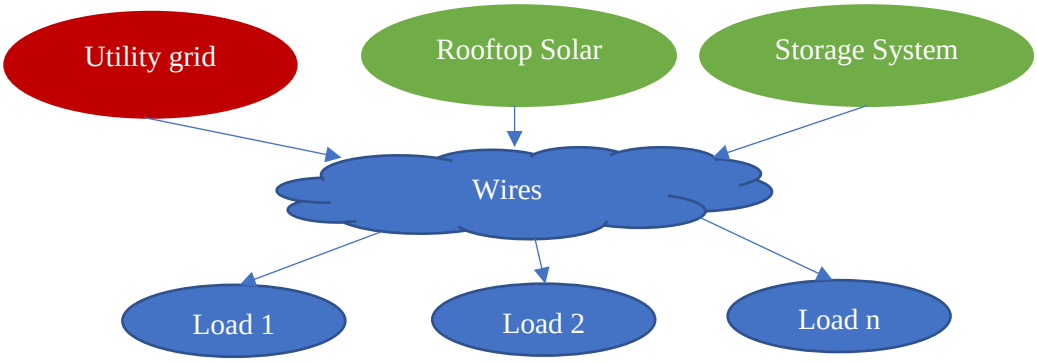

Figure 1.1 Concept of prosumer

In addition to the internal functions, prosumers would like to interact with external entities in order to consume or produce energy while participating in market operations. Some expectations of prosumers can be highlighted as follows.

- Make important decisions regarding economical energy utilization.
- Involve in the operations of a small- or large-scale power grids.
- The ability to control the system and flexibility of operation.
- Resiliency and reliability at grid faults
- maximize utilization of resources.

In order to meet above mentioned requirements, microgrid architecture is required to define all components of SPV microgrid (Phillip Oliver Kriett, 2012). Thus,

existing architecture of solar PV system and microgrid should be rearchitected in customer perspective.

Even though SPV generation is attractive to consumers, its intermittent nature of power generation, dependency on the time and the weather conditions of the day, will affect high penetration of SPV and it further challenges the Distribution Network (DN) such as power fluctuations, reverse power flow, unreliability and instability.

Nowadays there is a rapidly increasing trend to integrate SPV array to the low voltage (LV) system with government support. However, there are critical issues with SPV systems to be completely solved in future. Here, critical problems related to grid connected SPVSs are discussed in the grid point of view and SPV system point of view and considering each subsystem of SPVSs. The possible major problems with SPV systems are mentioned in Figure.1.2 and are discussed as follows. (K.A.Himali Lakshika, 2020), (K. A. H. Lakshika, 2020)

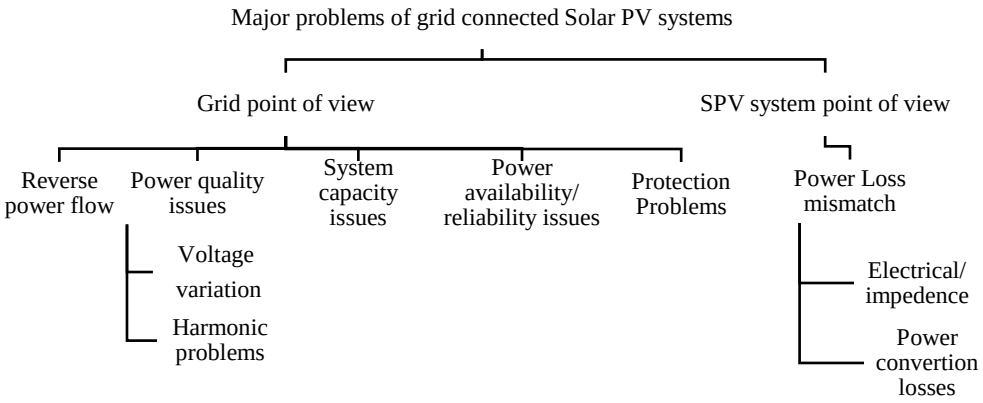

Figure 1.2 Problems with grid connected SPV systems.

1.1.1 Reverse power flow

With the connection of Distributed Generations (DG) such as SPV into the utility network, traditional centralized power generation architecture converts to a hybrid power generation architecture. Under a high penetration scenario, daytime solar generation is more than its consumption hence surplus power is exported to a neighboring feeder or the transmission lines. This causes reverse power flow in distribution substation levels, feeders, and sections. However, the distribution feeder of the distribution network was designed for unidirectional power flow.

Owing to that, it is affected by overcurrent protection coordination and the operation of voltage regulators. To overcome those issues, selecting the right protection methods after feeder-by-feeder basis studies and allowing to control bidirectional power flow in voltage regulators had been proposed in the literature (Farid Katiraei, 2011).

1.1.2 Power quality problems

The main critical Power quality problems with grid-connected systems are voltage problems and harmonic problems.

1.1.2.1 Voltage problems

Reverse power flow, due to excess solar power generation or operating at unity power factor without supporting for reactive power requirement leads for voltage rise at distribution feeder during daytime when maximum solar generation is occurs (Masoud Farhoodnea, 2012), (Leonard Mukwekwe, 2017). The magnitude of voltage rise depends on feeder configuration, the distance along the distribution feeder from the substation to SPV- DG, connection of fixed capacitors and level of solar irradiation. When voltage regulation function is not provided, solar generation spillage or unintentional islanding situations have occurred in industrial practice and it disturbs the penetration of a sustainable power generation into the main power system (S. Liu, 2016) . According to IEEE Std. 519-2014, limitations which have been laid down for voltage at PCC (Point of Common Coupling).

This problem is minimized by implementing new Flexible AC Transmission System (FACTS) devices, load tap changers (LTC), and line voltage regulators (LVR) etc. (Farid Katiraei, 2011).

Voltage fluctuations are produced by fast variation of solar irradiation changes and cloud passing. In a weak distribution network with a high PV penetration, it can create considerable voltage fluctuations. However, rapid voltage fluctuations cause the frequent operation of LTC, LVR and voltage-controlled capacitor banks. Hence, it reduces the life expectancy of each voltage regulator and requires frequent maintenance (Farid Katiraei, 2011).

In addition to those solutions, controlling reactive power through SPV, distributed network reconfiguration, clustering distribution network into several microgrids including SPV and creating PV based microgrids are proposed (Phillip Oliver Kriett, 2012) and they are the most effective solutions which reduce limitations to growth of DG connections to the grid in most of the research were concerned. Rather than that, PV-electrical vehicle (EV) charging based novel technique was proposed in (Phillip Oliver Kriett, 2012).

1.1.2.2 Harmonics

This problem is a critical power quality problem that appeared due to a power electronic inverter based SPV system. A solar power conversion unit is the heart of the SPV system which has been implemented with power electronic-based components and harmonics are generated at its switching operation of DC/AC power conversion. As a result of significant harmonic injection to the utility grid, overheating in capacitor banks, parallel and series resonances and transformers and mal function of protection devices have occurred (Masoud Farhoodnea, 2012).

According to IEEE Std. 519-2014, total harmonic distortion (THD) is the fraction of root mean square (RMS) of the harmonic content, and fundamental current as a percentage. In IEEE Std. 519-2014, possible maximum harmonic levels were laid down. According to that, voltage harmonic limit for bus voltages at PCC below 1kV, should be below 8% and individual THD should be below 5%.

According to IEEE Std. 519-2014, total demand distortion (TDD) is the fraction of the RMS of the harmonic content and specifically excluding inter harmonics maximum demand current (I_L) as a percentage. According to the IEEE Std. 519-2014, current harmonic limit for the systems which have (I_{sc} /I_L) < 20 and PVV voltage above 120V and below 69kV, should be below 5%. Where, I_{sc} = maximum short-circuit current at PCC.

Well-designed harmonic filters, multilevel inverters, Z-source inverters, and DC microgrids are the most promising solutions according to literature. At present, the Harmonic level of most modern pulse width modulation (PWM) inverter is considerably low (below 3% THD) which is better than some distribution networks

because most of the loads connected to distribution networks are consisting of rectifier front ends (Mohamed A. Eltawil, 2010). According to (Orawan Poosri, 2016), the maximum possible penetration of SPV (with THDi < 2%) into the distribution network was determined as 60% of rated power from the power transformer by considering the limits of harmonic distortion voltage of the distribution network.

1.1.3 Power availability and reliability

The contribution of SPV for existing demand is limited to the daytime. Nevertheless, the peak demand of most power systems is in the nighttime. Utilization of this expensive asset limited to the daytime due to the mismatch between solar generation and the existing demand. The intermittent and unpredictable nature of solar energy generation discourages its effective utilization. These inherent issues of SPV reduce the reliability of power generation. Therefore, separate battery backups, main grid, etc. should be integrated with these SPVSs to overcome demand-supply mismatches. In addition to that, the introduction of optimum dispatching algorithms, shifting suitable loads with the modernization of the power system into the smart grid concepts will increase controllability of the power system and these solutions may harvest the maximum available solar power.

Considering those challenges, self-sustained, residential SPV microgrid (MG) is the first step to overcome those challenges by decreasing power exchange between the PV system and utility grid while adding value to the SPV systems (S. Liu, 2016).

1.1.4 System capacity

Power generation from solar panels is limited for the daytime. However, in most developing countries, the peak load of domestic activities is in line at nighttime when solar power is not available. Even though there is a SPV connection into the grid, the Capacity of the transmission and distribution system of the country should be expanded to supply nighttime peak load. Hence, maximum benefits from a SPV system cannot be achieved without using energy storage devices for load ends or peak shifting methods at the load side.

1.1.5 Power losses

The main problem with SPV systems is the reduction of actual energy extraction from SPV rather than its potential energy generation. The main factors which are causes for that are an electrical mismatch of the SPV array, the impedance mismatch between the SPV system and the load, and power conversion losses in the whole system.

1.1.5.1 Impedance mismatch losses

To extract maximum power from SPV module, impedance should be match in load and source side. The impedance of the SPV module is varying with heat, insolation, type of solar cells and partial shading conditions. It causes the reduction of efficiency of the SPV array. Hence, Maximum power point tracker (MPPT) is used as a solution for that. There are dc/dc converters that utilizes an MPPT algorithm to track the MPP, under varying environmental conditions.

1.1.5.2 Power conversion losses

In conventional SPV systems consist of a single power conversion stage which is utilized for DC/AC conversion. At the event of higher or lower voltage exists beyond the required voltage, a line transformer or high-frequency transformer or buck or boost converter is used. Here, there are additional power loss. In literature, the Z source inverter based SPV system has achieved satisfactory results to overcome this problem.

At present, grid connected PV systems are utilized to convert the maximum available solar energy into active power. Utilization of Solar System is zero during nighttime (5.00 pm - 6.30 am next morning). Recently, reactive power controlling function at nighttime through solar inverters is investigated for the distribution networks which exists voltage rise or voltage dips during the nighttime to maintain the system voltage within its limits while increasing the efficiency in the use of net metering installation and helping maintain the grid voltage stability at PCC (Phillip Oliver Kriett, 2012), (M. Malinowski, 2017), (Damiano La Manna, 2014), (Masoud Farhoodnea, 2012). It is successfully proven technically and economically to control the voltage fluctuations of long distribution feeders (N. Solanki and J. Patel,

2016), (R. K. Varma, 2011), (K. Kanchanee Navoda, 2017). Hence, reactive power compensation at night is an expected function in the future residential microgrids.

However, microgrid architecture is vital to achieve above mentioned technical factors such as customer perception as many more features like power flow control, voltage regulation, and harmonic mitigation are expected from grid connected inverters while increasing utilization factor of the SPV system. Microgrid architecture can be defined in two perspectives: control architecture and power architecture. In literature, different microgrid control architectures and microgrid power architectures have been proposed for residential microgrids. Centralized, decentralized, and hierarchical control architectures are the main microgrid control architectures which can be utilized for MGs (Most Nahida Akter, 2017), (J. M. Guerrero, 2013). Multi-agent-based MG control architecture is another control architecture which has proven significant benefits for microgrid operation (Ho, 2016), (J. M. Guerrero, 2013) Based on combinations of different types of distributed resources (solar, wind, microturbines, fuel cells, battery energy storage), different microgrid power architectures were proposed. As per the combination of distributed generations, solar-wind micro hydro, solar-wind, solar–battery microgrids are widely discussed as power architectures (Lubna Mariam, 2013), (E. Rodriguez-Diaz, 2017). However, wind and micro hydro generations are not much feasible for residential MGs due to site limitations. Having plug and play capability, SPV with battery energy storage is the ideal DG to create residential MG. The conventional microgrid architecture is AC microgrid (A. M. R. Lede, 2017). But, considering residential loads and DC power generations like solar battery energy storage devices, DC microgrid architectures are proposed (E. Rodriguez-Diaz, 2017). A pure DC voltage supply is not yet a conceivable method for residential microgrids. Hence, AC/DC hybrid microgrids are being proposed (Ho, 2016), (A. Arulampalam, 2010), (E. Rodriguez-Diaz, 2017).

The reconfigurable power system is one of the concepts which has proposed the utilizing of the system components while reducing cost, size and weight and to increase the controllability and flexibility of the existing power system. In addition to that, reconfigurable systems allow the existing system to act in different configurations or as different systems to achieve different objectives by reducing

system failures due to external problems and adopting dynamic changes of SPV generation and the utility grid. At the end, it increases system reliability (A. Siddiqi, 2008).

The major controllable component of the SPV system is solar inverter and it will be the key component of the reconfigurable architecture. Hence, solar inverter should be developed to operate in given operating mode and it should be switched to the optimum mode of operation automatically.

Having a large amount of power conversion stages, poor fault tolerance capacity (Ravikumar, 2016), higher voltage stress on inverter and harmonics injection to the power network are common drawbacks in existing SPV inverters (Yi Huang, 2006). Early SPV inverters were simply DC/AC converters that deliver power to the utility grid. New designs highlight safety, cost reduction, and intelligent grid integration to improve their performance. Z-Source Inverter (ZSI) is the current trend for the research of the SPV inverter since it safe from short circuit operation by reducing inverter failures while reduces power losses by reducing power conversion stage (Single stage DC/AC power conversion with controllable buck boost operation with two control variables 1) Shoot through duty (Dst) and 2) Modulation Index (M). Not only that, but it also improves power quality by minimizing output voltage and current harmonics through reducing dead time, (Peng, 2003), (A. Florescu, 2010).

The operation of ZSI based solar systems have been considered for MPPT (S. A. K. Mozafari Niapoor, 2010), dual mode operation (grid connected and islanded) (Ahmadi, 2017) and reactive power control (R. Gharakhany, 2009). The combined operation of grid connected mode and islanded mode while nighttime reactive power compensation is not proposed for a residential system. Furthermore, SPV systems based reconfigurable systems will play a major role in future distribution networks. Hence, this research is carried out to develop ZSI based reconfigurable architecture for SPV microgrids as a solution for current issues in SPV systems and to meet future demands of utilities and SPV prosumers.

1.2 Objectives and specific contribution

As mentioned in the introduction, customer expectation and technical issues with solar PV integration, need change in Solar PV system connecting architecture to utility grid to increase SPV penetration. Therefore, objectives of the research were set to propose a new Reconfigurable Architecture for, Z source inverter based SPV microgrid.

- To obtain maximum power from solar generation
- To provide uninterrupted power supply to the MG
- To provide reactive power requirement PCC

Based on the literature review research gaps have been identified as follows,

- One type of ZSI, Quasi-Z-source inverter used to supply uninterrupted power supply to loads, but not ZSI and not considered reactive power control as a configuration in microgrid situation.
- Reconfiguration in microgrids was limited to grid connection mode and to islanded mode, but not to Reactive power control in distribution network.
- Grid initiative and consumer initiative microgrid reconfiguration is critical fact to maintain healthy power network, but not considered in reconfigurable control architectures.

As per the identified research gap, ZSI based reconfigurable architecture was proposed to operate the residential solar PV microgrid in three different operating modes; 1) current control mode (To obtain maximum power from solar generation), 2) voltage frequency control mode (To provide uninterrupted power supply to the MG), 3) reactive power control mode (To provide reactive power requirement PCC). In addition to that, this architecture added feature to select reconfiguration priority to utility or consumer accordingly.

1.3 Methodology

Since, this research work going to propose a microgrid architecture, it focus on the functionality of each microgrid component in each configuration. Therefore, firstly, a Qualitative analysis of available research works on ZSI based Solar PV, reconfigurable Solar PV and reconfigurable microgrid architecture was done. Then, research gap was identified and proposed a new conceptual reconfigurable architecture for ZSI based reconfigurable Solar PV system to improve its functionality. The proposed conceptual reconfigurable architecture is designed, developed, and simulated in MATLAB/Simulink interface as an experimental testbed. Functional improvement is verified according to simulation results as per the following table (Table 1.1).

Table 1.1 Parameters considered for validation.

Objective	**Parameters considered for to evaluate the performance of proposed reconfigurable architecture**
Z source inverter based Reconfigurable Architecture SPV microgrid	• Different configurations with different objectives and functions.
Obtain maximum power from solar generation	• Accuracy of MPPT.
Provide uninterrupted power supply to the MG	• Resource's availability • Maintain power quality limits. • Capability to provide uninterrupted power supply for critical loads.
Provide reactive power requirement PCC	• Maintain power quality limits.

1.4 Thesis outline

The structure of the thesis is as follows.

- Chapter 2 summarizes the literature related to these research topics such as ZSI and reconfigurable architecture implementations.
- Chapter 3 presents the proposed reconfigurable architecture and its function in detail.
- Chapter 4 describes mathematical modelling of each component of the proposed reconfigurable architecture.
- Chapter 5 discusses the simulation of reconfigurable architecture in MATLAB/Simulink environment.

- Chapter 6 discusses the simulation results implemented through MATLAB/Simulink and other salient achievements in the research followed by recommendations for future improvements.
- Chapter 7 summarizes the conclusion and limitations of the research were discussed.

2 LITERATURE REVIEW

2.1 Reconfigurable architecture

According to (T. Considine, 2012), (A. Siddiqi, 2008), configurations and reconfigurable systems are defined as follows (Figure 2.1).

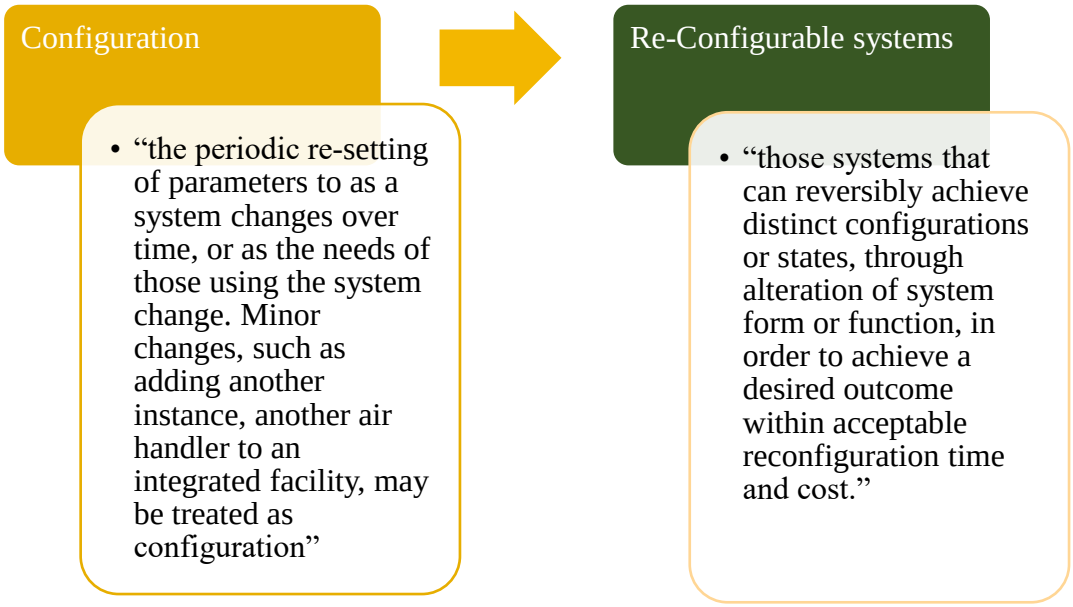

Figure 2.1 Definition of reconfiguration

Reconfigurable architecture,

- Increase flexibility of operation.
- Fully utilize the system components while reducing cost, size and weight enhances reliability.
- Increases the benefit from the microgrid.
- Provides a solution for an existing problem with SPV microgrid.

2.2 SPV systems

SPV concept arose with rural electrification with standalone SPV systems. But, due to increasing its economic value with technological development and environmental concern, SPV systems are connected to the utility grid. Hence, there are mainly two kinds of SPV systems called standalone SPVSs and grid-connected SPVSs. In this study, grid-connected SPV systems are under consideration. Depending on the functions and system architecture, grid-connected SPV systems are categorized as rooftop SPV systems, solar farms. The system architecture of those systems is given in Figure. 2.2.

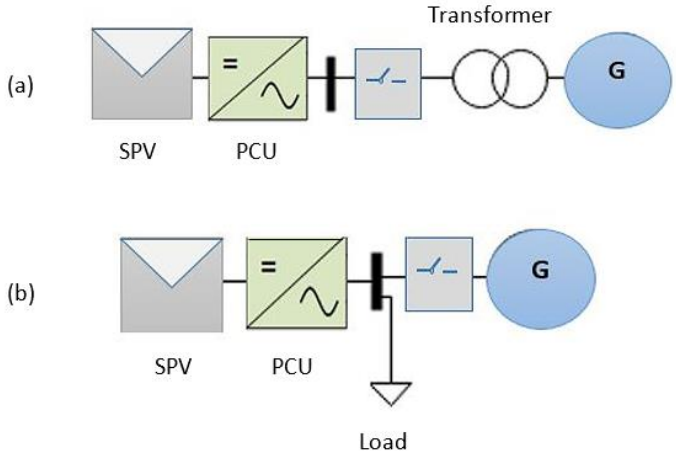

Figure 2.2 SPV system architectures (a) Solar farm (b) Rooftop SPV

Generally, the rooftop SPV system may be a SPV home system or an industrial or commercial building mounted SPV system, and supply power to the local demand and the utility grid. Nevertheless, SPV farms are not feeding to the local loads and they directly supply power to the utility grid. SPV systems are connected to the utility grid through, low voltage or medium voltage distribution network or through high voltage transmission network. According to the scale of the SPV system, we can observe utility-scale (above 1MW), medium-scale (1MW-10kW) and small scale (below 10kW) SPVSs. Solar farms are connected to the medium voltage distribution system or high voltage transmission network. Industrial or commercial building connected SPV systems are medium scale PV systems that are connected to the medium voltage (MV) distribution network or low voltage distribution network. SPV home systems are considered small-scale SPV and connected to the LV distribution networks. The connection of each SPV system into the utility grid is as in Figure. 2.3.

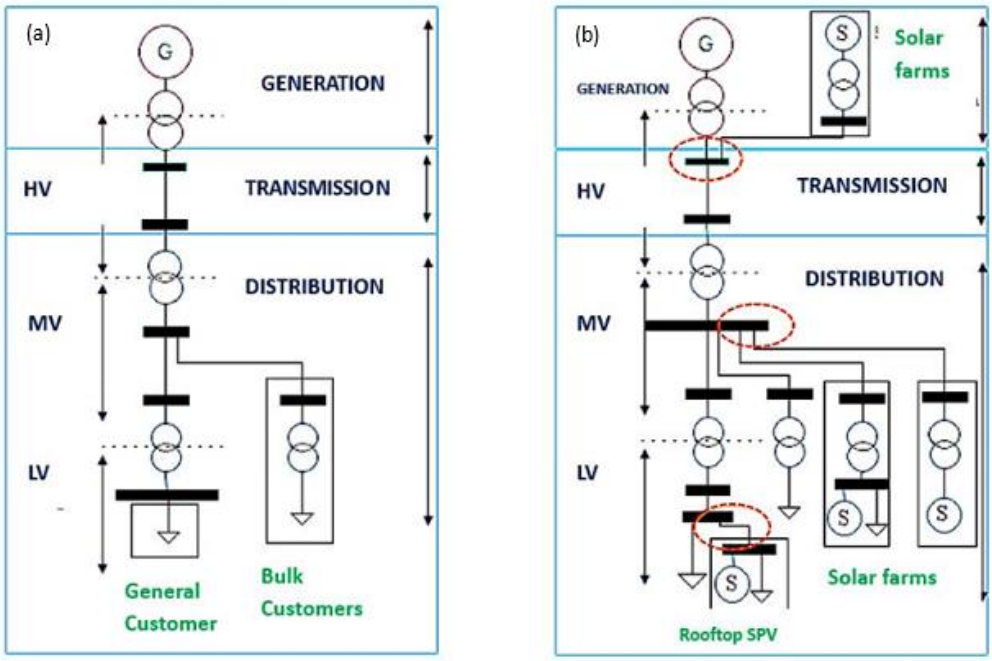

Figure 2.3 Structure of (a) conventional utility grid (b) with the connection of different types of SPV

2.3 SPV generator

SPV cells perform non-linear characteristics. Hence, an appropriate model is required to perform real electrical characteristics of SPV cells beyond using a just current source or a voltage source. The ideal solar cell is symbolized by a current source and the diode. However, different models were proposed in the literature, but the 5-parameter model (single-diode R_p model) is the most commonly used and accepted model due to its simplicity and accuracy. Where, the model is proposed as a combination of current source, diode, series resistance and parallel resistance and the model is given in Figure. 2.4. The series resistance denotes the contact resistance of the elements of the PV cell is made, while the parallel resistance represents the leakage current of the P–N junction (Ahmed Saidi, 2017).

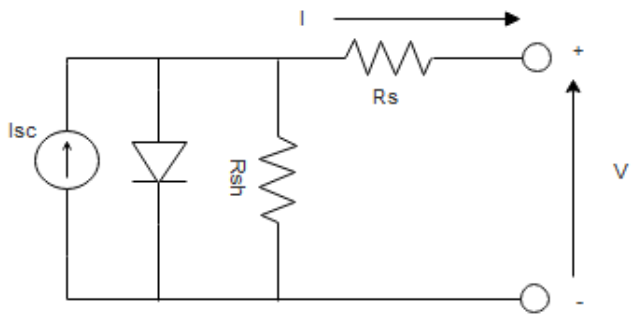

Figure 2.4 Electrical equivalent 5 parameter model based on one diode theory (Ahmed Saidi, 2017)

$$I = I_{PV,Cell} - I_{s,Cell}\left(exp^{\frac{V}{aVt}} - 1\right) \quad (2.1)$$

The first term in Eq. 2.1, $I_{s,Cell}$, is proportional to the irradiance intensity and the second term which is the diode current that expresses the non-linearity between the SPV cell current and voltage.

According to the equations, it clearly shows, SPV characteristics depend on different factors: solar irradiation, cell temperature. The relationship between the temperature and irradiation consequences in non-linear I-V characteristic as in Figure. 2.5. Therefore, it can be identified that the MPP is not a fixed point and it alters continuously with temperature and the irradiance. Due to these dynamics, an MPP tracker is needed.

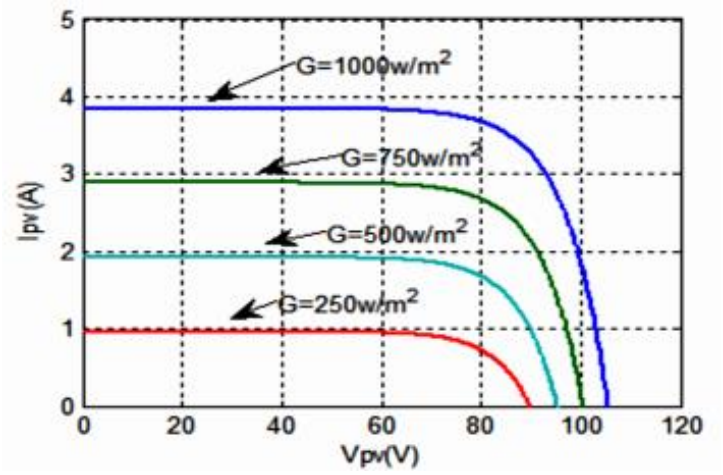

Figure 2.5 I-V Characteristics of solar panel for different solar irradiation

2.4 Power conditioning unit

Proper design of power conversion architecture of grid-connected PV systems is required since the number of inverters and the configuration significantly affects the performance, mismatch rejection, reliability, and costs of the SPV system.

Based on the type of power conditioning units in real-world cases, different architectures for the PV systems exist. The commonly reported architectures are the central inverter, string inverter, multi-string inverter and modular inverter (Damiano La Manna, 2014). They are shown in Figure. 2.6. and compared as in Table 2.1.

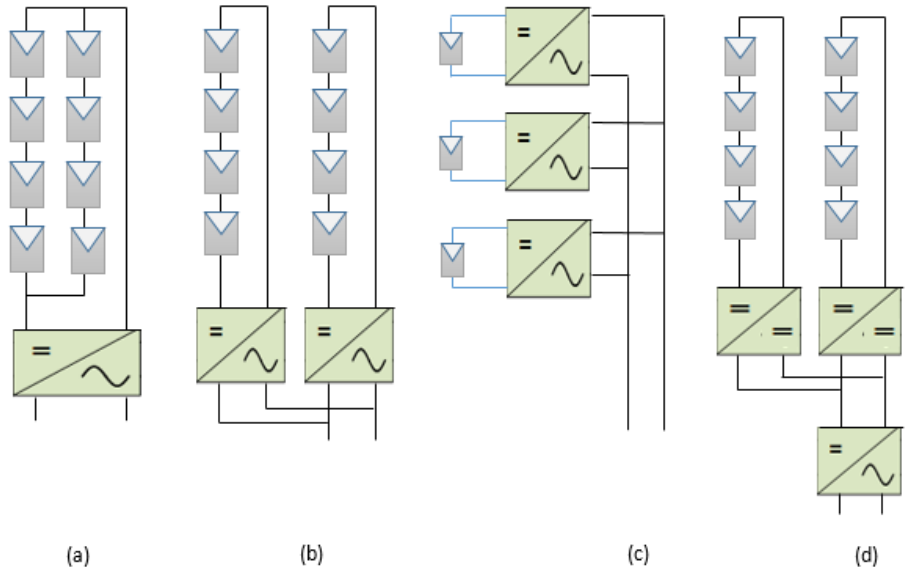

Figure 2.6 SPV architectures (a) Central inverter (b) String inverter (c) Micro/Modular inverter (d) Multi-string inverter

Table 2.1 Comparison of inverters (Central inverter, String inverter, Multi-MPPT inverter Module-integrated inverter)

Topology	Characteristics
Central Inverter	• Implement MPPT for whole array • Simple and cheep • Have higher mismatch losses
String Inverter	• Higher input DC voltage is obtained by making PV panels in series • Single PV string or few PV strings are connected to one string inverter and MPPT implemented itself • MPPT tracking is good and cost is high compared to central inverters
Module-Integrated Inverter	• Each PV modules are connected to the Module inverter • MPPT is implemented itself and performance are very high • System is very expensive • Lesser power conversion stages compared to Multi-MPPT Inverter
Multi-MPPT Inverter	• Few, separate MPPT / DC/DC converters which are feed from each individual PV strings, are connected to single inverter. • Higher power conversion losses compared to string inverters • Costly than string inverters • Good in MPPT tracing

2.4.1 Types of solar inverters

Mainly there are three types of solar inverters as Voltage source inverter (VSI) Current source inverters (CSI), and Z-source inverters (ZSI) (Peng, 2003).

2.4.1.1 Voltage source inverter

As shown in Figure. 2.7 VSI consists of a 3-ph bridge circuit and a DC source which is consist of a DC voltage source and a capacitor which has a relatively larger capacitance.

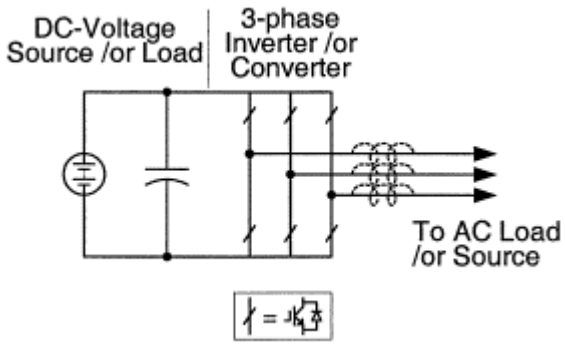

Figure 2.7 Structure of voltage source inverter

2.4.1.2 Current source inverter

CSI is consisting of a DC source, and 3-ph bridge as Figure. 2.8 and it feeds the converter circuit by DC source. But the dc source shall be a comparatively large dc inductor fed by a voltage source.

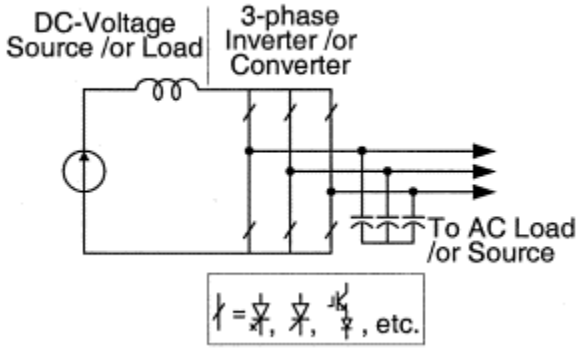

Figure 2.8 Structure of current source inverter

2.4.1.3 Z source inverter

ZSI consists of a dc source, a two-port network (impedance source (Z-source) coupling) that comprises of a split-inductor (two inductors, L_1, L_2) and two capacitors (C_1, C_2) which are connected in X shape Figure. 2.9 and it feeds the main converter circuit by DC source through impedance source coupling. Where the DC source can be either a voltage or a current source. ZSI propose a simplified single-stage power conversion topology providing additional benefits since the shoot-through (ST) doesn't destroy the inverter and it add DC/DC power conversion (buck boost mode) in addition to the DC/AC power conversion to the inverter. It gets rid of most of the problems challenged by the traditional VSIs and CSIs.

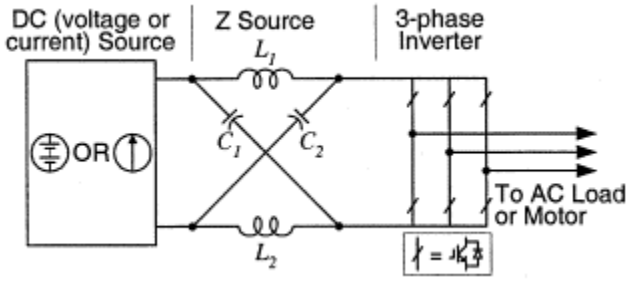

Figure 2.9 Structure of Z source inverter

The limitations and relative advantages of VSI, CSI, and ZSI are presented in Table 2.2.

Table 2.2 Limitations and advantages of VSI, CSI, and ZSI

VSI	CSI	ZSI
▪ Short-through state leads to fail the inverter ▪ Then, dead time is required and it increase harmonics injection more ▪ Filter should be sized to reduce the harmonic injection ▪ Voltage cannot boost at DC/AC conversion. ▪ Additional boost converter is necessary to boost the Voltage	▪ Open circuit state leads to fail the inverter ▪ Overlap time is required ▪ Voltage can boost at DC/AC conversion. ▪ Additional boost converter is necessary to boost Voltage	▪ Reliable due to safety in short through stage (Dmitri Vinnikov, 2016) ▪ Low harmonic injection ▪ Capability of buck-boost operation, (Peng, 2003) ▪ Additional boost converter not necessary ▪ Low cost, small size, reduced weight, more efficient rather than two stage power converters

2.4.2 Solar inverter categorization based on the function.

Solar inverters may be classified according to its function Stand-alone inverters, Grid-tie inverters, Battery backup inverters, intelligent hybrid inverters**.**

2.4.2.1 Stand-alone inverters

These types of inverters are used in islanded/isolated microgrids from utility grid, where the inverter draws its DC power from photovoltaic arrays or other DC generation to charge batteries and to provide AC power for Loads. As it is not connected with the utility grid, anti-islanding protection is not required.

2.4.2.2 Grid-tie inverters

These inverters match the phase in conjunction with a utility grid sine wave to generate AC power from DC source and they are programmed to automatically turn off itself at grid failures to ensure safety. Henceforth, they don't provide emergency power during grid failures. Grid code of most of the countries are accepted to connect these types of inverters to connect utility grid for net metering customers. Grid tie inverters are required to install with anti-islanding protection.

2.4.2.3 Battery backup inverters

These inverters are created to get power from the DC source and manage the energy from the battery through the onboard charger, and passe the excess energy to the

utility grid. They are capable to supply AC power to critical loads or particular loads during a power outage through battery back-up but it may be for a certain time. This type of inverter is also required to install with anti-islanding protection.

2.4.2.4 Intelligent hybrid inverters

These inverters are all-in-one system for grid-connected solar-plus-storage systems that are highly adaptable and can be used for grid-tie, backup, or stand-alone applications. And it can be installed without batteries and connecting other continuous power supplies such as wind generators. It is intelligent and programmable for maximizing overall system efficiency and savings. Generally, these types of inverters have less efficiency and less design flexibility compared to other inverters.

2.4.3 Operating conditions of DGs

Grid connected AC microgrids operation of DG are very important for voltage and frequency controlling. Generally, DGs are possible to operate in three different conditions. They are grid-forming units, grid-feeding units and grid supporting units. As per the operating conditions, the control methods of DG units are given in Table.2.3. (Xiongfei Wang, 2010)

Table 2.3 Control methods for DER units based on different operating conditions

Operating Conditions	Functions	Control Methods
Grid-forming units	Voltage and frequency control	Hybrid ac voltage and current control, ac voltage control, and indirect current control
	Load sharing	Active current sharing and Voltage and frequency droop-based control
Grid-feeding units	Power dispatch	Current control and AC voltage control, VOC and VFOC, direct power control
	Active/reactive power support	Positive sequence control, unity power factor control and constant active and reactive power control
Grid-supporting units	Maximum active power output	MPPT
	Reactive power support	AC voltage control

2.4.3.1 Grid-forming units

For continuous operation of microgrid during islanded mode, the MG voltage and frequency should be regulated by avoiding demand supply mismatches. This is achieved through grid-forming units as its name implies. In the grid connected operation, since the voltage and frequency regulations are done through the utility grid, these grid forming units change its operation from grid-forming mode to grid-feeding mode to feed active and reactive power as its generation. Therefore grid-forming units should be designed and controlled to operate in both islanded and grid connected modes.

The islanded and grid connected modes are controlled by voltage-frequency control and current control modes respectively. In addition to these conventional methods indirect current control algorithms and AC voltage control loops are used to overcome inherent issues of the conventional control methods such as voltage instability resulted by the delays in identifying unplanned operational mode transitions.

In case of more than one DGs which act as grid-forming units, complex control methods such as voltage and frequency droop-based method and active current sharing techniques are required to balance out demand sharing among these units.

2.4.3.2 Grid-feeding units

Grid-feeding units operate under current controlling mode as conventional grid connected DGs. However, these DGs regulate the active and reactive power output depending on the power dispatching requirements or voltage and frequency dynamics of the load or the feeder. In addition to the current control methods, power control methods are available such as voltage-oriented control (VOC) and virtual flux-oriented control (VFOC).

Grid feeding units are important in maintaining the power system stability with DER units not only by meeting grid requirements but also by absorbing small duration disturbances of the grid. Therefore, it is important to distinguish the faults in both the utility grid and the microgrid.

2.4.3.3 Grid-supporting units

Grid-supporting units are controlled such that the maximum active power can be extracted from the energy source together with the required reactive power to handle the sagging of grid voltage and supply local reactive current demand. These units should be distinguished from parallel units.

2.5 Energy storage systems

Another significant element of the proposed PV microgrid is the battery. It is required when backup power is needed and a need for the fluctuating power supply such as solar or wind to quick response for prevailing demand from charging and discharging. Comparatively, batteries have higher energy density compared to other storage devices like compressed air systems, ultra-capacitors, etc. Thus, the battery energy storage system (BESS) is the best flexible energy management solutions for microgrids, while improving its power quality.

Due to the nature of the application of this battery in microgrid a rechargeable type of battery is compulsory to select. There are mainly 6 types of rechargeable batteries as Lead acid, Nickel-metal hydride, Nickel-cadmium, Lithium-ion, Lithium-polymer, and Zinc-air batteries. The widely used batteries in residents are Lead acid and Lithium-ion batteries. The most developed electrochemical battery is lead acid battery due to its age. Low cost and low requirement of maintenance are the main advantages and low cycle life is the biggest disadvantage of this type of battery. The lithium-ion battery is a fairly new technology. Having a considerable range of energy and specific power density, high storage efficiency, better discharge performance are the main advantages, and the high cost is the biggest disadvantage (Bello, 2017).

Energy storage units generate more value when they are utilized for multiple stacked services. Most of the conventional systems utilize energy storage for one of the following applications.

- For peak shaving
- For backup power requirements
- For maximum utilization of renewable generation

This reduces the optimum utilization of batteries over its useful lifetime. As an example, if a battery is only used for peak shaving, it is utilized only for 5% to 50% of its useful life span. Therefore, it is beneficial to assign primary duties for batteries and then contribute them in multiple stacked services to add more value to the system. However, it is difficult to generalize the net value of the energy storages to the power system.

Because of hundreds of variables and related feedback loops, the net benefit of delivering any of the thirteen services at various grid levels (transmission level, distribution level, or behind the meter) varies significantly across and across all electricity markets. Therefore, energy storage values will differ drastically from analysis to analysis, influenced by grid-specific variables. Under current cost structures, batteries implemented for a primary key operation typically do not have a net economic gain (i.e., the present value of lifetime sales does not surpass the present value of lifetime costs), except for such use cases in certain markets. (Garrett Fitzgerald, 2015).

2.6 PV microgrid

A microgrid is a group of interconnected loads and distributed energy resources within clearly defined electrical boundaries that act as a single controllable entity with respect to the grid. It has the capability to connect and disconnect from the utility grid to allow it to operate in both grid-connected and island mode. Hence, SPV microgrid (PV MG) is defined as a group of interconnected loads and SPV systems which act as a single controllable entity and in both grid-connected situations and islanded situation. Generally, conventional SPV systems are not able to stand at islanded mode. Hence along with SPV systems, it cannot build a PV microgrid. However, this problem is solved with battery energy storage. Hence, SPV microgrid consists of SPV systems, battery storage units, controllable loads (critical loads noncritical loads), and controllers. A comparison between the SPV system and SPV microgrid is given in Table 2.4. Depend on the connections of components each other and its functionality, different PV microgrid architectures are created.

The relationship of SPV microgrid with other SPV is given in Figure. 2.10.

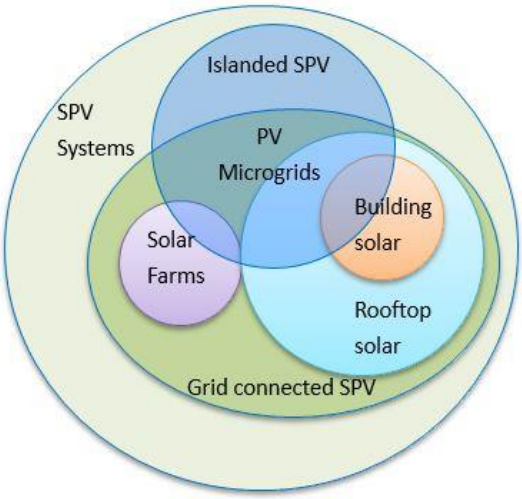

Figure 2.10 Relationship of PV microgrid with other SPV

Table 2.4 Features of SPV microgrid over a solar home system

Solar home systems	**SPV microgrid**
Loads are highly depending on Grid supply and intermittent, uncontrollable SPV generation only	When SPV power is not available
Utility grid have to bear more stress at night peak	Reduce the stress on the grid at night peak
System capacity should bare peak demand	Having the ability to control loads, utility grid capacity can be reduced

2.6.1 PV microgrid architecture

Based on various factors, we can identify various architectures in literature.

Considering the customer base of the PV microgrid, the PV microgrids can be categorized as single customer microgrid, multiple customers Basic PV microgrid. Single customer microgrids are powered through rooftop SPV systems while multiple customer microgrid may be powered through rooftop SPV systems or solar farms or both. Hence, single customer based microgrid be a home microgrid or commercial building microgrid or an industrial microgrid while multiple customer microgrid may be a partial feeder microgrid, full feeder microgrid based on the number of customer base and the geographical area.

Possible electrical boundary and PV microgrid according to the customer base is given in Figure. 2.11.

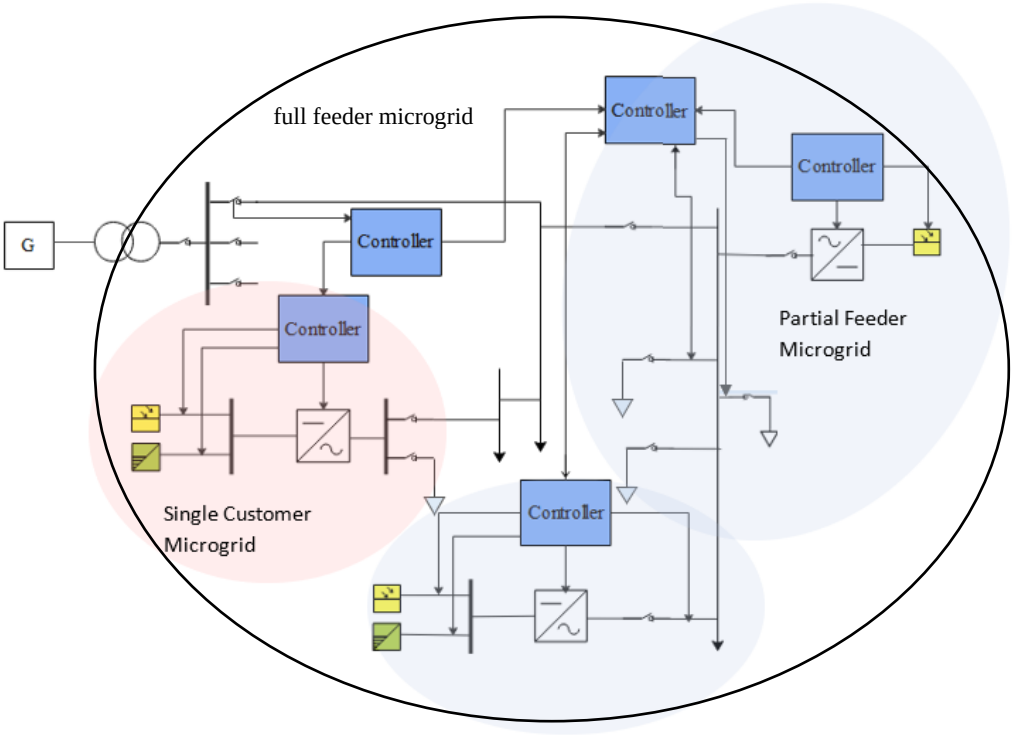

Figure 2.11 Different PV microgrid structures according to (Energy, 2015)

Based on the AC and DC systems, PV microgrids are present in different architectures. They are AC PV-microgrid, DC PV-microgrid, hybrid PV-microgrid and illustrated as Figure. 2.12. In AC PV microgrids, the main bus is an AC bus where AC loads are connected directly while DC power sources (solar and battery) and DC loads are connected through DC/AC converters and AC/DC inverters respectively. In DC PV microgrids, the main bus is a DC bus where DC loads are directly connected while DC sources (solar and battery) and AC loads are connected through DC/DC converters and DC/AC converters accordingly. However, hybrid PV microgrids are created by connecting both AC and DC microgrids through interleaving bidirectional converters. (Ravikumar, 2016).

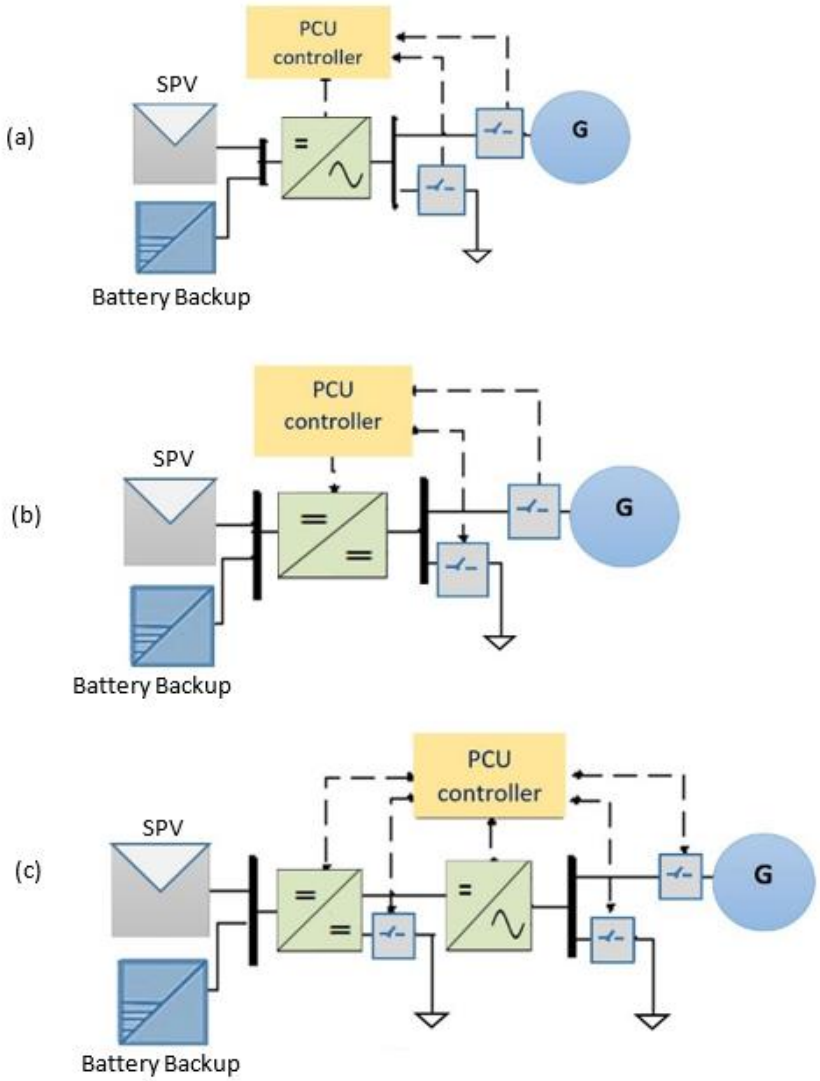

Figure 2.12 PV microgrid structures according to AC/DC systems (a) AC microgrid (b) DC microgrid (c) Hybrid microgrid

- ❖ According to the nature of sources
  - o Solar-Battery based power architecture
  - o Solar -Wind-based power architecture
  - o Solar - diesel-based power generator architecture
  - o Solar - mini-hydro based power architecture
- ❖ According to the operation
  - o Static Architecture
  - o Reconfigurable architecture

Based on the control architecture, PV MG architecture can be recategorized as demonstrated in Figure. 2.13 (Sushil S. Thale, 2015),

- ❖ Centralized control architecture
- ❖ Decentralized control architecture
- ❖ Hierarchical Architecture
- ❖ Multi-agent-based MG control architecture
- ❖ Reconfigurable Control Architecture

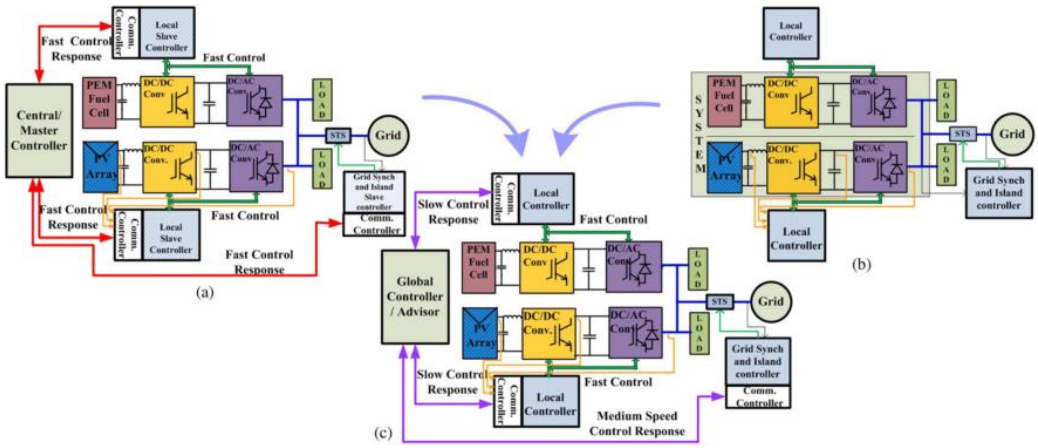

Figure 2.13 Different microgrid control architectures (Sushil S. Thale, 2015)

In the centralized concept, the sources are controlled by a central controller which may place at a remote location. In the decentralized concept, each source is individually controlled to share the demand change, without any interaction between controllers. The multilayer (hierarchical) control architecture is a better approach to overcome most of the issues related with centralized and decentralized control. A multi-agent-based system is an advanced version of a decentralized system, in which controllers interact with each other in achieving microgrid functions. The reconfigurable control architecture is the latest concept which increased reliability, flexibility, and controllability of power systems to use available resources in an optimized way to get reliable power supply while having cost benefits.

2.7 Reconfigurable SPV based power systems (RSPVS)

Reconfigurable systems are the systems that can attain different configurations at different times thereby altering their functional capabilities. Such systems are mainly suitable for specific type of applications in which their ability to undertake changes effortlessly, can be used to fulfil new demands, and to improve survivability by enhancing reliability (Weck., 2008).

By now, most of the power system components are not come up with isolated hardware only, and it is interconnected through different control and monitoring systems. For the modern world, existing traditional monitoring and control approaches are no longer satisfactory to face emerging needs for observability and controllability. Hence, moving towards reconfigurable power system components is the solution to fill the future requirements. Where reconfigurability can introduce for the power system at the hardware level as well as in the control level to adapt to the on-demand functional requirement though changing its hardware topology or control methodology.

In literature, reconfigurable solutions were proposed for different sections of SPV based systems such as SPV array, SPV power conversion unit and PV connected microgrids, and the summary of the application of it is described in Figure. 2.14 and Figure. 2.15. Hence, RSPVSs which were proposed in the literature, are discussed through the categories of reconfigurable SPV array, reconfigurable SPV power conditioning unit, and reconfigurable microgrids.

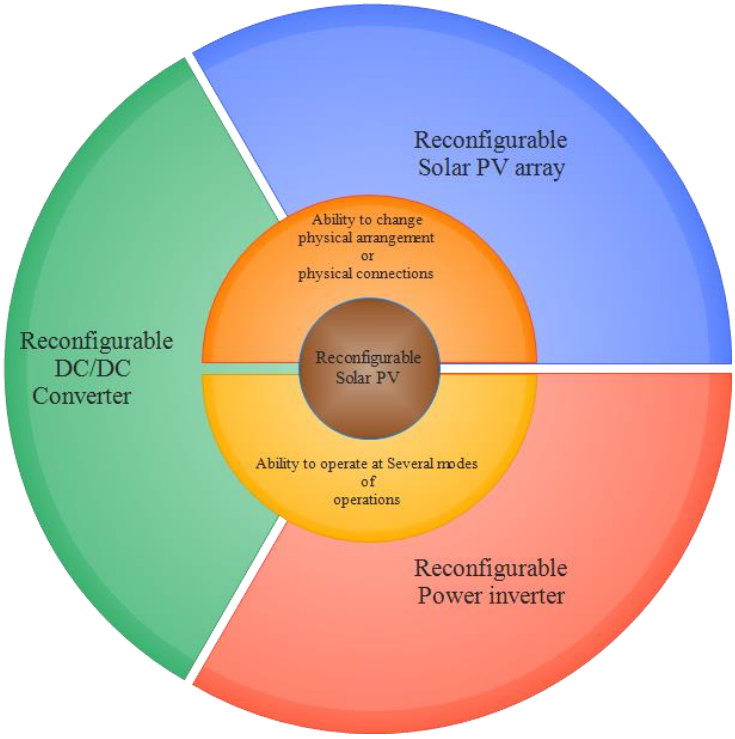

Figure 2.14 Summary of the function of reconfigurable SPV systems

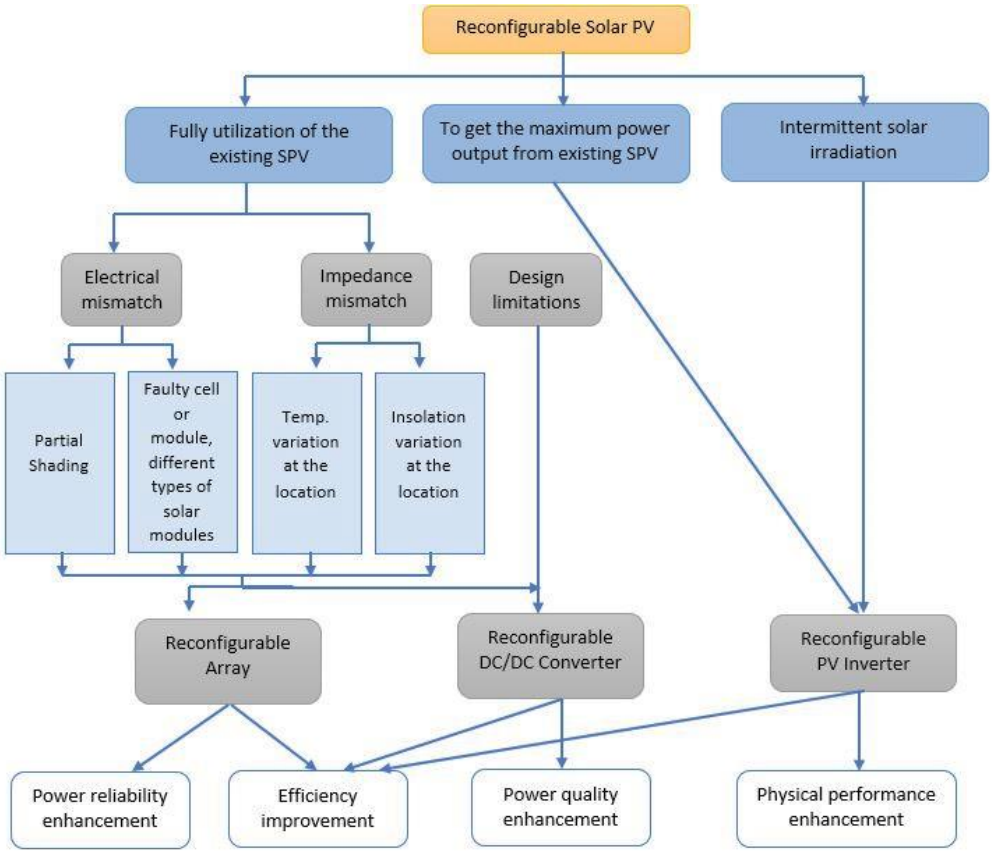

Figure 2.15 Summary of the application of reconfigurable SPV systems

2.7.1 The reconfigurable operation for SPV array

The SPV array reconfiguration is one of the solutions for electrical mismatch losses in SPV systems by changing its inter-connections of solar modules in a SPV array. Reconfiguration approach is applied only for central inverters, string inverters, multi-string inverters not for the module inverters, since module inverters are not much affected by electrical mismatch problem.

According to the configuration of connections of SPV modules in a SPV array, they can be categorized as,

- Series
- Parallel
- Series-Parallel (SP)
- Honeycomb
- Total cross tied (TCT)
- Bridge-linked (BL)

They are given in the following Figure. 2.16 (Damiano La Manna, 2014). Where series and parallel connection are the basic configurations to provide required power output and other configurations have been proposed with modification to these basic configurations to minimize the partial shading effect while providing the same power output as the basic configurations (Abdalla, 2013).

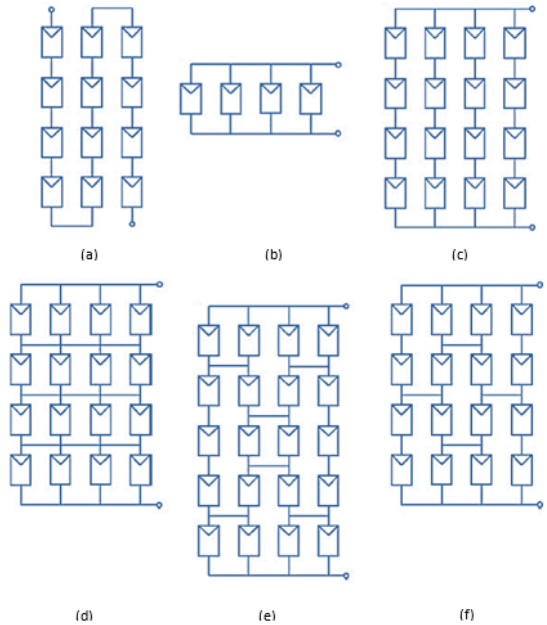

Figure 2.16 Reconfigurable array basic structures (Damiano La Manna, 2014) (a) Series (b) Parallel (c)Series-Parallel (d) Honeycomb (e) Total-cross-tied (f) Bridge-linked

In literature, ample of research papers were published regarding reconfiguration approach where Series-parallel (SP) and Total-crossed-tied (TCT) configurations are the main configurations most of the research has considered. Most of them, the irradiance equalization technique had been implemented as a control objective. The reconfigurable array basic structure is given in Figure. 2.17.

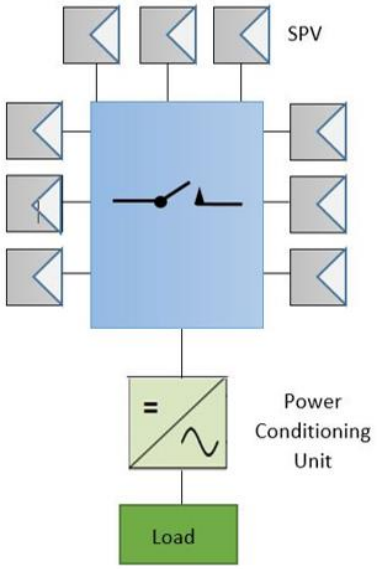

Figure 2.17 Reconfigurable array basic structure (Abdalla, 2013)

2.7.2 The reconfigurable operation for power conditioning unit for a SPVS

In a SPV system, the solar inverter is the main controllable device that is engaged with MPPT and grid synchronization in addition to the DC/AC conversion. Different types of solar inverters have been proposed considering different perspectives. Throughout them, the reconfigurable solar inverter has been taken considerable attraction and this concept was applied not only for DC/AC converter but also for DC/DC converter.

2.7.2.1 Reconfigurable solar converter

In (Hongrae Kim, 2013), a new concept called Reconfigurable Solar Converter (RSC) with minimum modification to the utility-scale, conventional 3-ph SPV converter was proposed. Its system configuration was SPV plant type with battery backup. The system structure of the proposed converter is given in Figure. 2.18. The key components of the RSC are SPV array, battery backup, conventional 3-ph inverter, harmonic filter, transformer, and additional switches. Here, the reconfigurable unit was a single-stage power conversion unit (VSI) and its controllability was improved to change its configurations according to the requirement of grid, battery, and availability of SPV generation. The proposed power conversion unit has the ability to operate into 5 major modes of operations through additional switches and it is described in Figure. 2.19. They are,

- PV to the grid - SPV provides power supply to the grid
- PV to the battery - SPV provides power supply to the for charging the battery
- PV-Battery to the grid - Both SPV and battery supply power to the grid
- Battery to the grid - Battery is sending power to the grid
- Grid to the battery - Battery is charging from the grid

Here, reconfiguration was proposed to reduce power conversion efficiency compared to the dual-stage power converter and to maximize its utilization, whenever peak shifting is required. As a result of that, the proposed converter could reduce its cost, weight, and volume, and dispatch it economically. Hence, this new converter added technical, financial and economic value to the existing SPV system, and it can be applied for even SPV home systems and also SPV microgrids.

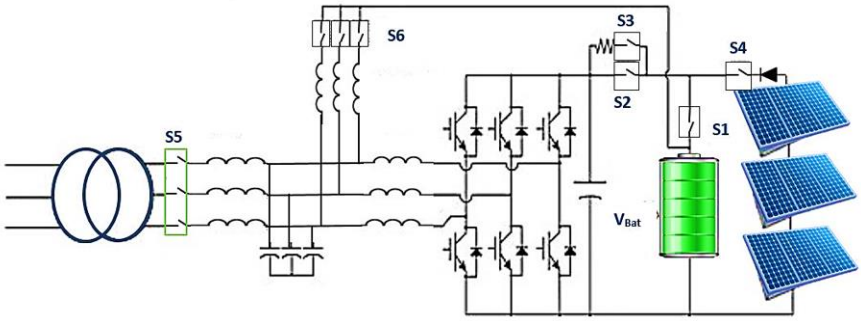

Figure 2.19 Structure of RSC (Hongrae Kim, 2013)

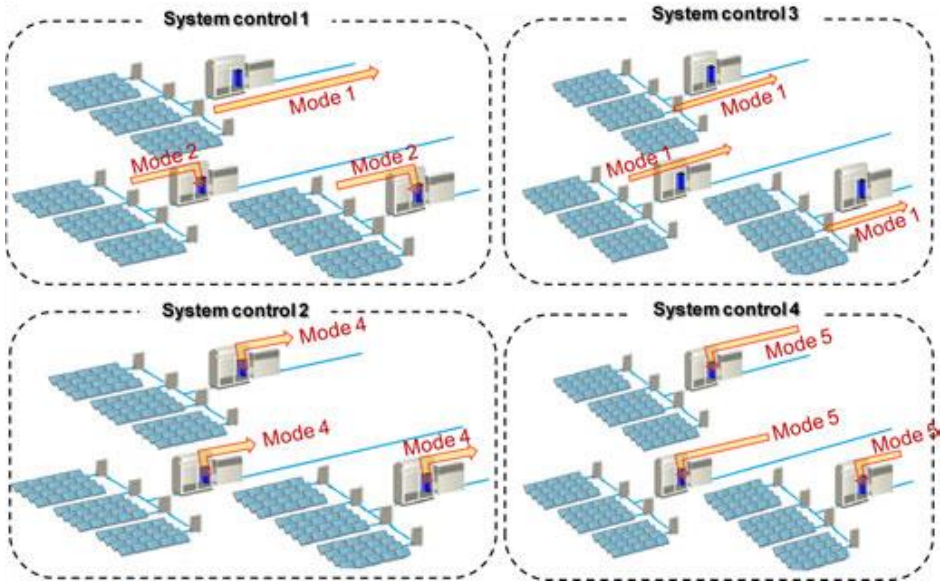

Figure 2.18 Modes of operation of RSC (Hongrae Kim, 2013)

Referring to this research work in (Hongrae Kim, 2013), several pieces of research were formulated to use this concept for different applications further.

Another application of RSC was proposed for distributed PV-battery architecture by (Iman Mazhari, 2014) for a solar farm, to reduce the effect of the intermittent nature of SPV generation throughout the day. Here, RSC in (Hongrae Kim, 2013) was modified to a single-phase RSC and it was used for peak shifting function. The same modes of operation in (Hongrae Kim, 2013) was used. By connecting these

modified modular RSCs in series with additional separate battery backup, the grid side transformer was eliminated. Hence it proposed a transformer less architecture while reducing power loss and additional cost due to the transformer. Due to its modular nature, RSCs have the ability to control each array independently and provide the ability to connect small and different energy storage systems. The separate storage system which was used to control power variations smoothly through ramp rate control.

Recently, a new inverter topology for solar-powered AC/DC hybrid homes was supposed by improving the concept of RSC in (Nikhil Sasidharan, 2017). The same modes of operation in (Hongrae Kim, 2013) was used. Through this new inverter, it mainly considered reducing harmonic distortion which is created due to extra power conversion at supplying DC load from DC power supply while increasing maximum utilization of utility-scale solar inverter. Performances at each mode of operations and transitions between each mode were considered. THD was compared in between the two conditions; connecting a dc load with the same rating with additional DC/AC and AC/DC converter and proposed new topology. Developed topology was implemented and validated practically. Significant harmonic reduction by 16% from THD and efficiency improvement was obtained due to introducing DC supply for DC loads (creating DC microgrid)

2.7.2.2 Reconfigurable single-input dual-output (SIDO) converter

A new concept for reconfigurable single-phase converter was proposed in (R. Rizzo, 2015) and it was introduced as a single-input dual-output (SIDO) converter to supply DC loads that require high and low voltage level in domestic microgrid operation (Electronic equipment, EV, scooter charging). Here, higher DC voltage is provided for higher DC loads such as EV charging, scooter charging, and low DC voltage was provided for smaller DC loads such as electronic equipment. This proposed new converter, it is having the ability to operate in three different modes by changing its configurations through static switches considering the availability of the SPV generation and DC load demand as in Figure. 2.20.

- RES DC/DC SIDO mode - two different voltage supply was provided through solar power generation according to the DC load requirement and solar power availability. Here, the converter is operating as a single input separate buck

converter output and boost converter output.

- In Grid/RES double DC output mode - Here, the SIDO converter was reconfigured into separate H bridge converter and buck converter. Here, SPV is connected to smaller DC loads buck converter and the grid was supplied to higher DC loads through H-bridge converter.
- Grid double DC output mode - Where SIDO converter is reconfiguring into a single input double cascade converter by series connecting H bridge converter and buck converter. Here, two-level of DC loads are supplied from this converter topology by means of static switches.

The aims of the converter were to reduce the number of components as necessary while utilizing MG components maximum with local DGs to meet a mixed supply-demand (AC and DC loads) successfully.

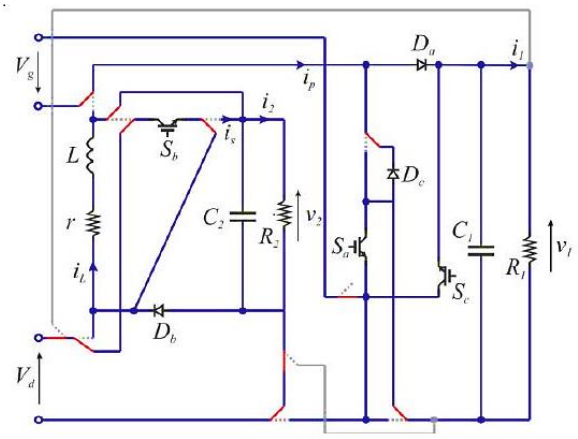

(a) Structure of SIDO (R. Rizzo, 2015)

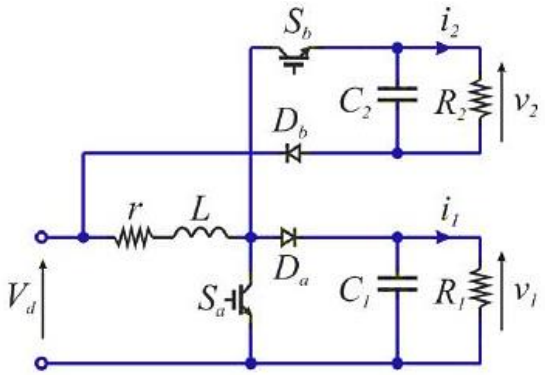

(b) Structure of SIDO at RES DC/DC SIDO mode (R. Rizzo, 2015)

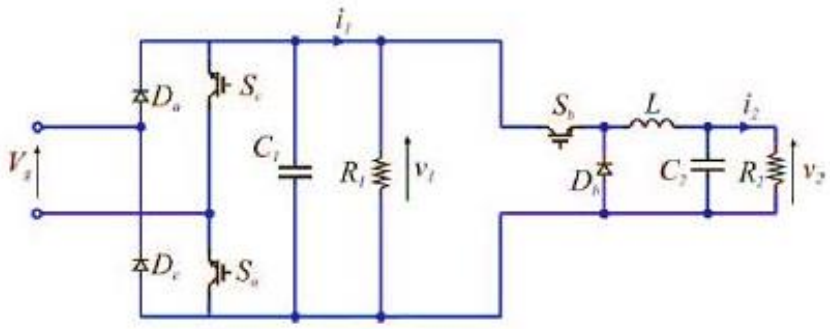

(c) Structure of SIDO at grid/RES double DC output mode (R. Rizzo, 2015)

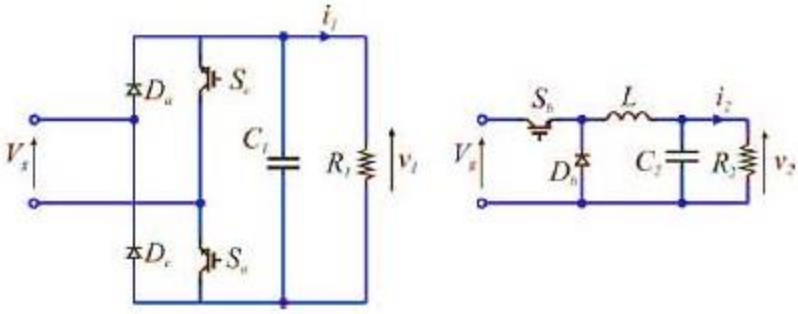

(d) Structure of SIDO at grid double DC output mode (R. Rizzo, 2015)

Figure 2.20 Modes of operation of RSC (R. Rizzo, 2015)

2.7.2.3 Reconfigurable PV system

In (Ming-tang Chen, 2016), another new concept for a single-phase reconfigurable SPV system which was equipped with quasi-Z-source inverter was proposed to supply uninterrupted power to the loads at grid failure. Proposed system structure was given in Figure. 2.21.

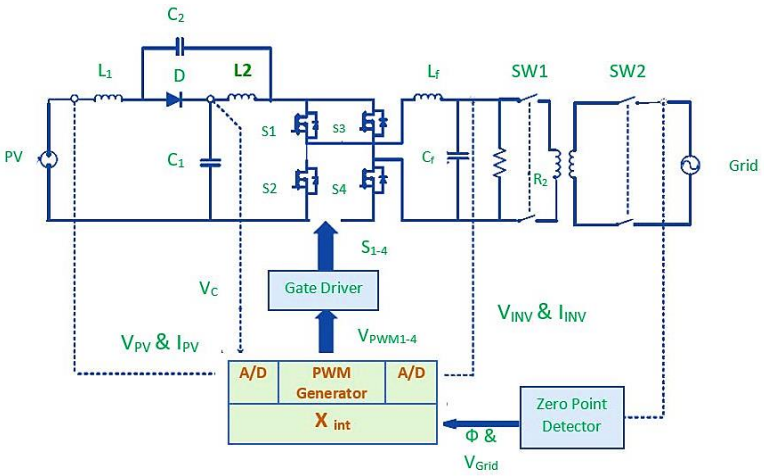

Figure 2.21 Structure of single-phase reconfigurable SPV system (Ming-tang Chen, 2016)

This reconfigurable system was operated at two operating modes,

- Grid-connected mode - normal operation of the grid-connected inverter
- Standalone mode - operated at grid failure where the grid is disconnected from the system and it is work as a standalone system

Where transient problems at due mode changes were considered. Hence, the indirect current controlling method was proposed to compensate for those problems. The proposed indirect current controlling method was implemented in MATLAB/Simulink environment, implemented and tested the system under different load conditions. But the Simulink model is not presented. With this proposed reconfigurable operation, system reliability at grid failure was improved. Another reconfigurable DC/DC converter was proposed in (P. K. Peter, 2012).

2.7.2.4 Quasi-Z-source series resonant DC/DC converter (qZSSRC)

In (Andrii Chub, 2017), the reconfigurable operation was proposed for quasi-Z-source series resonant DC/DC converter (qZSSRC) which was proposed in (Dmitri Vinnikov, 2016). It was proposed to track MPP at partial shading conditions and different temperatures of solar panels. Here, the incremental conductance method was used to calculate reference input voltage. Through this new converter, provides a wide range of input voltage and loads regulation capability to the SPV system. The proposed system has the capability to change its configuration into two different configurations such as full-bridge or traditional series resonance converter (SRC) or a single switch quasi z source dc/dc converter as given in Figure. 2.22 and it is operated in three different operational modes depending on its operating point as in Figure. 2.23.

- Buck mode - is operated at the startup the qZSSRC from its open-circuit voltage and when the system is operated at low-temperature conditions. Here, the system is operated as a single switch quasi-Z-source dc/dc converter.
- Normal mode - This is a boundary in between buck mode and boost mode. The system is operated as full-bridge qZSSRC at the resonant frequency in half cycle discontinuous conduction mode.
- Boost mode - is operated at high-temperature conditions and partially shaded

conditions. Here, the system is operated as a full-bridge qZSSRC and it is operated at the resonance frequency in half cycle discontinuous conduction mode.

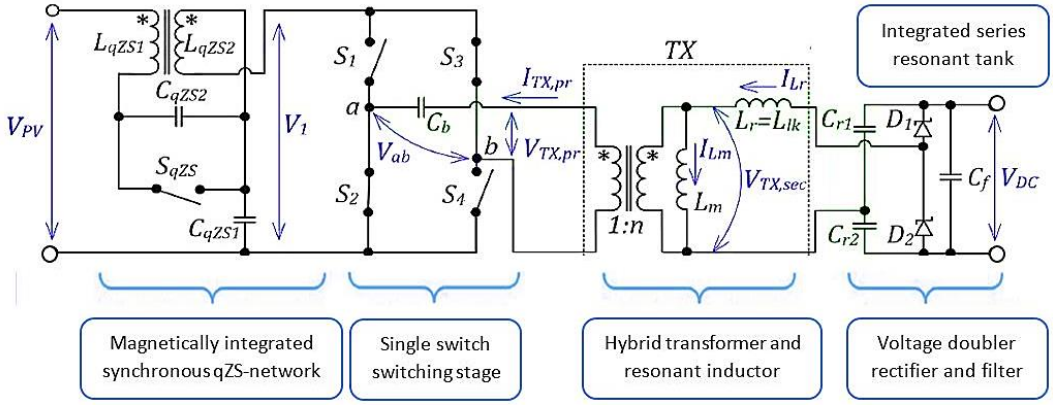

Figure 2.22 Structure of qZSSRC (Andrii Chub, 2017)

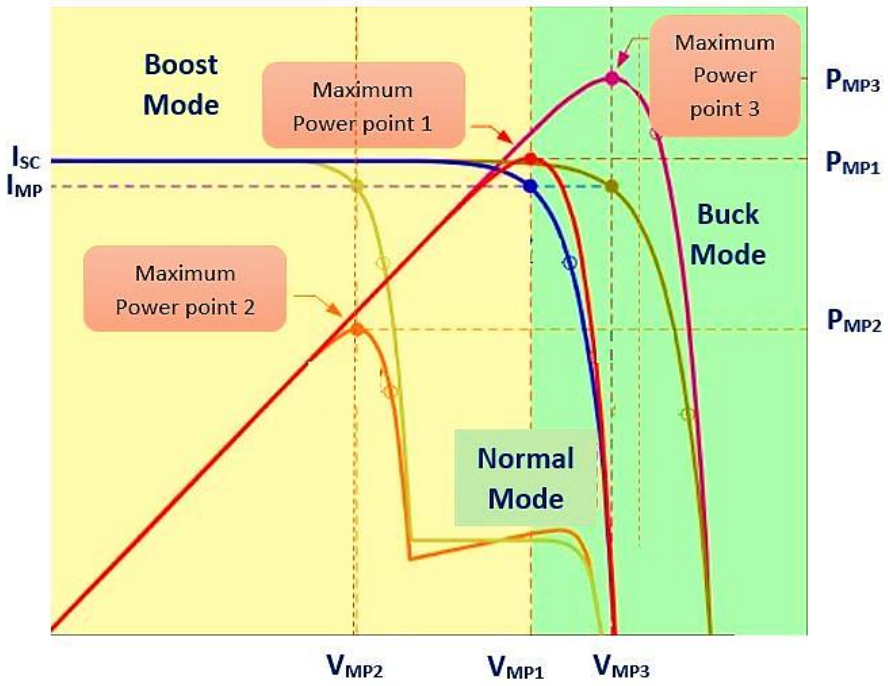

Figure 2.23 Characteristics of qZSSRC (Andrii Chub, 2017)

The main modifications done to this is the implementation of the magnetically integrated synchronous quasi-Z-source network and a resonant voltage-doubler rectifier (VDR) circuit, reconfigurable buck-boost switching stages for maximum power point tracking, and a distinct control algorithm with smooth transition in between each operating mode. The proposed control algorithm was proposed good dynamic behavior at MPP tracking with smooth transition between three modes of operations and peak efficiency was improved to almost 97% at nominal voltage

including all losses in the converter. Here, no passive components at a time and the number of switching devices are higher when compared to other DC/DC converters. That is the main disadvantage of this converter.

2.7.3 Reconfigurable inductor

Previous researchers were considered reconfigurability for the entire converter. But did not consider reconfigurable operation for a single element to change its effective size according to the situation. In (Chapman., 2007), reconfigurable inductor was proposed as a solution for the low efficiency of SPV boost converter at low insolation with high current and voltage ripple, and design limitation for the inductor size to prevent saturation at high insolation level. Where standard boost converter was modified with an additional three switches and replaced inductor with coupling inductor such that it can be reconfigured into two modes.

- High-L - where, inductors are connected in series and successfully reduce the output current and voltage ripple of the SPV system at low insolation.
- Low-L - where, inductors are connected in parallel and prevent saturation at high insolation.

Hardware implementation was done for this research study and considerable power efficiency improvement was performed for the 20W SPV system. It is useful to recharge batteries of the standalone solar system or to supply for load under low insolation level. Here, two-stage power conversion architecture was considered. The structure of the converter is given in Figure. 2.24.

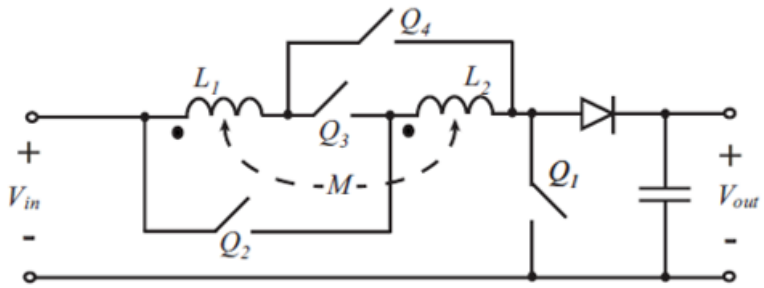

Figure 2.24 Structure of boost converter with reconfigurable inductor (Chapman., 2007)

2.7.4 Reconfigurable microgrids

In literature, reconfigurability was introduced for microgrid control architectures as well as for microgrid topology architecture.

According to (Singh, 2017) grid-connected SPV-battery and hydro generation based reconfigurable systems were proposed. Here, grid, microgrid, and non-linear load were connected at the PCC. Depending on the grid availability, the proposed reconfigurable microgrid was operated at two operating modes;

- Grid-Connected mode
- Islanded mode

In this system, Reconfigurable operation was applied for the control strategy of the microgrid. This reconfigurable system as consisting of three different controllers as MPPT controller, bidirectional inverter controller of Battery energy storage system (BESS) and VSC controller of the SPV system. But Solar Inverter was the main component that performs the reconfigurable operation by changing inverter control mode as the current controlling mode in grid-connected mode and as voltage-frequency controlling mode in islanded mode. Key features of this research work were automatic synchronization of the microgrid to the utility grid, providing uninterrupted power supply for critical loads, maintaining power quality in the microgrid and consideration the effect of non-linear loads. The reconfigurable microgrid structure is given in Figure. 2.25.

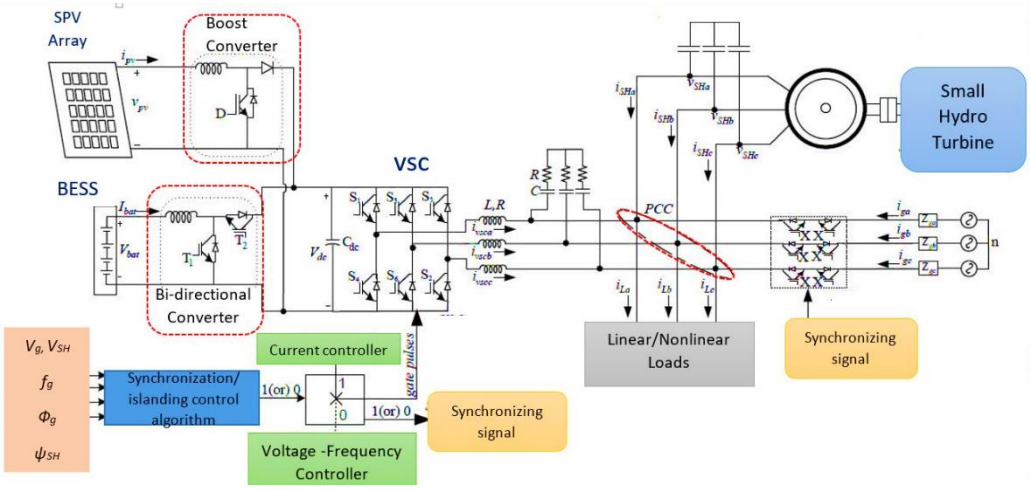

Figure 2.25 Structure of reconfigurable microgrid (Singh, 2017)

In (Chamana, 2014), the performance of this RSC (Hongrae Kim, 2013) was compared over conventional two-stage inverter (TSI) (with bidirectional converter for battery power controlling) while both are connecting to MG. The operations of RSC were proven its economic benefits and controllability over TSI while

performing similar power output characteristics as TSI even though it is a single-stage converter to control both SPV and battery.

2.7.5 Reconfigurable control architecture

The modern SPV inverters are expected to provide novel control features (e.g., voltage regulation, ramp-rate control, power curtailment, communication-assisted protection etc.) and targeted to enhance the communication with SPV-DGs with utility grid and provide coordinated control and operate over local or utility wide supervisory controllers.

Considering existing centralized, decentralized and hierarchical microgrid control architectures, a new hierarchical and reconfigurable architecture was proposed for a photovoltaic, wind, micro-hydro, and fuel cell-based microgrid with power backup from ultra-capacitor (UC) and battery storage in (Sushil S. Thale, 2015). The main objective of this new architecture was to increase the reliability of microgrid by creating a high fault tolerance microgrid at any failure or malfunctioning of microgrid controllers and communication links, through reconfigurability. This control architecture is consisting of 4 level control layers (local controller (LC), emergency controller, secondary controller, and global controller) and an additional control layer called adversary layer (ADVC). Here, the global and secondary layers are residing in the Master microgrid controller (MMC) while the emergency control layer is residing in ADVC, MMC, and LC. Here, all controllers are interconnected via the communication layer to operate a centralized controller. According to proposed reconfigurable architecture, the microgrid is operated through a decentralized controller. But, during a failure of LC MMC takes the controller as a centralized controller. In case of emergency, if MMC also failed during LC failure, ADVC takes control of LC again as a centralized controller. The proposed reconfigurable microgrid was implemented laboratory environment and tested for reconfigurable operation and various operating modes and events. This proposed reconfigurable control architecture was given in Figure. 2.26.

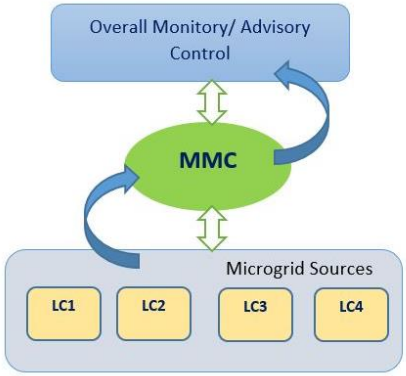

Figure 2.26 Proposed reconfigurable control architecture (Sushil S. Thale, 2015)

2.7.6 Reconfigurable distribution networks

After introducing distribution generations into distribution networks, the distribution network being active from its passive nature. High penetration of distributed generation even SPV creates critical problems in power reliability, power quality, harmonic level, and protection. Problems related voltage such as voltage fluctuations, voltage flickers, voltage sags and dips, and harmonic problems are the main power quality issues with SPV.

To overcome those problems, the distribution network reconfiguration into a cluster of microgrids or connecting distributed generations like solar, wind through microgrid, was the promising solution that was proposed in the literature (Sicong Tan, 2012). Moreover, it leads to self-consumption in the microgrid itself and reduces the power consumption from utility grid.

The possibility of a reconfiguration of the radial DN into MGs are proposed by developing algorithm in (E Ghiani, 2005) considering two main features: 1) cost of energy 2) financial loss of interruptions. The proposed algorithm showed major benefits from the reconfiguration of the network into MGs can be obtained by selecting opportune nodes carefully to create MGs. The suggested planning procedure may be beneficial to distribution system operators (DSOs) that strive to offer new high-level services to the customers having minimum interruptions.

Another application of distribution network reconfiguration was proposed in (Sicong Tan, 2012), where distribution network reconfiguration was proposed to

create microgrids accordingly with economic load dispatch considering uncertainties such as load variations and cost of SPV and wind generation and battery storage. Uncertainties are forecasted through a support vector regression-based machine learning approach. The promising multi-model optimization technique, Vaccine-enhanced artificial immune system (Vaccine-AIS) was used to solve the optimization problem. The network can adjust its configuration by itself, to allow the maximum utilization of renewable energy with power loss reduction in the distribution network.

Recently, a new robust optimization technique was proposed in (Phillip Oliver Kriett, 2012), to reconfigure distribution feeder into multiple microgrids for optimum microgrid planning under uncertainties. Here, the distribution feeder was partitioned into several microgrids through SSW feeder, and TSW feeder provides the ability to change the configuration of the distribution feeder. The optimum configuration of microgrids was decided according to the solution of optimization problem considering economical, technical and reliability point of view under uncertainty. Here, robust optimization was used to solve the optimization problems under uncertainty such as electricity price, load demand, and power generation from renewable sources. Multi-integer nonlinear programming model was used to formulate a microgrid planning model based on reliability, technical and economic aspects and it was solved by Grey Wolf Optimization (GWO) algorithm. The

Figure 2.27 Reconfigurable microgrids (Phillip Oliver Kriett, 2012)

proposed microgrid planning model was implemented and validated on the IEEE 30-bus distribution network in MATLAB/Simulink environment. Throughout the reconfigurable approach, it reduced energy not supplying cost, voltage fluctuations and power loss in distribution feeders. Its robustness was confirmed through Monte-Carlo simulation. Furthermore, the proposed model design was proved that the reconfigurable topology for microgrids have better performances rather than a fixed structure for practical applications. The proposed reconfigurable microgrid structure was given in Figure. 2.27.

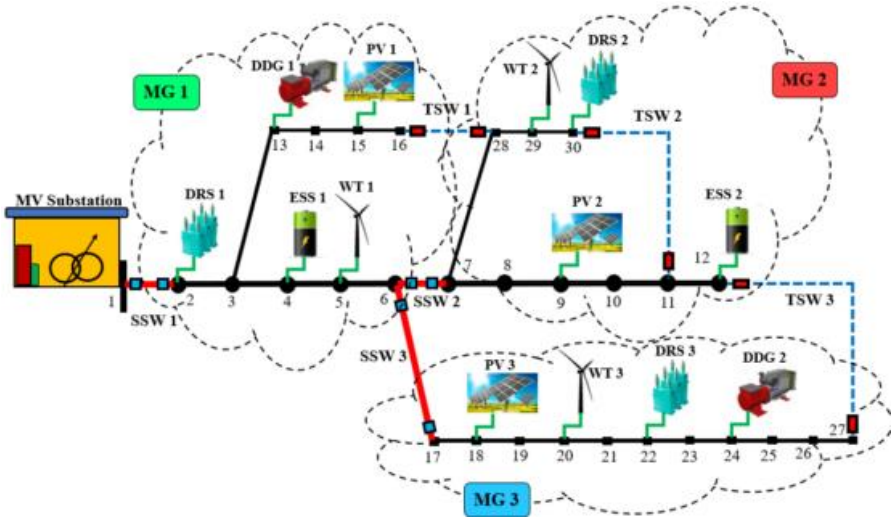

2.7.7 Summary of available reconfigurable solar PV systems

According to literature, the existing reconfigurable systems differ considerably in the application, objectives as well as reconfiguration methods and structures and described in Table 2.5 and 2.6. The main objective of proposed all reconfigurable solar arrays was to reduce partial shading losses. However, PCUs were used on different objectives such as to reduce partial shading losses, electrical mismatch losses and cost, weight, and volume to enhance performances overcoming its design limitations, to maximize its utilization, while reconfigurable microgrids were introduced to improve its reliability and power quality. Where predefined controlling function is there for each configuration, they may be changed from configuration to configuration and change of configuration may occur when existing mode goes beyond its set limits. Different control methods were proposed for each reconfigurable system.

DN reconfiguration was widely discussed to achieve common objectives for every configuration such as enhance the availability of power supply for critical load, power loss reduction and to increase quality and stability of the DN, considering the effect of DG into the distribution network. Where different optimization strategies were used to select its' best configuration considering the above objectives.

Multi-agent based microgrid control architecture was widely discussed with hierarchical control architecture. But hierarchical reconfigurable architecture was not discussed with multi-agent architecture.

According to literature, reconfigurable architecture was proposed to power architecture and control architecture of SPV based systems and microgrids. There is a positive trend for reconfiguration of power system components specially for solar PCUs, microgrids and microgrid control architecture for maximizing its utilization or increasing reliability of its operation. The reconfiguration of both power architecture and control architecture ability to provide more benefit to the future microgrids and it will be a key function.

The reconfigurable concept was applied for conventional microgrid, DC microgrid or grid-connected SPV generation, but not to Reactive power control in distribution network. Few pieces of research were carried out on reconfigurable architecture with the quasi-Z-source network for DC/DC converter operation, but others have not used the advantages of Z source inverter.

Consequently, policies, consumer needs, expectations of operations and services at the distribution level are changing. SPV connection and BESS are required to participate in power quality maintaining functions beyond its main functions such as backup power generation and balance power supply. Hence, the control architecture should as consider BESS as dispatchable power source. Grid initiative and consumer initiative microgrid reconfiguration is another fact to be highly study to maintain healthy power network, but not considered in existing reconfigurable control architectures.

Here after, critical changes are needed in the assembly of control systems, communications, coordination frameworks and regulatory changes. However, it is critical do big changes and to be understood, rearchitected, and accomplished at the same time, since these systems are extremely interconnected. Hence, new technologies, methodologies should be developed to meet customer demands in future considering above facts.

Table 2.5 Summary of available reconfigurable solar PV systems

	Micro grid	Advantages	Reconfigurable section	Modes of operation	Added features	Validated through
RSC (Hongrae Kim, 2013)	No, (Utility scale SPV power plants)	• Single stage power conversion system to perform different operation modes • Due to flexibility of operation, solar plants is controlled more effectively, and its power is dispatched more economically Maximize its utilization and reduced cost, volume and weight	VSC (3ph)	1) PV to grid 2) PV to battery 3) PV-Battery to grid 4) Battery to grid 5) Grid to battery	• Added additional cables and mechanical switches to conventional the three-phase PV inverter system to operate as a dc/dc converter in addition to its dc/ac conversion. • Optional inductors are added when ac filter inductance is not enough for battery charging. • Power control : synchronous reference frame PI current control	Hardware implementation
RSC for distributed PV Battery systems (Iman Mazhari, 2014)	No, (Utility scale SPV power plants)	• Possible for peak shifting • Possible for Smooth power variation • Enable to connect different types of PV modules and small energy storage systems • Reduced power conversion losses by removing step up transformer	VSC (1ph)	1)PV to grid 2)PV to battery 3)PV-Battery to grid 4)Battery to grid 5)Grid to battery	• Grid side transformer is removed from distributed multilevel modular RSC • Power controlled through ramp rate controlling method • Additional, separate battery is used to help ramp rate controlling	MATLAB - Simulink simulation

RSC with DC bus (Nikhil Sasidharan, 2017)	Yes (AC/DC, domestic microgrid)	• Improve efficiency, reduce volume, and enhances the reliability. • Increased dc side of the inverter efficiency (90%) • Reduce 16% of current harmonics (THD)	VSC (1ph)	1)PV to grid 2)PV to battery 3)PV-Battery to grid 4)Battery to grid 5)Grid to battery	• Same as RSC (Hongrae Kim, 2013), utilize single stage conversion of ac power to dc and vice versa • DC loads are directly connected to the DC link without connecting to AC side through AC/DC converter	Hardware implementation
Reconfigurable SIDO inverter (R. Rizzo, 2015)	Yes (Domestic Microgrid)	• Flexible to operate different power conversion modes • Solution to meet demand of mixed power supply (AC and DC) with single converter • Good performance in both steady-state and slow and fast transient conditions. • Reduced no of components, maximize its utilization, reduced cost, volume and weight	Single-input dual-output (SIDO) converter (DC/DC and AC/DC converter (1ph))	1)RES DC/DC SIDO mode 2)Grid/RES double DC output mode 3)Grid double DC output mode	• SIDO converter has been modified adding 11 static switches • Measures have taken to meet mixed power supply demand (AC and DC) • Supply two level of dc loads demands	MATLAB - Simulink simulation
Ref (Ming-tang Chen, 2016)	Yes	• Enable to supply uninterrupted power supply for critical loads at grid failure • Improved reliability of the SPV system	Quasi Z-source inverter (DC/AC converter (1ph))	1)Grid connected mode 2)Islanded mod	• Single-phase quasi-Z-source inverter is used as SPV converter • Indirect current control-based controller is developed	MATLAB - Simulink simulation and hardware implementation
Reconfigurable quasi-Z source Inverter	No	• Capability of wide range voltage regulation for MPP tracking	DC/DC converter	1)Boost mode (full bridge qZSSRC)	• Implementation of magnetically integrated synchronous qZS network	Hardware implementation

(Andrii Chub, 2017)		• Reduced power losses due to partial shading and impedance mismatch • Improved peak efficiency of converter closed to 97% • Smooth transition between three modes of operations	(quasi-Z source Inverter)	2)Normal mode (full bridge qZSSRC) 3)Buck (single switch qZSC)	and resonant voltage-doubler rectifier (VDR) and its specific controller	
Ref (Chapman., 2007)	No (residential SPV System)	• Increase solar energy capture at low irradiance conditions. • Reduce current ripple without increasing the inductor volume to meet peak current saturation requirements. • Reduce the required PV panel size, inductor volume, or both.	Inductor in DC/DC converter	1)High L (High Inductance) 2)Low L (low inductance)	• A standard boost converter has been modified by replacing source side inductor from coupled two inductors and adding 3 additional semiconductor switches.	Numerical simulation and hardware implementation
Ref (Singh, 2017)	Yes (small hydro, PV, battery microgrid)	• Extracting maximum power from SPV system • Providing uninterrupted power supply for critical loads • Maintaining power quality in the micro grid • The THD of load voltage and grid current is below 5% even under nonlinear loads	VSI (3ph)	1)Grid connected mode 2)Islanded mode	• Small hydro generator was connected at PCC • Consideration the effect of non-linear loads • Compensation of load reactive power. • Performance of the reconfigurable system was proved under all types of disturbances	MATLAB - Simulink simulation

Table 2.6 Summary of objectives applied reconfigurability in SPV based power system

<table>
<tr><td colspan="4">For SPV systems</td><td colspan="2">For microgrid</td></tr>
<tr><td rowspan="2">For SPV arrays (Damiano La Manna, 2014), (Abdalla, 2013)</td><td rowspan="2">DC/DC converter (Andrii Chub, 2017), (Chapman., 2007)</td><td colspan="2">DC/AC inverter (Hongrae Kim, 2013), (Nikhil Sasidharan, 2017), (R. Rizzo, 2015) , (Ming-tang Chen, 2016)</td><td rowspan="2">Control architecture (Sushil S. Thale, 2015)</td><td rowspan="2">Microgrid operation (Distribution network), (Singh, 2017)</td></tr>
<tr><td>Conventional Inverters</td><td>ZSI</td></tr>
<tr><td>• Solution for Electrical mismatch</td><td>• Solution for Electrical mismatch (Andrii Chub, 2017)
• Solution for Impedance mismatch (Andrii Chub, 2017)
• Solution for design Limitation (Chapman., 2007)
• Maximize its utilization and reduced cost, volume and weight (Chapman., 2007)</td><td>• Maximize its utilization and reduced cost, volume and weight (Hongrae Kim, 2013), (Nikhil Sasidharan, 2017), (R. Rizzo, 2015)</td><td>• To increase the reliability (Ming-tang Chen, 2016)</td><td>• To increase the reliability</td><td>• Optimum MG operation
• Distribution network power loss reduction
• Load balancing
• Service restoration for critical loads
• To improve power quality at PCC (Singh, 2017)</td></tr>
<tr><td colspan="4">System efficiency increased, power availability, power quality and power reliability at PCC is improved. Maximize its utilization and reduced cost, volume and weight.</td><td colspan="2">Reliability increased</td></tr>
</table>

2.8 MPPT control

To achieve MPP, different controlling methods are proposed in literature. There are well recognized MPPT methods in literature proposed to achieve MPP in SPV system under uniform irradiance condition and Partial Shading Conditions (PSC) (Amit Kumer Podder, 2018). Under uniform irradiance conditions, following MPPT control techniques have been discussed: perturb and observe (P&O), Hill Climbing (HC), Incremental Conductance (INC), short circuit current (SCC), current sweep, load I or V maximization, DC link capacitor droop control, dP/dV or dP/dI feedback control etc. Under PSC conditions following MPPT control techniques were discussed as partial swarm optimization (PSO), state based (SB), array reconfiguration (AR), etc.

This research is focused on INC as it is ideal to enhance the tracking accuracy and dynamic performance (provides less oscillation around the MPP) under quick changing conditions and uniform solar irradiance, and its simplicity even through it has disadvantage of tracking true MPP at Partial Shading Conditions.

2.9 ZSI controller

Even though ZSI provides advantages to the SPV systems over conventional voltage source inverters (VSIs), the controller of ZSI is more complex to implement due to its ST state in addition to the active state and zero state from PWM. Active states are used to control output AC Voltage (DC/AC conversion) using modulation index (M) while ST state is used to control DC link voltage (DC/DC power conversion) though ST duty ratio (D_{st}). However, D_{st} and M had been controlled in independent and dependent way in literature. Where, independent control of D_{st} and M is adopted in this application.

Keeping constant dc-link voltage of Inverter Bridge at the presence of input and output voltage variations is necessary. The dc-link voltage of the ZSI can be controlled in both direct and indirect methods as mentioned in (Yam P. Siwakoti, 2015). In the direct dc-link voltage control method, the voltage across the dc-link (in between Z source network and Inverter Bridge) is measured by special sensing method directly and scaling circuits as in Figure. 2.28 and feeds forward to control DC link constant.

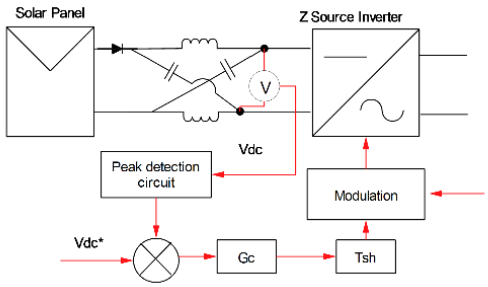

Figure 2.28 Direct DC link control structure of ZSI.

In the indirect method, dc-link voltage is controlled without sensing dc-link voltage directly. Where, the capacitor voltage of impedance network is sensed and compared with the expected value of capacitor voltage or capacitor voltage and input DC voltage of the impedance network is sensed to estimated dc-link voltage as shown in Figure. 2.29 (a) Figure. 2.29 (b) Figure. 2.29 (c).

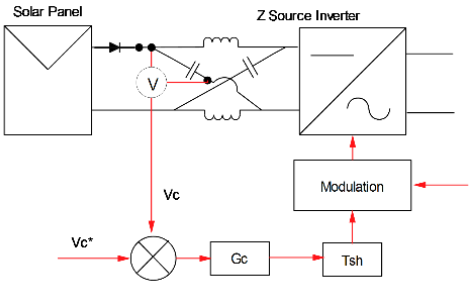

(a).

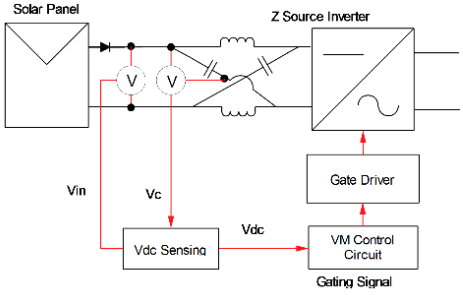

(b)

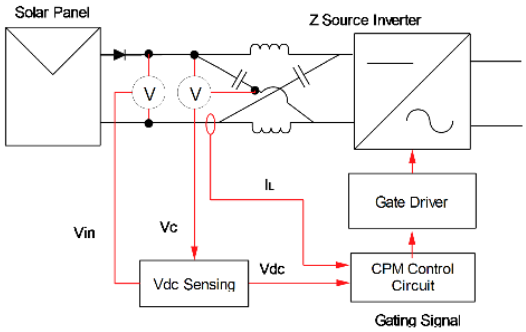

(c)

Figure 2.29 Indirect DC link control method of ZSI

In indirect dc-link control approaches, the peak dc-link voltage is overwhelming, while regulating fast changing input voltages with shoot through duty. It may produce high semiconductor stress and then it increases the THD in the output waveforms. However, for fast changing input voltage it can be controlled by direct control method even though dc link measurement becomes more complex with additional circuitry in hardware implementation. Therefore, direct DC link close

loop control method is adopted in this study to generate reference sinusoidal signal to the inverter.

2.10 Importance of reactive power controlling capability

Residential consumers in most of rural distribution networks who are fed from long distribution feeders have low power demand at day peak and off peak. They experience under voltage conditions during peak time and voltage rise at PCC during day peak and off-peak hours. Therefore, in rural areas with long length feeders are not allowed solar connection because the solar PV connection makes this voltage worse. Voltage control is important for a power system to maintain the power quality of the system and to save the system voltage without collapsing the operation of equipment. Voltage fluctuations may result in overheating of generators and motors, transmission losses, etc. To control voltage at PCC, several methods were proposed in literature. Since the voltage depends on the active and reactive power, the voltage can be controlled by controlling them. (Eiríksson, 2017).

- Voltage control: direct control of voltage by using FACTS.
- Active power control: 1) battery charging batteries, 2) Active power curtailment: disconnect DG when over voltage.

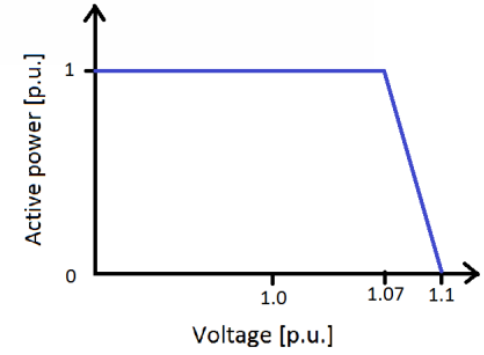

Figure 2.30: Active power curtailment (Eiríksson, 2017).

- Reactive power control: the most common methods proposed to control voltage by DG units are mentioned here. 1) Constant reactive power control, 2) Constant power factor control, 3) Cos Ø (P): change power factor as a function of active power, 4) Cos Ø (U): change power factor as a function of voltage and 5) Q (V): Change reactive power as a function of voltage. Where DG work as STATCOM and possible to control voltage when

nonproducing hours of solar energy. In this research, this reactive power control method was considered for reactive power controlling mode.

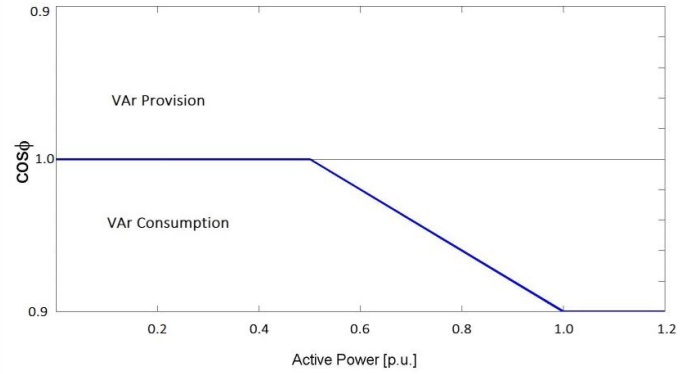

Figure 2.31: Operation of Cos Ø (P) control (Eiríksson, 2017).

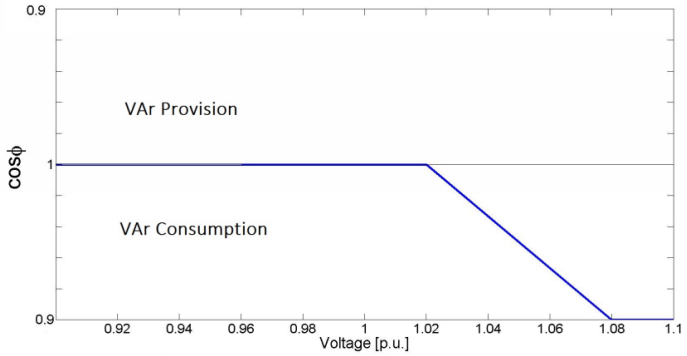

Figure 2.32: Operation of Cos Ø (U) control (Eiríksson, 2017).

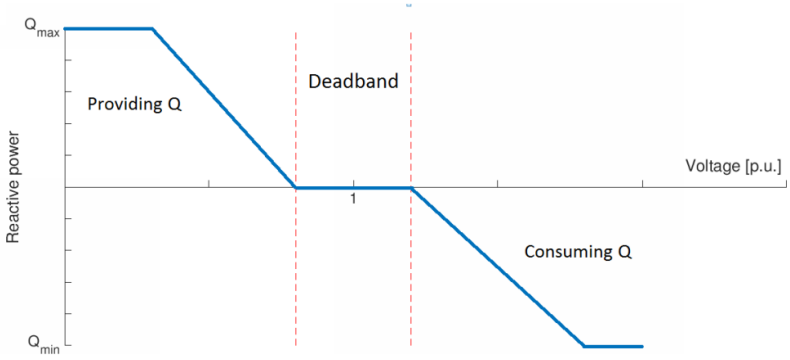

Figure 2.33: Operation of Q (U) control (Eiríksson, 2017).

2.10.1 STATCOM

STATCOM is a power electronic device which is used to control the reactive power flow through a power network and thereby reduce the instability of power network due to reactive power demand and it is a shunt device of FACTS devices family. STATCOM can either absorb or generate reactive power from power network to stabilize the voltage of the power network. If the PCC voltage is lower than the set

minimum limit, the STATCOM generates reactive power (STATCOM capacitive). When PCC voltage is higher than the set maximum limit, it absorbs reactive power (STATCOM inductive).

2.10.2 Working Principle of STATCOM:

The following reactive power transfer equation can be used to understand the working principle of STATCOM. Let's simply represent MG and grid as two voltage sources and consider output voltage of them as V1 and V2 and they are connected through an impedance of $Z = R_a + jX$ as shown in Figure. 2.30 below. Where, resistance R is negligible. Therefore, $Z = jX$ consider the angle between V1 and V2 as δ and reactive and active power flow equation (Eq. 2.2 and Eq. 2.3) can be expressed as follows.

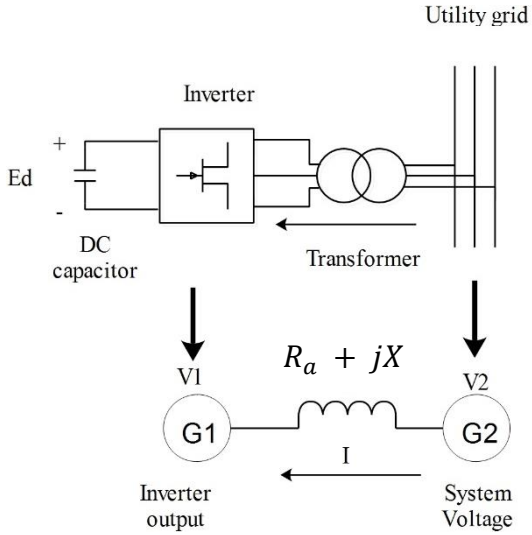

Figure 2.34 Basic structure of MG and utility grid to understand STATCOM working-principle

$$Q = \left(\frac{V_2}{X}\right)(V_1 \cos\delta - V_2) \qquad (2.2)$$

$$P = \frac{V_1 V_2 \sin\delta}{X} \qquad (2.3)$$

The angle δ is maintain 0 with synchronous operation of DSTATCOM with utility grid by using Phase Locked Loop (PLL), then Reactive power flow will become,

$$Q = \left(\frac{V_2}{X}\right)(V_1 - V_2) \qquad (2.4)$$

and active power is,

$$P = \frac{V_1 V_2 \sin\delta}{X} = 0 \qquad (2.5)$$

In summary, when the angle between V_1 and $V_2$is zero, then the active power flow between grid and MG becomes zero and the reactive power flow is contingent on $(V_1 - V_2)$. Therefore, when the MG voltage is greater than grid voltage, reactive power will flow from MG to utility grid and vice versa. Hence, this concept is applied to control reactive power for proposed STATCOM mode.

In voltage control/reactive power control mode, the V-I characteristic is denoted by following equation and Figure. 2.31.

$$V = V_{ref} + X_s I \qquad (2.6)$$

where,

V	Positive sequence voltage (pu)
I	Reactive current (pu/P_{nom}) (I > 0)
$X_s I$	Slope or droop reactance (pu/P_{nom})

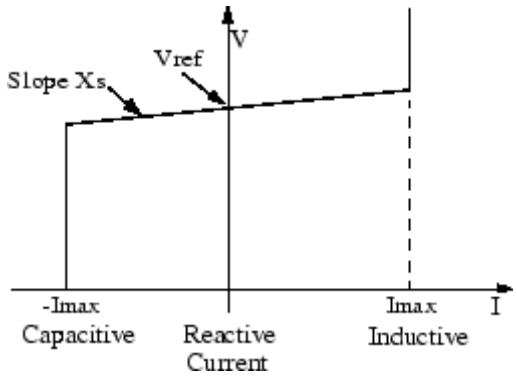

Figure 2.35 Voltage current characteristics of STATCOM

2.11 **Islanding detection**

The disconnection of the Microgrid from utility grid is called islanding, which can be either intentional (Planned) or unintentional (Unintentional). Intentional islanding is the formation of power "island" during utility grid disturbances, such as faults. Undetected island leading to formation of a micro-grid is generally called "unintentional islanding". (Mehdi Hosseinzadeh, 2020).

Intentional islanding is scheduled with the purpose to reduce load when power generation capacity is not enough to meet the forecasted demand or system augmentations or due to the maintenance occurs. Since it is planned and announced islanding situation it reduces undesirable consequences to consumers, DG owners and distribution feeders.

Undetected or unplanned islanding may result in many undesirable consequences. Instability of grid operation, damages to DG units and the converters and other sensitive customer side equipment due to voltages and frequencies out of the allowed limits, unnecessary operation of fuses, over current relays, etc. in which the settings are adjusted for grid connected operation, low quality power supply, safety issues for the workers engaged in the utility side, re-tripping of the system circuit breakers due to the reconnection without synchronization. These are several consequences of unintentional islanding.

The most momentous performance indicators of islanding detection methods are the detection time and non-detection zones (NDZs) (Gerald Cham Kpu, 2019) for a best islanding detection method should have the shortest detection time and should be free of NDZs. NDZs is the operating range of active power (ΔP) and reactive power (ΔQ) deviation between the utility grid and microgrid where the proposed islanding detection methods are not able to detect islanding. Islanding detection control techniques are mainly categorized into two; 1) remote and 2) local techniques.

The remote techniques utilize communication infrastructure between the utility grid and the microgrid and signal processing techniques. These islanding methods have negligible NDZ and high reliability compared to local islanding detection methods. However, cost of implementation is very high due to the extra costs for communication equipment. (Gerald Cham Kpu, 2019).

Local schemes are further classified into active and passive schemes, Hybrid Techniques. (Wei Yee Teoh, 2011)

Active islanding methods can detect islanding when the perfect matching between generation and load is occurred. They are generally created on the concept of perturb

and observe technique. Here, an external signal is injected to create disturbance in the voltage and current waveforms so that to distort the current/voltage waveform, causing a change in its amplitude, phase or frequency. In the grid connected mode, the distortions are absorbed by the utility grid as the PCC voltage and frequency are controlled by the grid. But, when the Microgrid is in islanded mode, effective change is observed in the system that triggers the system protection devices (A.Y. Hatata, 2016) (Gerald Cham Kpu, 2019). Thereby the inverter trips. Active islanding detection methods are more efficient than the local methods and are generally zero NDZs. But they are not fast as some passive methods due to system's reaction time, and it's cost of implementation is higher. (Gerald Cham Kpu, 2019)

Passive islanding detection methods are achieved by observing significant deviations into the system's output parameters such as voltage imbalance, total harmonic distortion of current, unusual change in active power and frequency, change in reactive power, phase jump and vector shift detection, over/under voltage and over/under frequency (OUV/OUF), and the rate of change of frequency (ROCOF). Besides, new research has been carried out using advanced tools like the wavelet transform, decision tree classifier, neural network to control passive islanding. However, these passive islanding methods are easy to implement. But these methods may fail to detect exact islanding condition. Therefore, passive methods have large NDZ.

Hybrid islanding detection methods are implemented by combining active and passive methods to make use of both methods. Here, disturbance is injected only where islanding is probable. Therefore, this method faces less power quality problems compared to active methods. These methods take lower islanding detection time and narrow NDZs. (Gerald Cham Kpu, 2019).

2.12 Islanded mode control methods

2.12.1 Master-slave control

In master slave concept, there are two types of controllers called Master controller and Slave controllers. Apart from master-slave control, all DGs perform the same function, namely when microgrid operates in the islanded mode, each of DGs performs its droop characteristics. Each DGs will rebalance the load variance based

on the drop characteristics during a transient load, and the system automatically achieve a new balancing point. During this process, the microgrid operates continuously without any intermediate reconfiguration when any energy source is disconnected or connected from the MG, thus achieving 'plug and play' feature. Initially, droop control method was used to handle load sharing between multiple DGs in the MG, including primary frequency control. Frequency can be adjusted by controlling real power, and voltage can accordingly be controlled by regulating reactive power appropriately (Zhou Yang, 2016).

2.12.2 Hierarchical control

As the name implies, three control layers, which are primary, secondary and tertiary control layers, are included in this control system. Primary control is essentially at the level of converter control, where the method of P/Q droop is used to share active and reactive power between DGs. The secondary control is used to absorb fluctuations in frequency and voltage formed by the primary control, also ensuring the utility grid synchronization process. Tertiary control is an advanced control layer that takes account of the economic issue and decides when to sell or purchase power from or to the utility grid to control power flow between the MG and the utility grid is also controlled (Zhou Yang, 2016).

2.12.3 Multi-agent system control

Multi-agent system (MAS) is an evolving technology which enables each micro-source or load to be represented as an agent and it can share the information and data for a shared purpose with neighboring agents to cooperate. In fact, MAS control is a type of the peer-to-peer control family and it is a form of decentralized control method. Where, each microgrid agent is independent from utility to an extended limit so that it can make decisions according to its current state without external control. (Zhou Yang, 2016).

3 PROPOSED ARCHITECTURE

3.1 Introduction

The architecture of the SPV microgrid is the main concern of this study. The proposed reconfigurable power architecture of the residential MG is shown in Figure. 3.1 and control architecture is given as in Figure. 3.2. The power architecture consists of 6 major components ZSI based 1) SPV system, 2) ZSI 3) battery energy storage system, 4) DC/DC converter, 5) line filter (for absorbing switching ripple), 6) residential loads (critical and non-critical). The PCC is connected to the utility grid through Power Electronic Switch (PES). Critical and non-critical loads are directly connected to the PCC. ZSI based SPV system is responsible for MPPT, and maintaining power quality at PCC even in nighttime, in addition to the DC/AC power conversion. BESS are utilized to fill the gap between solar production and the demand of residential MG and, voltage and frequency controlling at islanded mode with SPV. PES is set for switching (ON/OFF) of the reconfigurable MG with utility grid, depending on synchronization and islanding signal state (K. A. H. Lakshika, 2020).

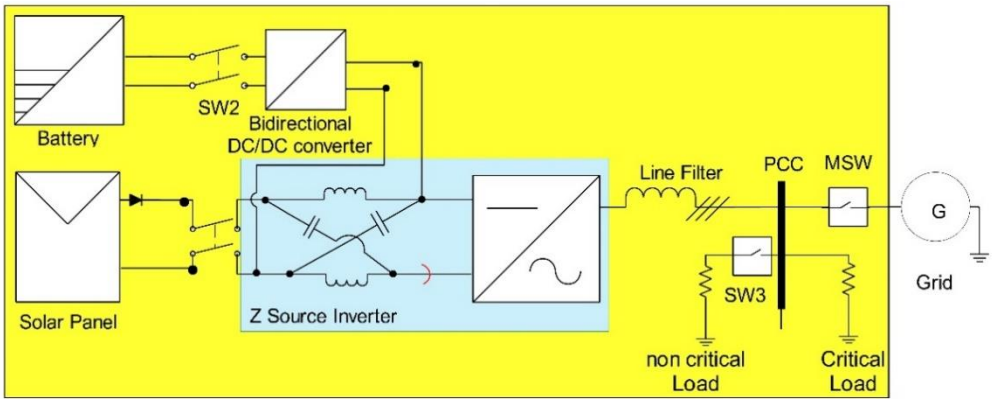

Figure 3.1 Proposed microgrid power architecture.

The novelty of this proposed control architecture is it consists of three different modes of operations with three different control objectives, and it is possible to select the mode of operation according to PCC power quality condition or utility grid request upon customer approval. Where, the residential microgrid play the role of current source or STATCOM during grid connected mode and or voltage source during islanded mode as shown in Figure 3.3.

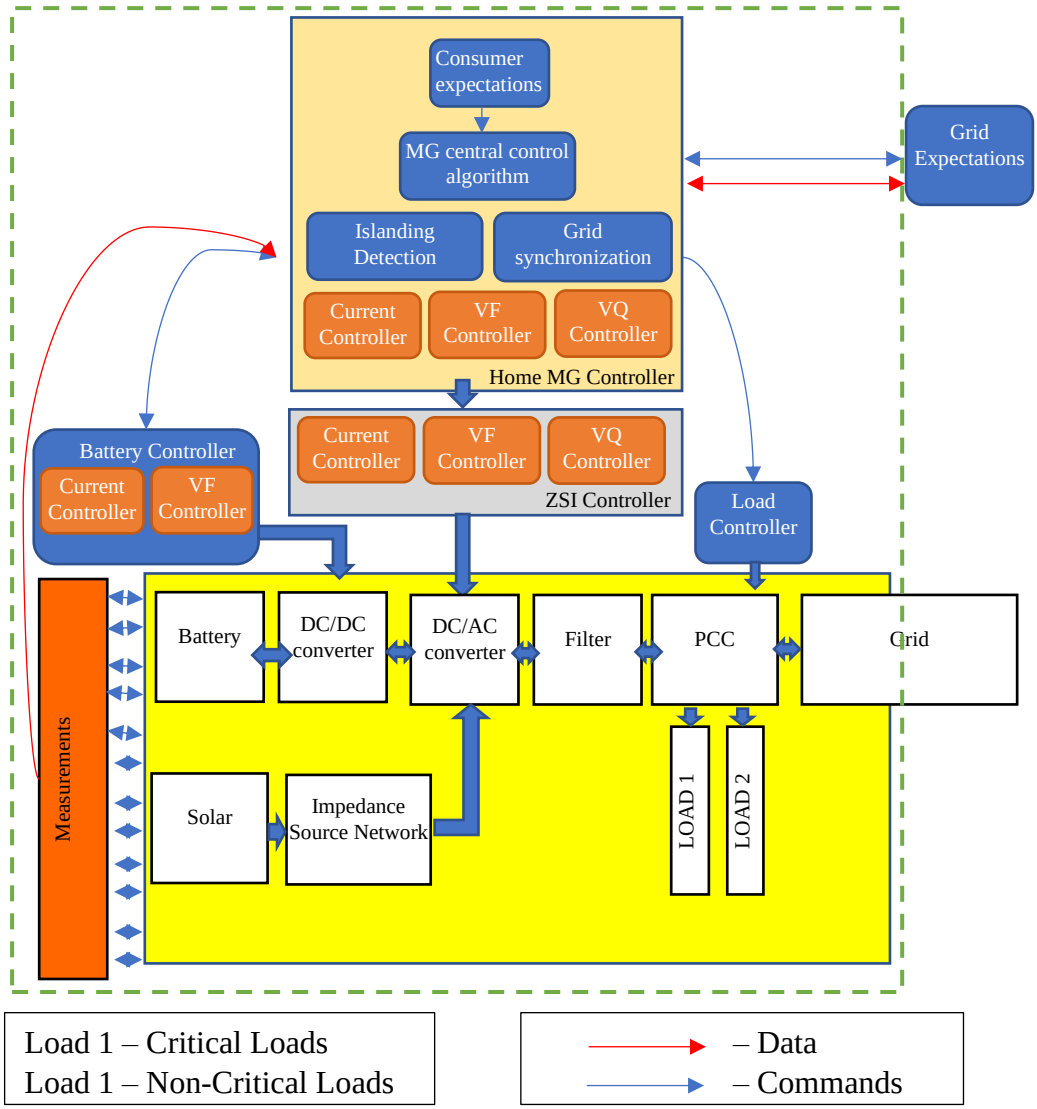

Figure 3.2 Control architecture of proposed residential microgrid

3.2 **Functions**

The algorithm for reconfiguration is explained in Figure. 3.4. The microgrid power architecture of each configuration and power flow regarding each configuration are given in Figure.3.5, Figure.3.6 and Figure.3.7.

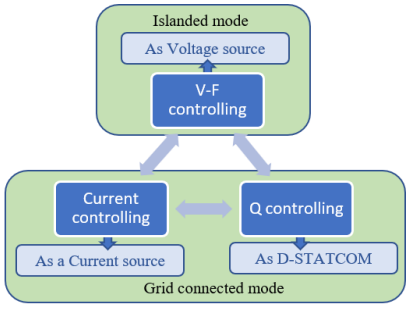

Figure 3.3 States of controlling of SPV system.

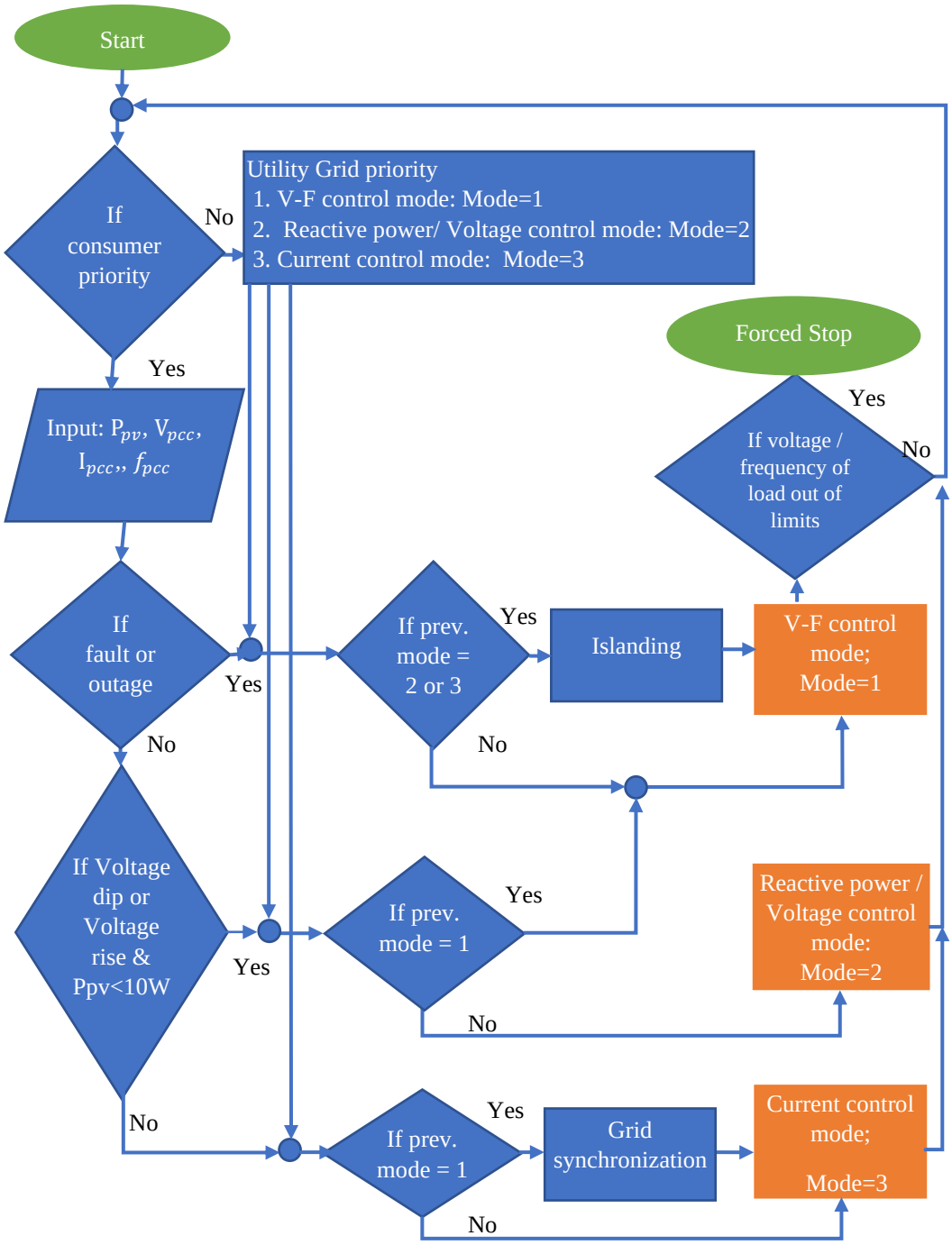

Figure 3.4 Algorithm for reconfiguration

When consumer select grid propriety, utility can select the operation accordingly. As the utility grid perspective, this option is very important during

- Thermal maximum period to reduce cost of oil-based energy generation at peak (Self generation): to keep solar PV microgrid in islanded situation while providing uninterrupted power supply to consumer.
- Blackout states: to keep solar PV microgrid in islanded situation while

providing uninterrupted power supply to consumer until utility grid is restored,

- During voltage rise and drop situation: to use this microgrid as STATCOM to generate and absorb reactive power.

When consumer selects consumer priority, the mode of operation is selected according to above algorithm. The system which is active or inactive, the control objective and function are decided according to each configuration. The main controllable device in the proposed power architecture is ZSI. It plays a major role in the reconfigurable operation of SPV microgrid.

When three phases to ground fault or single phase to ground fault or grid outage is detected, the MG is automatically disconnected from the utility grid itself (through islanding) after confirming the previous mode which is grid connected mode (current control mode or Voltage / reactive power control mode) and inverter controller is changed to Voltage-frequency controlling mode without any interruption to the residential loads. In this case, the customer is able to propose economic dispatch considering utility tariff and value of asset to recover his investment cost and consumer can decide when to island not only at ground fault and utility grid outage. However, in this research, that objective is not focused. Here, the ZSI is controlled to operate the SPV system as a Voltage Source. In this power architecture, utility grid and non-critical loads do not participate in this mode and the operating objective is changed to provide uninterrupted power supply to the critical loads and maintain power quality. Where, the excess solar power is stored in BESS. If the demand of

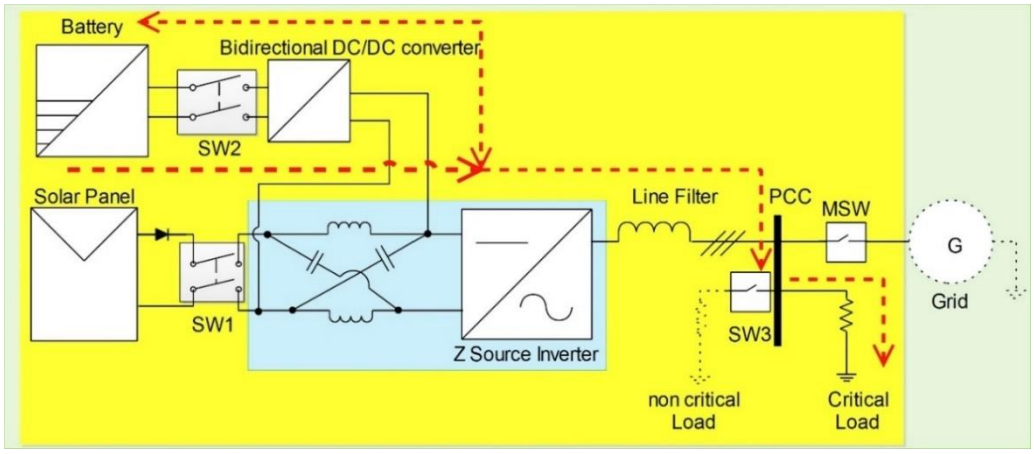

Figure 3.5 Configuration and power flow at the mode of V-F control mode

the MG is higher than the power from battery and solar, non-critical loads are disconnected from the MG. (K. A. H. Lakshika, 2020)

At nighttime when solar generation is not available, the SPV system is idle. During off peak, most of the long distribution feeders in rural distribution networks experience voltage rise due to low load condition. During night peak hours which has higher power demand, the scenario is inverse, and consumers experience voltage dips (K. Kanchanee Navoda, 2017). At this state, the residential microgrid is set to operate as a DSTATCOM to control reactive power after reconfiguration by confirming previous state of mode is not islanded operation, the solar PV generation is zero and voltage rise, or dip is identified. Where, the ZSI provide in reactive power support proportional to voltage limiting to its capacity, as discussed in section 2.10. The operating objective is set to utilize idle resources for supporting utility grid to avoid voltage problems along the distribution feeder by bordering power architecture without solar panels, battery, and DC/DC converter.

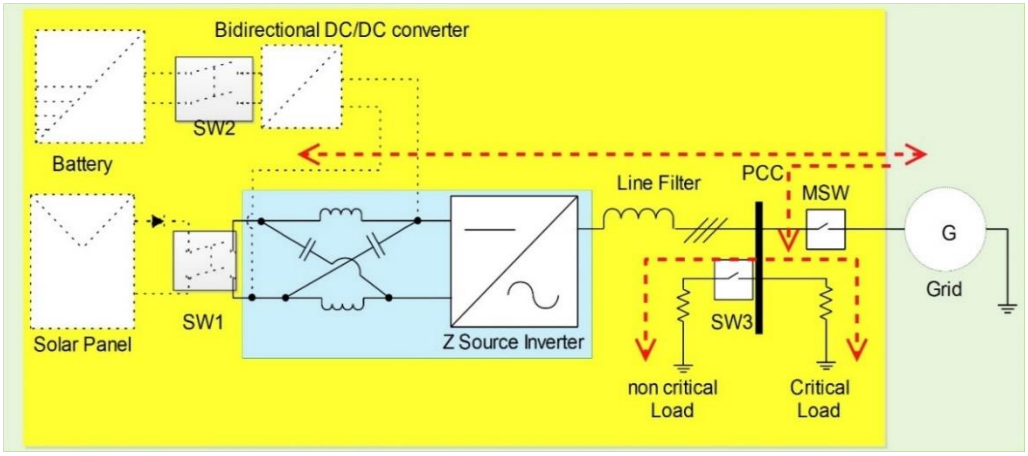

Figure 3.6 Configuration and power flow at the mode of reactive power control mode

For normal operation without ground fault or grid outage or PCC not experiencing voltage dip or rise, the residential MG is operated as a grid connected microgrid after checking previous state of mode and the inverter controller is operated in Current Controlling Mode. If the previous mode is V-F controlling mode, synchronizing should happen with utility grid. Here, the ZSI is controlled to operate the SPV system as a Current Source to feed the microgrid. When the previous state of mode is islanded situation (V-F control mode), the MG has to wait for grid synchronization to connect to the grid otherwise, it can operate current controlling

mode directly. In this power architecture, all components are utilized and the operating objective is changed to extract and maximum power from SPV. The battery and the utility grid provide the shortage of power demand to the residential loads if excess power generation from SPV, BESS is stored, and the rest of power is transferred to the utility grid.

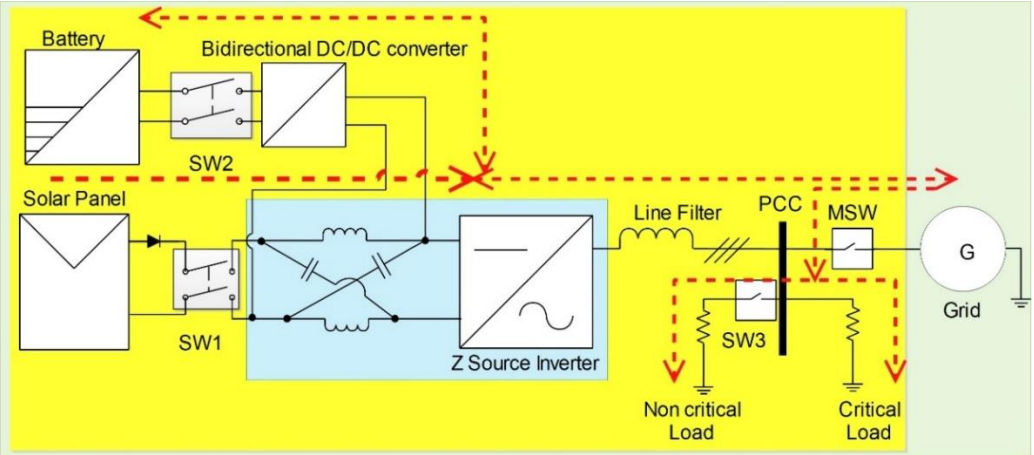

Figure 3.7 Configuration and power flow at the mode of current control mode

According to the IEEE standard 1547, operational limits during current control mode and V-f control mode are given in Table 3.1.

Table 3.1 IEEE standard 1547: Operational limits

Feature	Limitation
Maximum output voltage	±6% of the nominal grid voltage
Frequency range	± 1% of the nominal frequency
Total harmonic distortion	THD < 5

Following figures (Figure. 3.8 and Figure. 3.9) describe the voltage and current limits to decide reconfiguration limits to select operating modes.

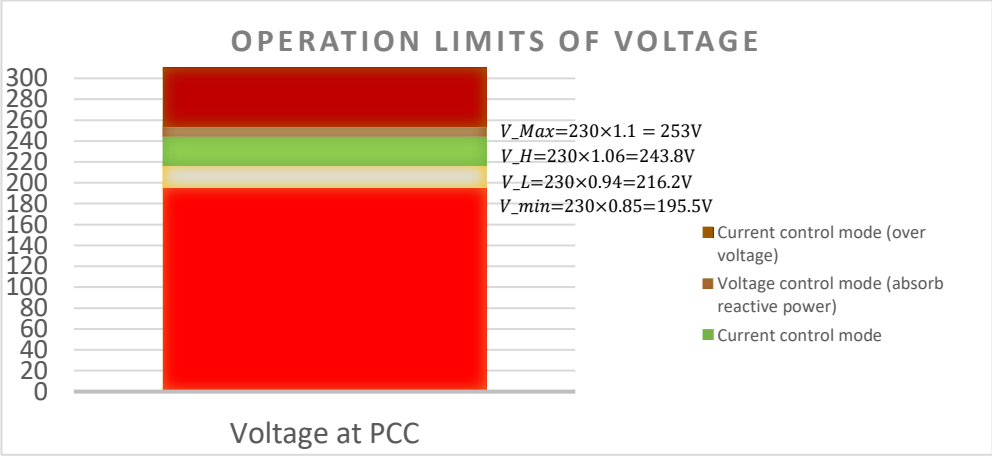

Figure 3.8 Voltage limits of reconfiguration

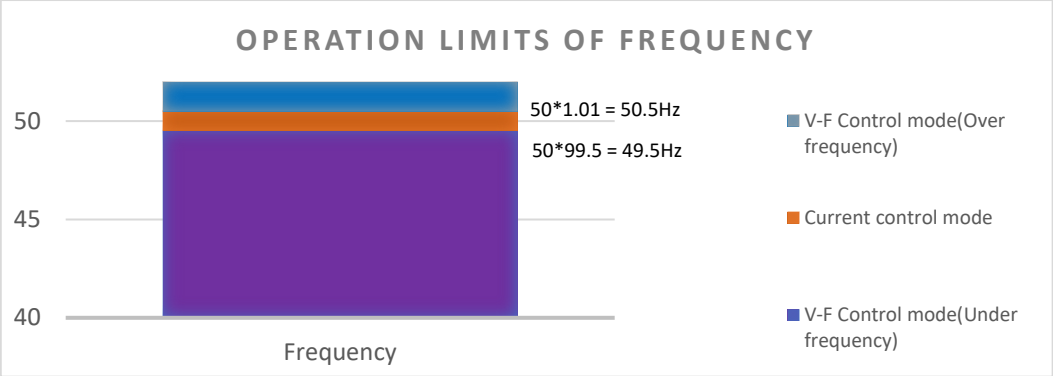

Figure 3.9 Frequency limits of reconfiguration

According to the three different control modes, the microgrid components has specific task and state to operate and they are given in Table 3.2.

Table 3.2 The state of MG components in each mode of operation

Components	**Grid connected microgrid**	**STATCOM @ off peak (night)**		**Islanded microgrid**	
		Voltage drop	voltage rise	Enough Solar	Not enough Solar
Microgrid	Grid connected	Grid connected		Islanded	
SPV	Generate maximum power	Disconnected		Generate maximum power	
ZSI	• 2nd order filter • MPPT • DC/AC conversion	STATCOM (Reactive power generation @ Voltage drop)	STATCOM (Reactive power consumption)	• 2nd order filter • MPPT • DC/AC conversion	
		Active power consumes for switching losses and Capacitor charging			
ZSI controller	Current controlling	Reactive power controlling		Voltage-frequency controlling	
Battery	Energy storage /Energy source	Disconnected		Energy storage	Source
Battery controller	Charging /Discharging	Disconnected		Charging	Discharging
Filter	Filtering	Filtering		Filtering	
Critical loads	Connected to the MG	Connected to the MG		Connected to the MG	
Noncritical loads	Connected to the MG	Connected to the MG		Disconnected	
Grid	Load/ Source	Source	Sink	Disconnected	

3.3 Benefits from this architecture

Consumer benefits

- At unexpected grid failure, the MG reconfigure itself in to islanded to supply power for critical loads for residentials.
- Possible maximum power generation is obtained from SPV system whenever solar power is available.
- Since ZSI is a main component, it improves inverter efficiency and lifetime of inverter (enabling shoot through).

Utility benefits

- Since ZSI is a main component, it improves the power quality (voltage distortions elimination) of the grid.
- Reactive power control mode is utilized to improve voltage profile at nighttime (Peak and off peak) and it provides benefits to utility by reducing cost for installing expensive capacity banks for utility.

Benefits to both parties

- It provides a fault-tolerant MG architecture with increasing reliability and controllability without introducing any significant severance to the MG.
- Capability of controlling Reactive power, increased grid stability and value addition to existing SPV system during non-production hours.

4 DESIGN AND MODELLING OF PROPOSED ZSI BASED RECONFIGURABLE, PV MG

Each of the five components is mathematically modelled and designed to operate in previously explained modes of operations and they are discussing as follows.

4.1 Solar panels

As discussed in Chapter 1, the solar cell is represented using 5 parameter model and it is described in Figure. 4.1. (Villalva et al.; 2009). When the current of current source; I_{ph} denotes the current produced by the occurrence of light. Non-ideal diode denotes the p-n junction of the PV cell. In practical conditions, resistive losses are considered, and it is represented by R_s and R_p.

The characteristic equation is developed, and the mathematical model is developed as follows. (Villalva, 2009)

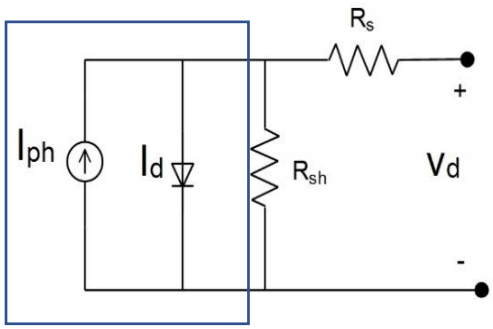

Resistive losses Rs and Rsh

Figure 4.1 Five parameter model of SPV cell

The light-generated current, which is known as photocurrent, is denoted as I_{ph} , the diode current as I_d, parallel resister current $I_p$and the net current and terminal voltage of solar cell as I_{cell} and Vcell, respectively.

$$I_{pv} = I_{ph} - I_d - I_p \quad (4.1)$$

$$I_{ph} = \frac{(I_{pn,n} + K_I \Delta T)}{1000} G \quad (4.2)$$

Where, $I_{pn,n}$ is the light-generated current at the standard conditions (25 ◦C and 1000W/m2), $\Delta T = T - T_n$, (being T and T_n the actual and nominal temperatures [K]), $K_I$is the temperature coefficient, G [W/m2] is the irradiation on the device surface,

$$I_d = I_o \left[\exp\left(\frac{qV_d}{nkT_{cell}}\right) - 1\right] \qquad (4.3)$$

Where, V_d: voltage across the diode, I_o : reverse saturation current of the diode, q = 1.602 × 10^{19}: electron charge, T_{cell}: cell temperature in Kelvin, n: diode ideality factor and k = 1.38065 × 10^{23} J/K: Boltzmann constant. The reciprocal term of (q/nkT_{cell}) is called the thermal voltage of the diode.

Therefore, the thermal voltage of the diode is:

$$V_T = \frac{nkT_{cell}}{q} \qquad (4.4)$$

$$I_p = \frac{(V_{cell} + I_{cell}R_s)}{R_p} \qquad (4.5)$$

$$I_{pv} = \frac{(\mathrm{I}_{pn,n} + K_I\Delta\mathrm{T})}{1000} G - I_o \left[\exp\left(\frac{V_{pv}+I_{pv}R_s}{V_T}\right) - 1\right] - \frac{(V_{pv}+ I_{pv}R_s)}{R_p} \qquad (4.6)$$

4.1.1 I-V characteristics

For PV array, the five-parameter model can be represented as in Figure. 4.2

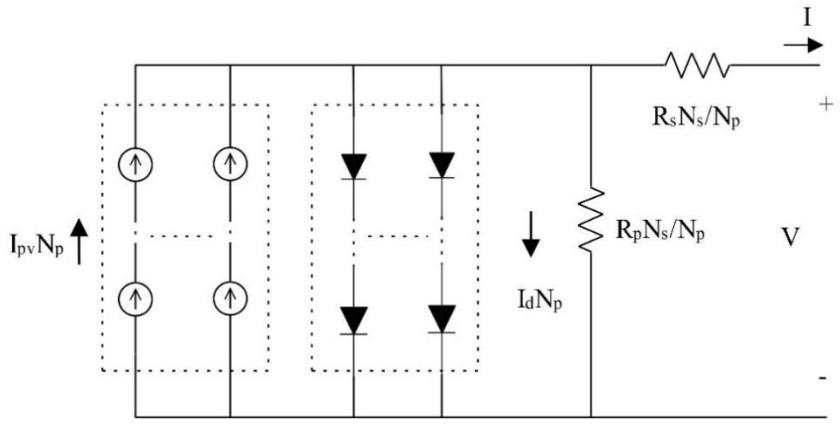

Figure 4.2 PV array represent in 5 parameter model

I -V characteristics of the PV array is described as follows,

$$[N_p \times N_s]I_{pv} = N_p \left\{\frac{(\mathrm{I}_{pn,n} + K_I\Delta\mathrm{T})}{1000} G - I_o \left[\exp\left(\frac{V_{pv}+I_{pv}R_s\left(\frac{N_s}{N_p}\right)}{N_s V_T}\right) - 1\right] - \frac{\left(\mathrm{Vpv} + I_{pv}\mathrm{Rs}\left(\frac{N_s}{N_p}\right)\right)}{\mathrm{Rp}\left(\frac{N_s}{N_p}\right)}\right\} \qquad (4.7)$$

4.1.2 P-V characteristics

P-V characteristics of the SPV array is described as follows,

$$P = V_{cell} \times I_{cell} = V_{cell}\left\{I_L - I_o\left[\exp\left(\frac{V_{cell}+I_{cell}R_s}{V_T}\right) - 1\right] - \frac{(\text{Vcell} + I_{cell}\text{Rs})}{\text{Rp}}\right\} \quad (4.8)$$

The mathematical model of the PV generator is developed according to above equations in MATLAB/Simulink and it is simulated under the irradiation of 1000 W/m2 at 25^0C which is the standard test condition (STC) and irradiation of 600 W/m2 at 25^0C. The parameters of MATLAB SPV block which is pre-set PV modules available from NREL System Advisor Model (Jan. 2014), are used to model the PV generator accurately as follows;

Tina Solar TSM-170D module parameters

- Maximum Power (W) = 170.4W
- Open circuit voltage: V_{oc} (V) = 43.6V
- Short-circuit current; I_{sc} (A) = 3.56A
- Shunt resistance R_p (ohms) = 145.757 ohm
- Series resistance R_s (ohms) = 0.49129ohm
- Light-generated current at 1000W/m2, $I_{pn,n}$ (A) = 4.24A
- Diode Ideality factor = 0.98
- Diode saturation current, I_o = 1.889e-10A
- Temperature coefficient, K_I = 0.042

The considered mathematical model for the simulation and its performances are given in Figure.4.3, and Figure.4.4.

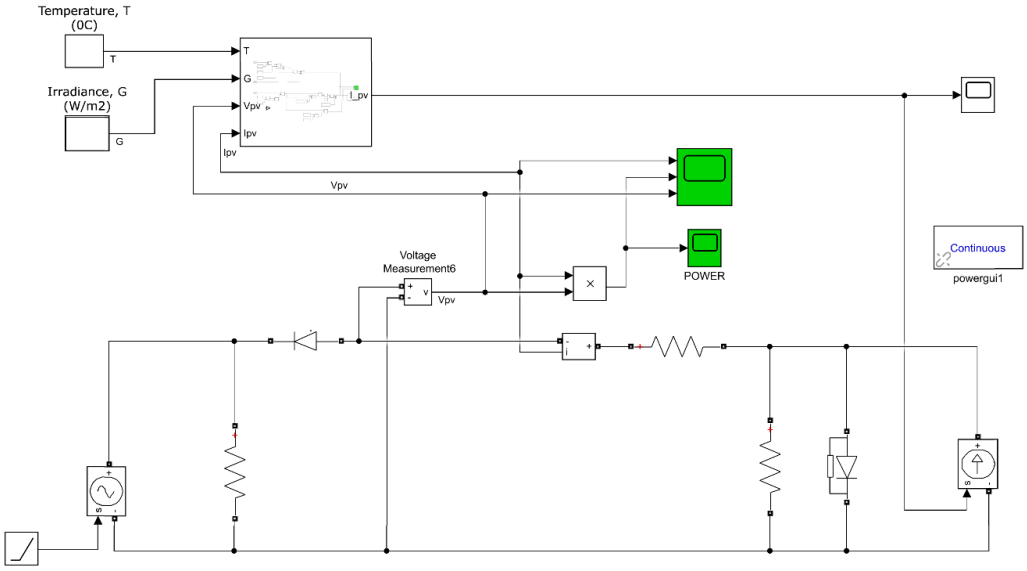

Figure 4.3 MATLAB/Simulink model of PV array

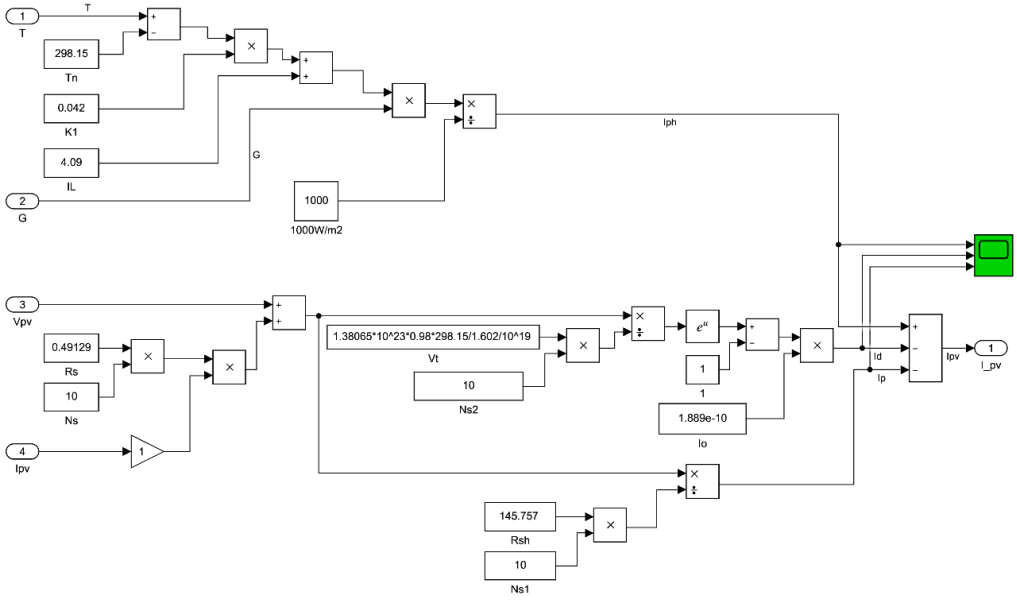

Figure 4.4 MATLAB/Simulink model to generate Ipv considering PV array temperature and irradiance

The I-V and P-V characteristics of SPV solar array model for different solar irradiance the is illustrated in Figure.4.5, and Figure.4.6.

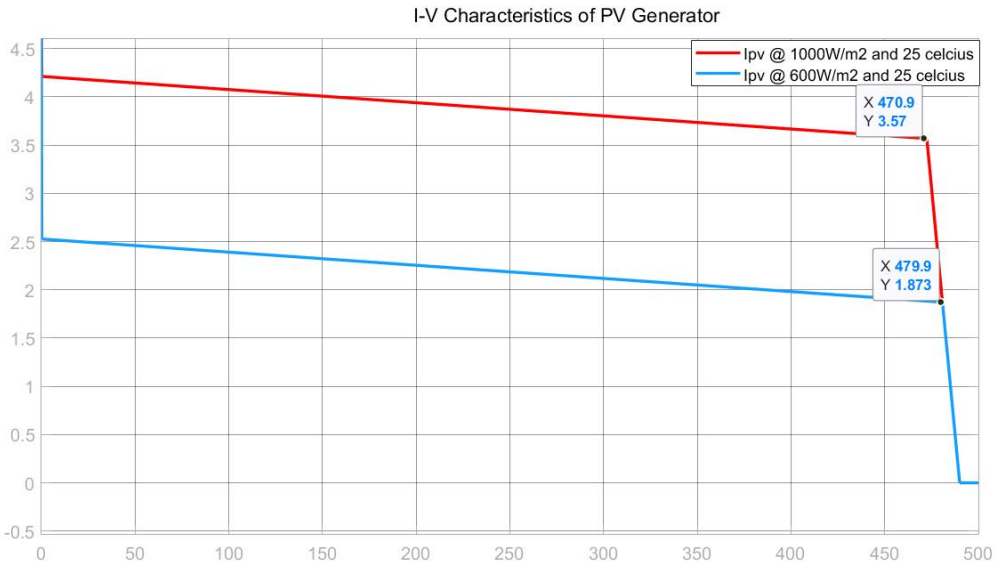

Figure 4.5 I-V Characteristics of PV array

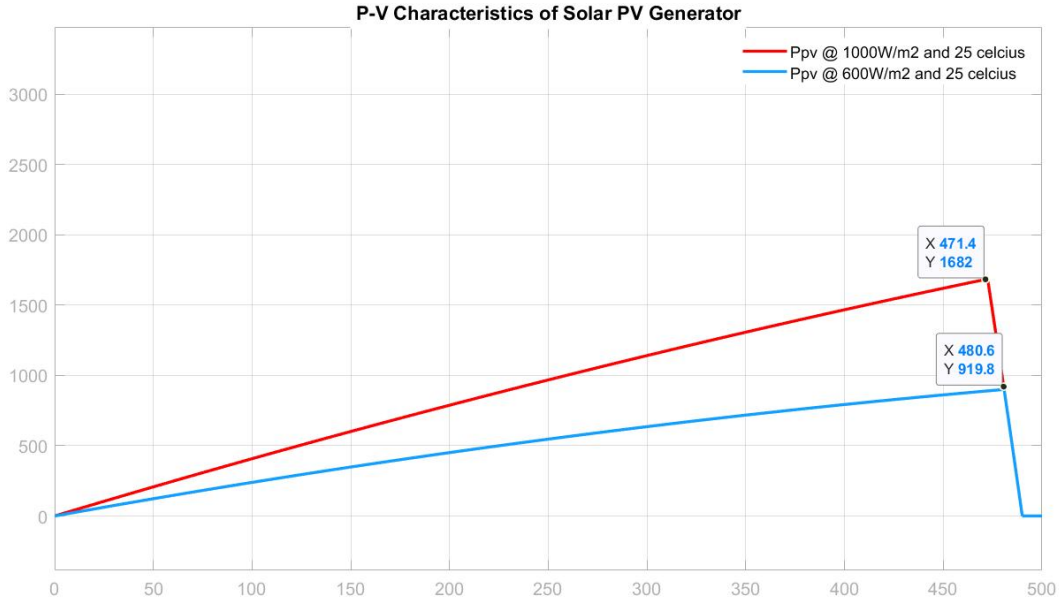

Figure 4.6 P-V Characteristics of PV array

- at 1000W/m2 irradiance, $Vmpp$ = 471V, $Impp$= 3.56A and $Pmpp$= 1,676W
- at 600W/m2 irradiance, $Vmpp$= 479V, $Impp$= 1.87A and $Pmpp$= 919W

The solar irradiation increase will result the increase of SPV cell current and maximum power and reduce Maximum Power Point (MPP) voltage. The I-V characteristics curve in Figure.4.7 clearly shows that the SPV panels are significantly different from P-V characteristics from a voltage sources, such as a battery or current source. However, it shows characteristics of both voltage source and current source

dependent to its operating point. Below the MPP voltage, the SPV cell behaves as a current source, the beyond the MPP voltage, it behaves as a voltage source and at MPP, it behaves as a constant power source.

4.2 Z source inverter

Design and parameter estimation of ZSI is carried out according to (M. Hanif, 2011). Since, same inductance and same capacitance are selected for split-inductor (two inductors, L1, L2) and two capacitors (C1, C2) where (L1= L2= L and C1 = C2 = C), respectively.

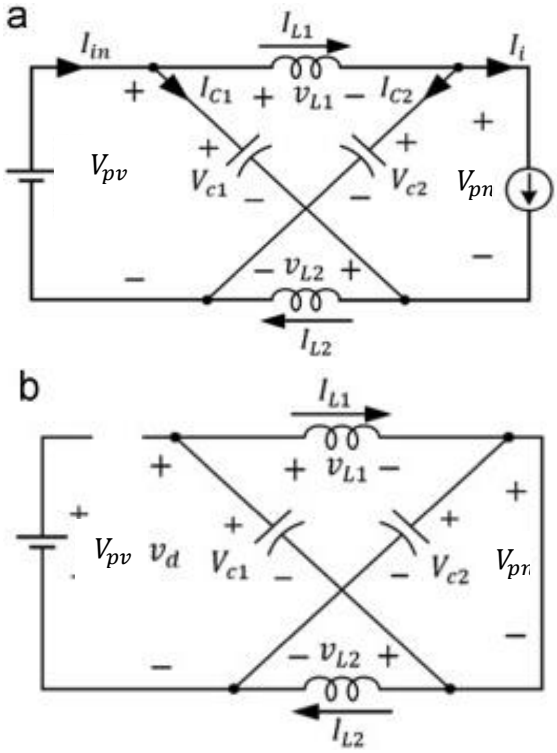

Figure 4.7 Z Source inverter circuit (a) during non-shoot through period, (b) non shoot through period

Considering voltages of ZSI as

$V_{L1} = V_{L2} = V_L$ (4.9)

$V_{C1} = V_{C2} = V_C$ (4.8)

During ST time (T_0 time interval)

$V_L = V_C$ (4.10)

$Vd = 2V_C$ (4.11)

$V_{PV} = 0$ (4.12)

Where, V_{PV} is PV output voltage, and V_{PN} is the inverter DC-link voltage (as given in Figure. 4.7 (a) and Figure. 4.7 (b).

During Shoot through and Non-Shoot through states (non-ST, T_1 time interval)

$V_L \neq V_C$, (4.13)

$V_D = V_{PV} = V_L + V_C$ (4.14)

$V_L = V_{PV} - V_C = V_C - V_{pn}$ (4.15)

$V_{pn} = V_c - V_L = 2V_c - V_{pv}$ (4.16)

Over a switching period T, the average voltage across $V_{L1} = 0$;

$\overline{V_L} = V_c * T_0 + (V_{pv} - V_c) * T_1 = 0$

$\frac{V_c}{V_{pv}} = \frac{T_1}{T_1 - T_0}$ (4.17)

Average DC-link voltage of ZSI,

$\overline{V_{pn}} = \frac{T_0 \times 0 + T_1(2V_c - V_{pv})}{T} = \frac{T_1(2V_c - V_{pv})}{T} = \frac{T_1}{T_1 - T_0} V_{pv}$

From (4.17)

$\overline{V_{pn}} = \frac{T_1}{T_1 - T_0} V_{pv} = V_c$ (4.18)

Peak DC-link voltage during T_0,

$\hat{V}_{pn} = V_c - V_L = 2V_c - V_{pv}$ (4.19)

Substituting V_c from (4.17) into (4.18),

$\hat{V}_{pn} = \frac{T}{T_1 - T_0} V_{pv} = B\, V_{pv}$ (4.20)

The boosting factor (B)

$B = \frac{T}{T_1 - T_0} = \frac{1}{1 - \frac{2T_0}{T}} \geq 1$ (4.21)

Since, $(T = T_1 + T_0)$,

The AC output peak phase voltage from the ZSI is,

$$\hat{V}_{AC} = V_{rms,grid} \times \sqrt{2} = \frac{MBV_{pv}}{2} \qquad (4.22)$$

M; modulation index (M ≤ 1)

Assume M=0.9 and considering three phase 230V/400V, 50Hz distribution system and solar panel data and equation 4.22,

$$B = \frac{2 \times V_{rms,grid} \times \sqrt{2}}{MV_{pv}}$$

$$= \frac{2 \times \sqrt{2} \times 230}{0.9 \times 471}$$

$$= 1.535$$

By picking the suitable buck–boost factor $B_B = MB$ (0 to infinity) the AC output voltage can be stepped up or down.

From (4.21)

$$B = \frac{1}{1 - \frac{2T_0}{T}} = \frac{1}{1 - 2D_{ST}}$$

$$D_{ST} = \frac{B - 1}{2B}$$

$$D_{ST} = \frac{1.535 - 1}{2 \times 1.535}$$

$$= 0.174$$

Capacitor voltage (V_c)

From (4.17) we have

$$V_c = \frac{T_1}{T_1 - T_0} V_{pv} = \frac{T_1}{T} \frac{T}{T_1 - T_0} V_{pv} = \frac{1 - \left(\frac{T_0}{T}\right)}{1 - \left(\frac{2T_0}{T}\right)} V_{pv} \qquad (4.23)$$

From (4.21),

$$\frac{T_0}{T} = \frac{B-1}{2B} \qquad (4.24a)$$

Therefore,

$$1 - \frac{T_0}{T} = \frac{B+1}{2B} \qquad (4.24b)$$

Substituting (4.21) and (4.24b) into (2.23), the capacitor voltage,

$$V_c = \frac{1 - \left(\frac{T_0}{T}\right)}{1 - \left(\frac{2T_0}{T}\right)} V_{pv}$$

$= \frac{B+1}{2B} \times B \times V_{pv}$

$$V_c = \frac{B+1}{2} V_{pv} \qquad (4.25)$$

Considering calculated boost factor

$$V_c = \frac{1.535 + 1}{2} 471$$
$$= 559.69V$$

Substituting (4.25) into (4.20) the peak DC-link voltage during non-ST,

$$\hat{V}_{pn} = B \times V_{pv} = \frac{1}{1-\frac{2T_0}{T}} V_{pv} = B \frac{2V_c}{B+1} = \frac{2B}{B+1} V_c \qquad (4.26)$$

Considering calculated boost factor;

$$\hat{V}_{pn} = \frac{2 \times 1.535}{1.535 + 1} \times 5596.9$$
$$= 674.1V$$

4.2.1 Z-network component design

4.2.1.1 Inductor sizing

During no-shoot through state, the input voltage is applied across the capacitor. But no voltage is applied across the inductor as only a pure DC current flows through an inductor. During shoot through operation, the duty of the inductor is to limit the current ripple through switches. During ST, the DC current passes through inductor and the voltage across the inductors are the same as the voltage across the capacitors. During non-ST mode the voltage across the inductors are the difference between the SPV input voltage and the capacitor voltage. The average current through inductors is derived as follows,

$$\overline{I_L} = \frac{P}{V_{pv}} \qquad (4.27)$$

Considering solar panel capacities,

$$\overline{I_L} = \frac{1678}{471}$$
$$= 3.56A$$

Where, P: total power through impedance source network,

V_{pv}: SPV string output voltage

Since the maximum current ripple through the inductors is happen during shoot through state, the peak-to-peak current ripple ($I_{\mathrm{pk-pk}}$) of the inductors should be calculated. Where, 10% (20% of $I_{\mathrm{pk-pk}}$) of current ripple is chosen for the inductor sizing.

The maximum inductor current,

$$\widehat{I_L} = \overline{I_L} + 10\%\overline{I_L}$$

The minimum inductor current,

$$\check{I_L} = \overline{I_L} - 10\%\overline{I_L}$$

Where $\Delta I = \widehat{I_L} - \check{I_L}$,

$$\Delta I = 0.2 \times \overline{I_L}$$

$$\Delta I = 2.136A$$

$T_0$is the ST period per switching cycle,

$$T = \frac{1}{F, Switching\ frequency}$$

For the design, switching frequency is 5000Hz,

$$T = \frac{1}{5000}s$$

During ST, $V_L = V_c = V$

$V = \frac{V_{unboosted} + V_{boosted}}{2}$ (4.28)

$$= \frac{1.535 + 1}{2}471$$

$$= 559.69V$$

Then, the inductor size can be calculated as,

$L = \frac{V \times T_0}{\Delta I}$ (4.28)

Therefore, inductors of the ZSI of this research is,

$$\mathrm{L} = \frac{559.69 \times 0.174 \times 2}{3.56 \times 0.2 \times 5000}$$

$$= 54.7mH$$

4.2.1.2 Capacitor sizing

Capacitors in the ZSI compensates the current ripple and they give a steady voltage to generate sinusoidal voltage at AC output. Inductors are charged by the capacitors during ST state. Where,

$$I_L = I_c$$

To limit capacitor voltage ripple to around 6% during peak power the capacitor size is roughly calculated using following equation.

$$C = \frac{\bar{I_L} T_0}{\Delta V_c} \qquad (4.29)$$

The capacitor size for this application is,

$$C = \frac{3.56 \times 0.174 \times 2}{5000 \times 559.69 \times 0.12}$$

$$= 3.689uF$$

Where, $\Delta V_c = V \times \pm 6\%$

4.2.2 ZSI as STATCOM

According to (Maknouninejad, Kutkut, Batarseh, & Qu, 2011), operation of STATCOM mode of grid connected Solar PV systems was discussed. Referring to that, the capability of operating in STSTCOM mode by ZSI was verified by matching both equivalent circuits of solar conventional VSC and ZSI, and described a following Figure. 4.8.

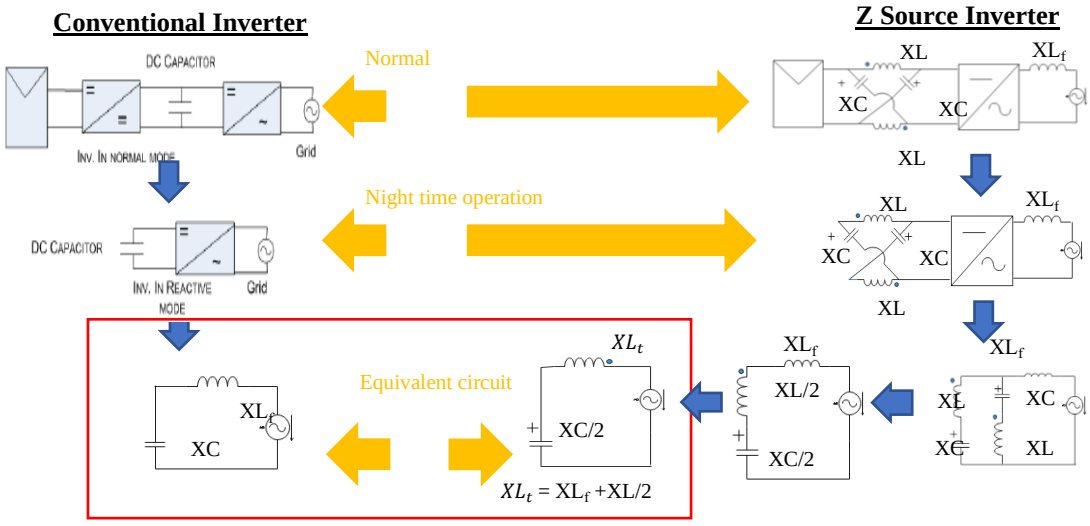

Figure 4.8 Capability of operating in STATCOM mode through equivalent circuits of solar conventional VSC and ZSI

STATCOM generally consists of VSC, DC Capacitor or energy source, Harmonic Filter. In this case, inverter has additional impedance source network at DC side to create VSI as we use ZSI. The impedance source network consists of two capacitors and split inductors and they act as voltage source and current source to VSC to generate reactive power and absorb reactive power accordingly. When the VSC is used to for DC/AC voltage conversion, the Harmonic Filter is used to diminish harmonics and other high frequency components that produce from VSC.

Considering above basic theories and based on past researches (Ruban Preet Kaur, 2014), ZSI based STATCOM is developed as a solution of reactive power requirement in distribution network. Since the usage of STATCOM is for distribution network, it is called as D-STATCOM.

Having X shaped impedance network comprising split inductors and two capacitors on the DC side of ZSI, it can act as both current source type and voltage source type inverter to behave characteristics of D-STSTCOM at PCC of this MG. The power electronic switches used here are IGBT which are a combination of IGBT and antiparallel diode. As mentioned in above chapters, the ZSI is capable of single stage power conversion by boosting low voltage to specific high voltage. The main feature of ZSI is that it reduces harmonic due to reducing dead zone and improve power quality at PCC. Hence, ZSI based D-STATCOM performs better in reactive power controlling in addition to the ripple reducing, enabling ST state. A simplified diagram and equivalent electrical circuit of ZSI based STATCOM is shown in figure below.

Since the inverter was designed to cater 1680MVA of SPV system, inverter can deliver this full capacity as reactive power capacity to control reactive power after reducing active power losses in power conversion and DC link regulation $S = \sqrt{P^2 + Q^2}$. Assuming this ZSI shows 98% efficiency and Considering Eq. X, the maximum controllable voltage range is,

$$(V_1 - V_2) = Q\left(\frac{X}{V_2}\right) \qquad (4.30)$$

For this application,

$$(V_1 - V_2) = 1680\left(\frac{2 * pi * 50 * 0.01}{230}\right) = 22.94V$$

Therefore,

$$V_{1\_Max} = 230V + 22.94V = 252.94V$$

$$V_{1\_min} = 230V - 22.94V = 208.06V$$

At the maximum reactive power output, the voltage droop is generally maintained within 1- 4%. The voltage will be regulated at the reference voltage as the reactive currents is within the constraints introduced by the converter ratings.

4.3 Battery storage system

Considering the facts mentioned in literature, Li-Ion battery is selected for the research and for the selection of battery capacity, considered energy efficiency is 85% and the DOD (Depth of Discharge) is 80% (Solar, n.d.). The capacity of the battery storage system is calculated as follows (Leonics, n.d.), When backup power is needed for 24hrs of autonomy for 1kW of critical load. The proposed battery backup arrangement is given in Figure. 4.9.

∴ Energy Stored by Battery

$$= \frac{Power\ requirnment \times required\ time\ of\ back\ up\ power}{Energy\ Efficiency} \quad (4.31)$$

$$= \frac{1000 \times 24}{0.8}$$

$$= 30kWhr$$

$$\therefore \text{Battery capacity} = \frac{\text{Energy Stored by Battery}}{DOD\% \times Battery\ voltage} \quad (4.32)$$

$$= \frac{30}{0.85 \times 96}$$

$$= 735Ahr$$

Battery backup arrangement;

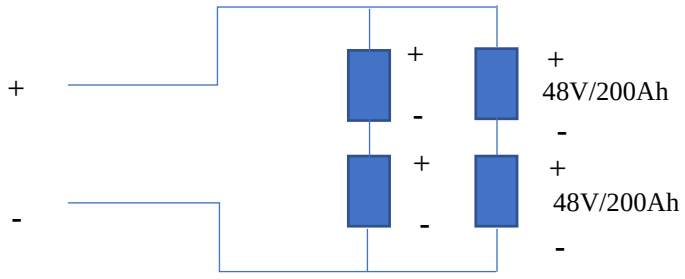

Figure 4.9 The proposed battery backup arrangement

4.4 DC-DC converter

The battery controller is used to control the power flow in between PV system, batteries and loads according to MG status such as acceptable state of charge (SoC) of the battery, charging and discharging current and the DC input voltage for the battery controller. (Hansen, Sørensen, Hansen, & Bindner, 2001)

When ZSI is implemented which is not like conventional inverters. Therefore, we cannot just connect the battery system across the DC-Link like conventional inverters as the DC link is participation the Shoot through operation, we have to connect a battery across the capacitor which maintains a stable voltage. Hence, Capacitor voltage is the reference voltage which gives information to active charge function or discharge function, in addition to SOC and the discharge and charge current. (Shaw, 2015):

Bidirectional DC/DC converters can power flow in both the directions. Basically, there are two types of bidirectional DC/DC converters which are 1) Non-isolated bidirectional DC/DC converters, 2) Isolated bidirectional DC/DC converters. The non-isolated converter is used as they are common and avoid additional cost and losses due to isolation transformer.

Out of other non-isolation dc/dc converters, the half-bridge converter has several advantages such as higher energy efficiency, lower switching and conduction losses and the topology requires minimal storage elements and two switching devices and the structure is given in Figure.4.10. It reduces cost and space. With the objective of minimizing the cost, weight, volume and having a reliable system, a simple half-bridge topology is selected for the MG. (Ung, 2011).The mode of charging or discharging decides the operation of Q1 and Q2 switches and battery controller is developed to meet the those switching signals. The design calculations are as follows;

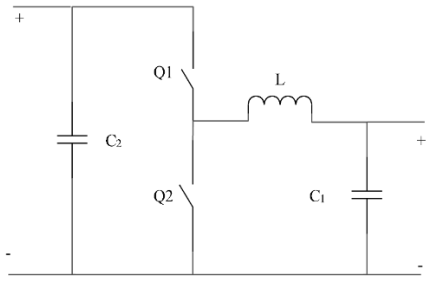

Figure 4.10 Half bridge buck-boost converter

The input and output voltages of this configuration are related through,

$$\frac{V_{out}}{V_{in}} = \frac{-t_{on}}{t_{off}} = \frac{-d}{1-d} \qquad (4.33)$$

According to the design parameters, the following calculations were made.

- The low side or Battery side voltage: 96V
- The high side or ZSI side voltage: 690V
- Switching Frequency and Period:

$f_{sw} = 5000Hz \quad T_s = \frac{1}{5000} = 0.2ms$

- Maximum load current $\frac{I_{o\,max}000}{96} = 10.4A$
- The minimum current in I_{com} at 10% of load current = $10.4 \times 0.1 = 1.04A$
- The output ripple voltage = $\Delta V = 1\% \times V = 690 \times 0.01 = 6.9V$

Boost Calculations:

$$D_{boost} = 1 - \frac{V_{in}}{V_{out}} \qquad (4.34)$$

$$= 1 - \frac{96}{690} = 0.86$$

Critical Inductance;

$$L = \frac{D\,(1-D)^2}{2f_{sw}}\,\frac{V_0}{I_{com}} \qquad (4.35)$$

$$= \frac{0.86\,(1-0.86)^2}{2 \times 5000}\,\frac{690}{1.04}$$

$$= 1.11mH$$

Output Capacitance;

$$C_2 = \frac{DI}{f_{sw}V_0} \qquad (4.36)$$

$$C_2 = \frac{0.86 \times 1.04}{5000 \times 6.9} = 0.25\mu F$$

Buck Calculations:

$$t_{on=}\frac{V_{battery}}{V_{grid}\times f_{sw}}=\frac{96}{690\times 5000}=27\mu s$$

Critical Inductance;

$$L_c=\frac{[\![(V]\!]_{ZSI}-V_{battery})}{2\times I_{com}}\times t_{on} \qquad (4.37)$$

$$=\frac{690-96}{2\times 1.04}\times 27\times 10^{-6}\ =7.7mH$$

Inductor Current Ripple $$=\frac{[\![D(V]\!]_{ZSI}-V_{battery})}{L_c\cdot f_{sw}} \qquad (4.38)$$

$$=\frac{0.86(\ 690-96)}{7.7\times 10^{-3}\times 5000}=13.26A$$

$$ESR=\frac{\Delta V}{\Delta L} \qquad (4.39)$$

Therefore,

$$ESR=\frac{6.9}{13.26}=520m\Omega$$

Output Capacitance;

$$C_1=\frac{65\times 10^{-6}}{ESR} \qquad (4.40)$$

Therefore,

$$C_1=\frac{65\times 10^{-6}}{0.52}=125\mu F$$

4.5 Three phase line filter

The inductor value is decided by basic inductor voltage equation, during PWM switching period Ts.

$$\Delta V=L\,\frac{\Delta i}{\Delta t}$$

$$L=\frac{\Delta V\times\Delta t}{\Delta i} \qquad (4.41)$$

The main objective of three phase line filter is to set fundamental current to passe to utility from ZSI. According to (F. L. Paukner, 2015), the largest ripple is happening during fundamental frequency period and it is considered here. Therefore, the calculations done considering rms current value during PWM switching period Ts.

$$I_{h_{rms}} = THD_i \times I_1 \qquad (4.42)$$

For three phase systems, the minimum injected current is calculated as,

$$I_1 = \frac{S_p}{3 \times V_{h_{pcc}}} \qquad (4.43)$$

Considering maximum solar generation and battery power

$$I_1 = \frac{30wk00}{3 \times 230}$$
$$= 4.348A$$

By considering maximum THDi, 5% using 4.28 equation,

$$I_{h_{rms}} = THD_i \times I_1$$
$$I_{h_{rms}} = 0.05 \times 4.348$$
$$= 0.217$$

However,

$$I_{h_{rms}} = \frac{\Delta i_p}{\sqrt{2}} \qquad (4.44)$$

$$\Delta i_p = \sqrt{2} \times I_{h_{rms}}$$
$$= \sqrt{2} \times 0.217$$
$$= 0.307A$$

The DC voltage on filter inductors is assumed as the 1/2 of $\hat{V}_{pn}$ at worst case to design the line filter for grid-connection of a three-phase ZSI.

According to Eq. (4.22), $\hat{V}_{AC} = \frac{MV_{pn}}{2}$ and Eq. (4.41) and considering output switching frequency is twice than ZSI switching frequency,

$$L = \frac{1}{2} \frac{MV_{pn}}{\Delta i_p . 4 . f_s} \qquad (4.43)$$

$$L = \frac{1}{2} \frac{0.9 \times 674}{0.307 \times 4 \times 5000}$$

$$= 49mH$$

Therefore, line filter parameters were decided as L= 49mH, R=0.2Ω.

4.6 Residential microgrid loads

Here, a residential microgrid is considered and expected Maximum peak load is 2k. The selected critical load is 1kW and the noncritical load is 1kW.

5 CONTROLLER DEVELOPMENT

As in Figure.39, the proposed home MG control architecture is enabled to accept utility grid commands to change the modes of operation of microgrid according to utility perceptions with consumer approval. Generally, Microgrid or utility grid with control consists of three layers. 1). Hardware layer, 2). Control layer, 3). Communication layer and data and control signals are exchanges in between relevant layers are given in Figure. 5.1. Where, MG and utility grid is physically connected through hardware layer to power flow and communication layer is connected to exchange data and control signals. The proposed MG is used as communication layer to exchange utility grid commands while connecting through hardware layer to power flow. When the home microgrid expects to exchange communication real time solar generation, real time load profile, to utility grid while residential MG receives data on planned outage of grid from the utility grid.

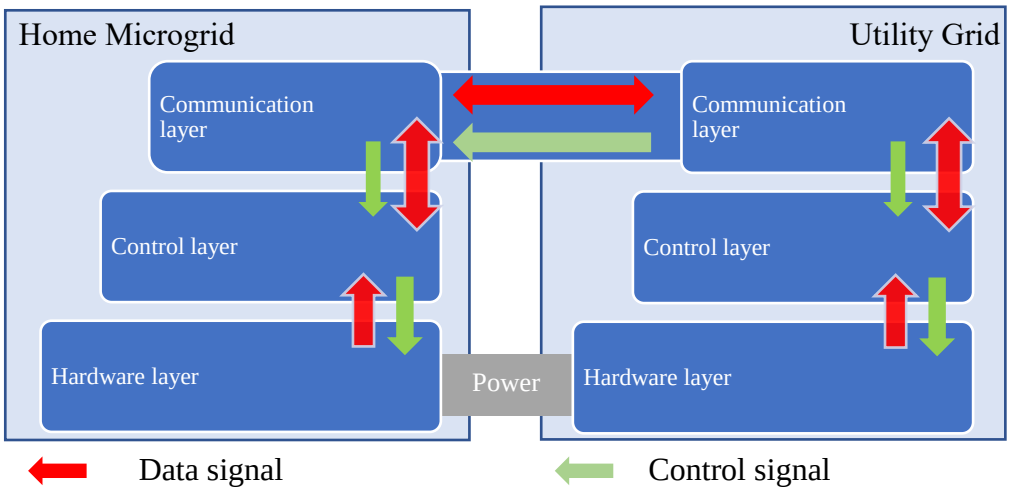

Figure 5.1 Inter connection in between PV MG and utility grid

According to the proposed reconfigurable architecture, this residential MG is centrally controlled by home MG controller and it gives control signal to battery controller, ZSI controller and to load controller according to the reconfiguration algorithm as discussed in Figure. 43 and are discussed in following sections.

5.1 Home MG controller

This is the central controller of proposed residential MG and it communicate with utility grid. The main objective of MG controller is to execute the MG reconfiguration algorithm as given in Figure. 3.4 and select operating mode according to consumer perspective and MG status or upon utility request. By

microgrid algorithm, the expected mode of operation of MG is decided and according to previous mode the algorithm decides whether islanding or grid synchronization is required. After islanding or grid synchronization happens, MG controller sends control signal relevant to the operating mode to ZSI controller and battery controller to set their control objective. Where ON/OFF signals are given to switches to create relevant configuration as per the new operating mode. If the consumer needs to add economic dispatch to get more benefit from this MG, he/she can integrate that controller to this home MG controller.

5.1.1 Islanding detection and synchronization

Under/over frequency protection methods (UOF) and under/over voltage protective devices (UOV) are a must to implement in all grid-connected PV inverter to protect the customer's equipment and they are used as an ant islanding detection method.

If an unplanned islanding occurs, there will be a demand supply deficit. As a result, the inverter detects the occurrence of islanding as its operation goes beyond the acceptable design limits. Whenever the voltage the PCC deviates beyond the voltage limits according to "SLS 1547:2016 (IEC 61727:2004): Response to abnormal voltages" (Table 5.1) and the frequency is beyond $\pm 1\%$ from 50Hz, the islanding detection takes place in this proposed reconfigurable MG.

Table 5.1 SLS 1547:2016 (IEC 61727:2004): Response to abnormal voltages

Voltage (at point of utility connection)	**Maximum trip time**
50% < V < 85%	2.0s
85% < V < 110%	Continuous operation
110% < V < 135%	2.0 s

This method is known as the fundamental detection mechanism for islanding in grid connected systems. (A.Y. Hatata, 2016). Due to its simplicity and its basic islanding detection method, this UOF and UOV methods are utilized for this research to implement reconfigurable architecture. When Grid synchronization is done through Closed loop three phase PLL method to follow grid voltage and frequency due to its effectiveness, simplicity and robustness are in numerous grid conditions.

5.2 Battery controller

The battery controller generates the control signal to bidirectional DC/DC converter for battery charging and discharging function. The main objective of the battery controller is to keep constant ZSI capacitor voltage to fulfil voltage limits at PCC. The constant capacitor voltage is preserved by charging or discharging function of the Li-ion battery to respond according to solar irradiance changes and load changes. Therefore, the battery controller acts to keep the ZSI capacitor voltage stable throughout the operation. The two cascaded PI controllers:1) internal current control, 2) external voltage control, regulate capacitor voltage. The inner current controller regulates battery charging and discharging current within battery and converter safe limits, and the outer voltage loop controls the capacitor voltage.

The capacitor voltage error is passed through the PI controller to produce reference battery current and it is compared with the actual battery current and the error signal is sent through PI controller to generate a battery control signal as given in the Figure.5.2. Then the battery control signal is compared with a high frequency triangular signal to generate the switching signal for DC/DC converter.

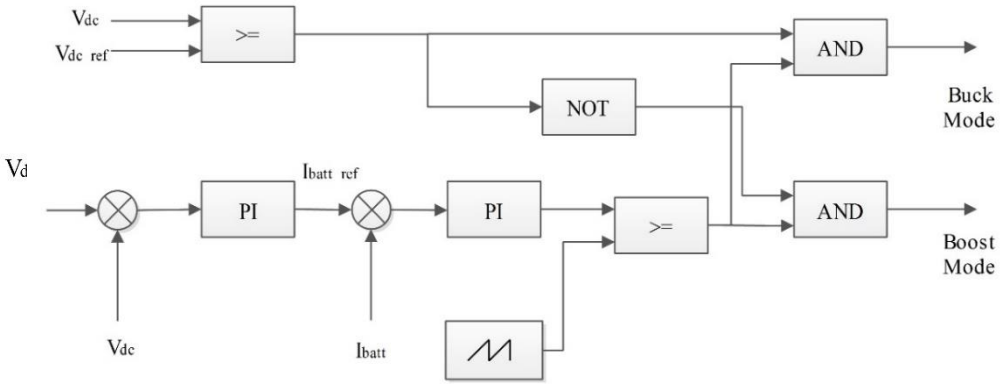

Figure 5.2 Controller of buck-boost DC-DC converter

In this study, the switching frequency of the DC-DC converter was taken as 5 kHz. Where, the PI controller parameters for voltage loop are Kp = 0.1 and Ki = 20 and for current loop are Kp = 0.3 and Ki = 20.

5.3 ZSI controller

5.3.1 Current controlling mode

The main objective of this mode is to extract maximum power from Solar panels and transfer to the residential loads and to the utility grid. The developed structure of controller for the current controlling mode of proposed residential MG is given in Figure.5.3.

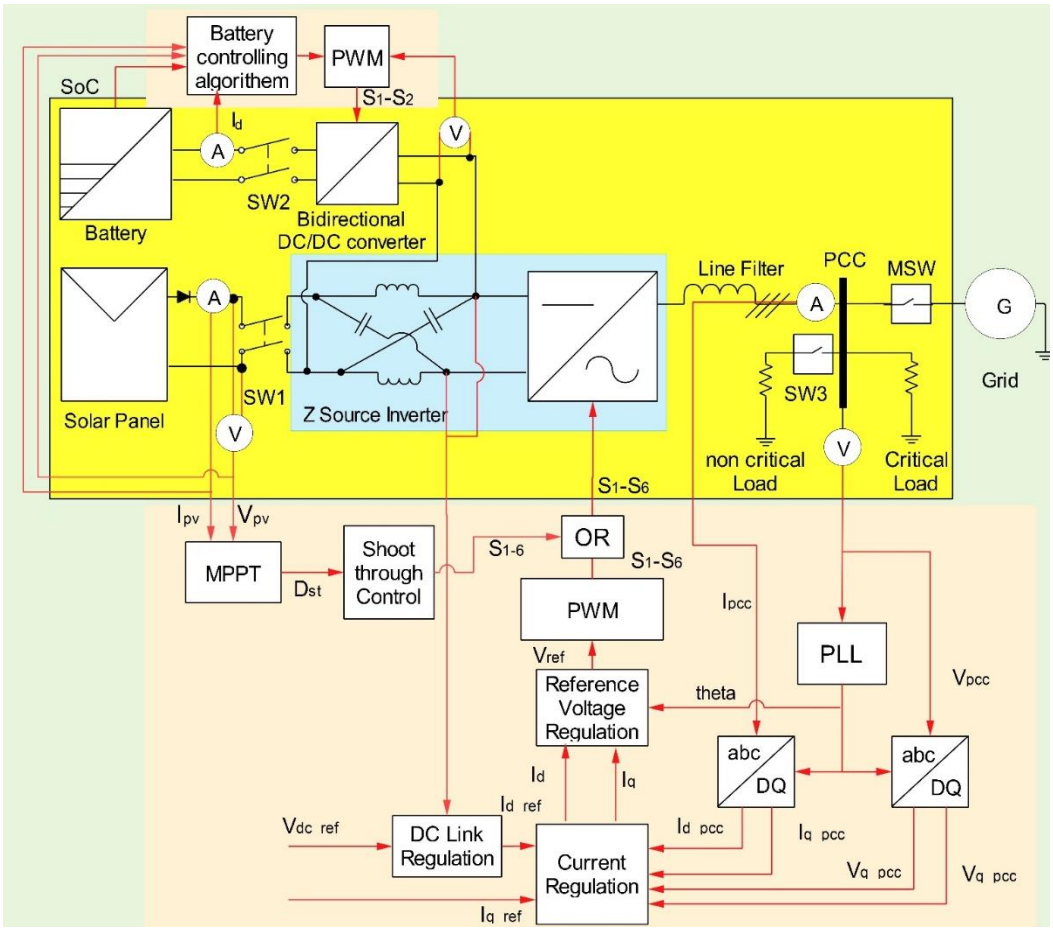

Figure 5.3 Z source inverter controller and battery controller for current control mode

As discussed in literature review, independent control of D_{st} and M is adopted in this application. Therefore, two main controllers were developed as 1. MPPT controller to control D_{st} 2. Close loop feedback controller to generate modulation index (M).

5.3.1.1 MPPT controller

The MPP point changes over a wide range, with PV array temperature and solar insolation. Hence, MPPT must be implemented to ensure an optimal operation of a PV array, irrespective of temperature and irradiance conditions and load variations.

Since ZSI is a single stage power converter MPPT algorithm is adopted to control PV array voltage through shoot through duty (D_{st}).

Thus, INC algorithm is adopted. The concept of INC MPPT algorithm be contingent on $\Delta P/\Delta V$ which is equivalent to zero at MPP as in Figure. 5.4. Theoretical background of this method is described as follows (Amit Kumer Podder, 2018).

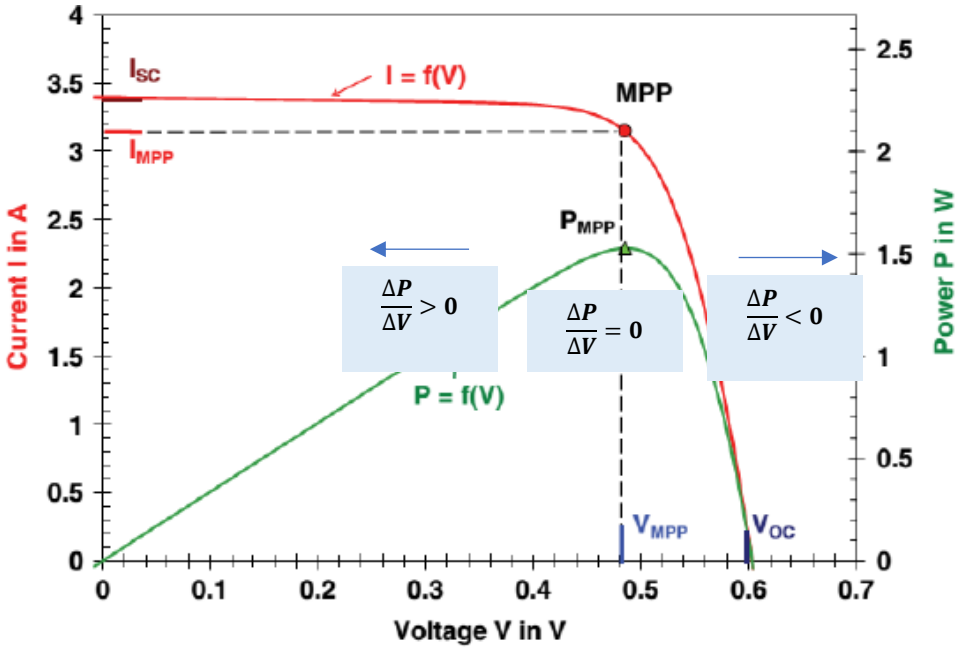

Figure 5.4 IV PV characteristics of solar array near MPP

$$\therefore \frac{\Delta P}{\Delta V} = \frac{d(V.I)}{dV} = I\frac{dV}{dV} + V\frac{dI}{dV} = I + V\frac{dI}{dV} = 0$$

$$\therefore at\ MPP, \frac{dI}{dV} = -\frac{I}{V}$$

Instantaneous impedance equals to incremental impedance at MPPP.

When the MPP voltage is higher than the current voltage, $\frac{\Delta P}{\Delta V}$ is greater than zero.

$$\frac{dI}{dV} > -\frac{I}{V}$$

When the MPP voltage is lower than the current voltage, $\frac{\Delta P}{\Delta V}$ is less than zero.

$$\frac{dI}{dV} < -\frac{I}{V}$$

The flowchart in Figure.5.5 describe the INC algorithm as given below.

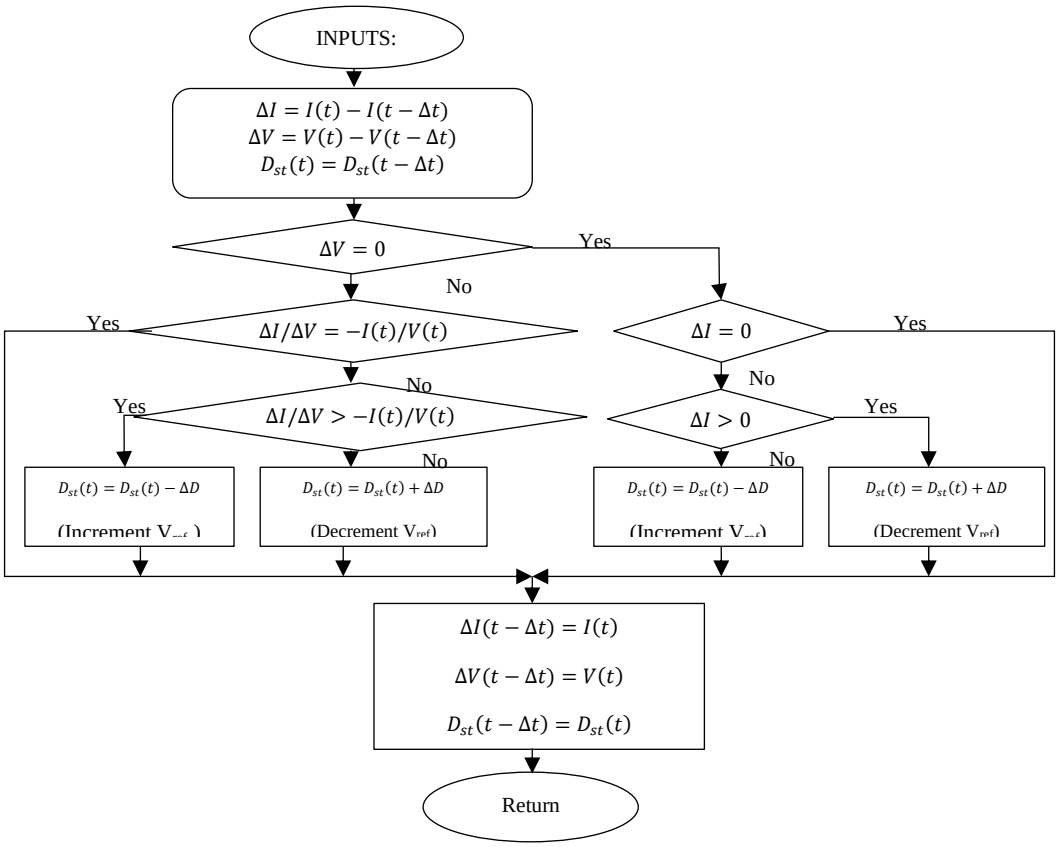

Figure 5.5 INC MPPT algorithm

Initially, in this algorithm, ΔV=0 is checked to confirm the previous state of voltage weather it is MPP or not. If ΔV=0, then check ΔI=0 to verify the irradiance change during sampling period to change if PV current happens or not. If ΔI=0, keep the current duty as it is. If not ΔI=0, again check ΔI>0, if answer is yes, irradiance has increased and MPP has been changed and have to increase PV voltage to converge at MPP. Otherwise, irradiance has decreased and have to decrease PV voltage to converge at MPP. If not ΔV=0, $\frac{\Delta I}{\Delta V} = -\frac{I(t)}{V(t)}$ is checked if it is true, it is at MPP and it is not true, again have to check how closed to MPP through $\frac{\Delta I}{\Delta V} > -\frac{I(t)}{V(t)}$. If it is true, current PV voltage is left side to the MPP. Therefore, voltage has to increase to converge at MPP. If not, PV voltage has to decrease accordingly.

According to those changes, it is decided to increase or decrease the PV voltage. However, PV array voltage is inversely proportional to the shoot through duty up to the 0.5 duty factor (ZSI operating boundary is below 0.5) according to the following equation.

$\hat{V}_{pn} = B \times V_{pv} = \frac{1}{1-2(D_{st})} V_{pv}$ (Peak DC Link Voltage kept to be at constant)

$$\hat{V}_{pn}[1 - 2(D_{st})] = V_{pv}$$

Therefore, shoot through duty (D_{st}) is increase or decrease opposite to the PV voltage.

5.3.2 Closed loop feedback controller

Feed forward voltage regulator is used to remove the effect of non-linear characteristics of SPV system and current control technique reduces THD level of the inverter. Therefore, closed loop feedback controller is adopted for this research work.

The main function of this feedback controller is to create reference voltage V_{ref} signal for PWM signal generator (Modulation) of the ZSI to follow grid voltage (V_{PCC}) to feed active and reactive power according to MG and utility grid requirement.

The synchronous operation of MG with utility grid is done though PLL which is used to get power angle (ωt) of grid voltage. Then, direct and quadrature transformed components of PCC voltage ($V_{d_{pcc}}$ and $V_{q_{pcc}}$) and ZSI current from PCC ($I_{d_{pcc}}$ and $I_{q_{pcc}}$), are considered as feedback signals for AC voltage and current loop.

Active and reactive powers injected can be calculated using the following relationships

$$P = V_{d_{pcc}} I_{d_{PCC}} + V_{q_{pcc}} I_{q_{PCC}}$$

$$Q = -V_{d_{pcc}} I_{q_{PCC}} + V_{q_{pcc}} I_{d_{PCC}}$$

In the Equation, the reactive power Q is given from cross coupling between the d-q current and voltage components. Due to PLL, it eliminates $V_{q_{pcc}} I_{d_{PCC}}$ component as it locks on the grid frequency to zero the quadrature component of the voltage at PCC. Then, the above equation will be simplified to,

$$P = V_{d_{pcc}} I_{d_{PCC}}$$

$$Q = -V_{d_{pcc}} I_{q_{PCC}}$$

Therefore, by controlling $I_{d_{PCC}}$, $I_{q_{PCC}}$, it is possible to control active and reactive power output from the inverter. Since feedback control method is used to control this inverter, reference $I_{d_{ref}}$, $I_{q_{ref}}$, is generated as per the required active and reactive power from the inverter.

This mode focused was to generate maximum power from solar and feed to residential loads, grid and store energy.

To extract maximum power generation from Solar PV, modulation index (M) of ZSI is controlled through direct DC link control method. Where, the DC link peak voltage is measured and error between measured DC link peak voltage and reference DC link peak voltage value are processed through PI controller. The output of this DC link voltage controller is produced $I_{d_{ref}}$.

Converting solar power to reactive power is not economical due to usable form of generated energy which is active power, not reactive power and most of utilities are not paid for reactive power. Therefore, here, $I_{q_{ref}}$, was set to zero, to make reactive power output from inverter is to zero and $I_{d_{ref}}$ was fed from DC link controller to extract maximum from solar PV. So, PV system is set to operate at unity power factor.

In the inner current regulator, the error between reference ($I_{d_{ref}}$, and $I_{q_{ref}}$) and measured PCC current (I_{d_pcc}, and I_{q_pcc}) is sent through PI controller to generate expected deviation of inverter output voltage $\Delta V_{d_{conv}}$, and $\Delta V_{q_{conv}}$ components) before the line inductor when all PI controllers have tuned through trial-and-error method. To generate converter output reference voltage, measured PCC voltage should be modified according to the line filer components. The converter output reference voltages ($V_{d_{conv}}$ and $V_{q_{conv}}$) can be determined including the effect of line filters as the following equation.

$$V_{d_{conv}} = V_{d_{PCC}} + RI_d - \omega LI_d + \left(K_p + {}^{K_i}/_{s}\right)\left(I_{d_{ref}} - I_{q_{pcc}}\right)$$

$$V_{q_{conv}} = V_{q_{PCC}} + \omega LI_d + RI_q + \left(K_p + {}^{K_i}/_{s}\right)\left(I_{d_{ref}} - I_{q_{pcc}}\right)$$

Thus $V_{d_{PCC}}$ and $V_{q_{PCC}}$ are generated from d-q transformation of measured PCC voltage. R and L are total resistance and inductance between Inverter Bridge and PCC. The two terms, $\omega L I_d$ and $\omega L I_d$ are used to compensate for the coupling between the d-q axis.

Finally, the converter voltages $V_{d_{conv}}, V_{q_{conv}}$ are transformed back into the three phase quantities $V_{abc_{ref}}$ to follow grid voltage according to power angel (ωt). The reference converter voltage is compared to the PWM carrier signal to give the switching signal to on/off the IGBT modules to generate inverter output voltage accodingly. Then $V_{abc_{ref}}$ for modulation is generated from converter reference voltage which is generated from PLL. The developed MATLAB/Simulation control block to generate $V_{abc_{ref}}$ is given in Figure.5.6. (Jayasundara, et al., 2018)

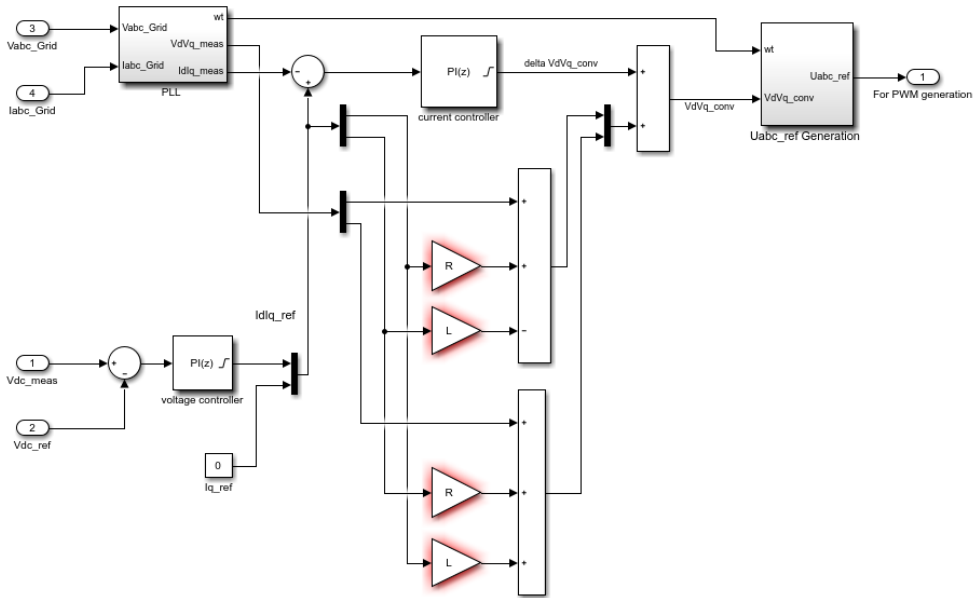

Figure 5.6 MATLAB/Simulation control block to generate $V_{abc_{ref}}$

For modulation of 3ph ZSI, several control methods are proposed in literature as simple boost control (SBC), maximum boost control (MBC), maximum constant boost control (MCBC) from sine PWM (SPWM) and modified space vector modulation boost control (MSVMBC) from space-vector PWM (SVPWM). According to their performances, MCBC and MSVMB methods provide wide range boosting capability and lower voltage across switching devices. However, SBC is the simple modulation method to implement, and it can provide satisfactory results to operate in current control mode. Hence, SBC is considered in this research work.

5.4 Reactive power control mode

In long distribution feeders, due to less active power load conditions at off peak hours or heavy load conditions at night peak hours or faults conditions make power quality issues such as voltage rise and dips. Since the most common use of DSTATCOM is for such voltage stability, and it is applied here. In this study, the control objective of this mode is to provide voltage regulating support at PCC during the nighttime to maintain PCC voltage within pre-decided limits by acting the PV MG as DSTATCOM. However, the proposed MG does not expect to activate this mode if the previous mode is islanded as it will create protection problem to utility. In this mode, PV panel and batteries and battery controller are disconnected from the MG and ZSI to operate in voltage regulating mode and critical loads stay connected.

The developed structure of controller for the Reactive power controlling mode of proposed residential MG is given in Figure.5.7.

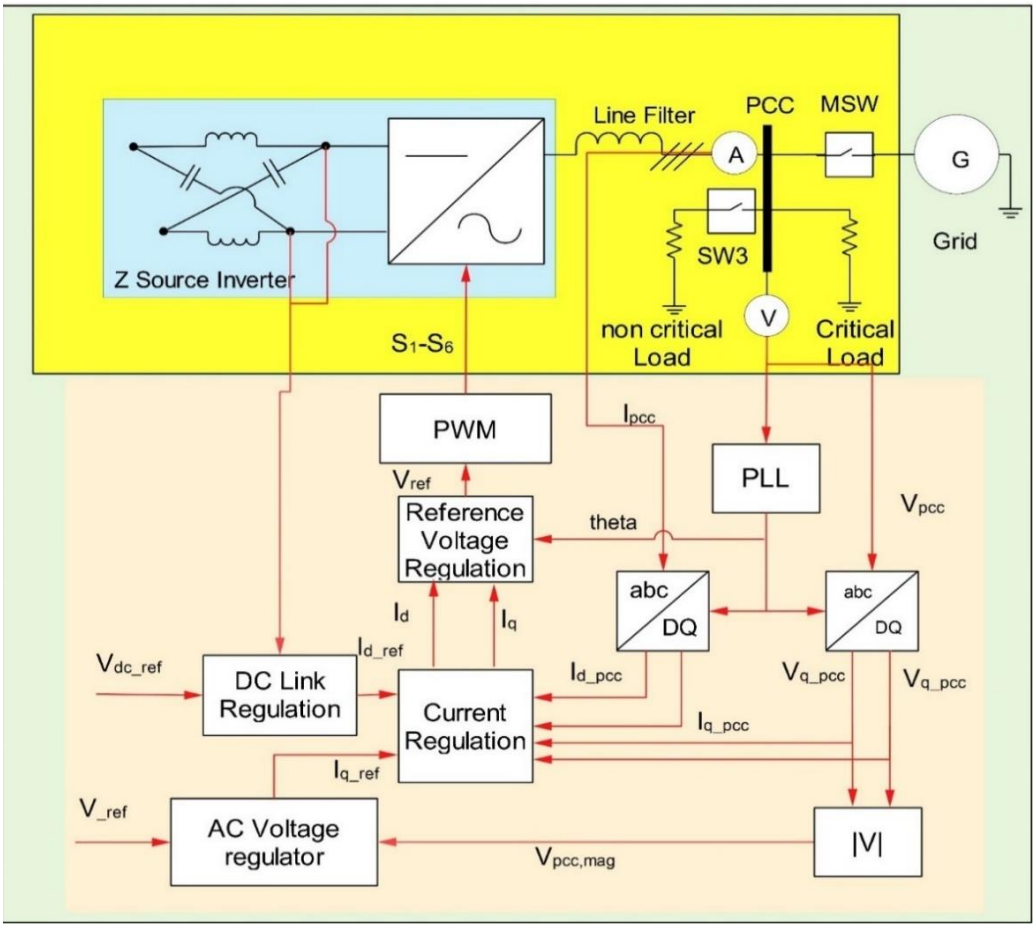

Figure 5.7 Z source inverter controller for voltage/reactive power control mode

As shown in Figure.3.8, when the grid voltage is between V_L and V_H , MG is operated as its general condition as in grid connected mode. This DSTATCOM mode regulates voltage when the PCC voltage is between V_H to V_{max} and V_L to V_{min} . When the PCC voltage is between V_{low} to V_{min} , DSTATCOM produces reactive power to PCC and the PCC voltage is in between V_{high} to V_{max} by absorbing reactive power.

The output voltage of DSTATCOM is generated by ZSI which is operated from an energy storage or capacitors. By varying the magnitude of output voltage of ZSI, the reactive power exchanges between DSTATCOM and Utility grid is controlled. This output voltage of the DSTATCOM can directly be controlled by directing the modulation index (M) and shoot through duty (D_{st}) of SPWM waves. The controller is configured to maintain the PCC voltage close to normal operating voltage (V_L during voltage dip, V_H during voltage rise) by absorbing or generating corresponding reactive power depending on the difference of magnitude of the PCC voltage and ZSI voltage.

The control system consists of a PLL, AC voltage regulator and a DC voltage regulator as outer regulation loop consisting, inner current regulation loop.

The PLL synchronizes line filter output voltage with utility grid voltage as in current control mode. The PLL generate phase angle (ωt) of grid voltage is used to compute the dq-axis components of the ZSI output voltage and currents. The outer regulation loops are consisting of AC voltage regulator and DC voltage regulator.

The AC voltage regulating outer loop compares the magnitudes of grid voltage and given reference grid voltage. Then the error is fed through PI controller to generate reference current $\left(I_{q_{ref}}\right)$ for inner current loop. Where $I_{q_{ref}}$ controls reactive power flow accordingly.

Since, there is no active source at DC side of ZSI in this mode, capacitors of impedance source work as dc source and charging of these capacitors are done through consuming active power from the utility grid to supply active power losses in the switching circuit and filter circuit during voltage control mode. To keep

charged capacitors, the DC link voltage should be kept constant. Therefore, the DC link voltage is compared with reference DC link voltage to generate reference current $I_{d_{ref}}$ regarding exchange of active power between ZSI and utility to provide the inner current regulator as in current control mode.

In the inner current regulator, the error between reference ($I_{d_{ref}}$, and $I_{q_{ref}}$) and measured PCC current (I_{d_pcc}, and I_{q_pcc}) is sent through PI controller to generate expected deviation of inverter output voltage $\Delta V_{d_{conv}}$, and $\Delta V_{q_{conv}}$ components) before the line inductor as in Current control mode. All PI controllers have tuned through trial-and-error method. The next control blocks (Outer voltage regulation loop, PWM reference signal generator) are developed as in current control mode. Then, simple boost control method is adopted for modulation as in current control mode.

5.5 V-F control mode

A clear concepts of VF controller (operation of islanded mode) for inverter and battery-based DG units in the portion of the CIGRE LV distribution, was presented in (Ghullam Mustafa Bhutto, 2017) and the same concept is followed for the operation of this islanded microgrid. The developed structure of controller for the V-F controlling mode of proposed residential MG is given in Figure.5.8.

Proportional Integral (PI) controllers are used to control the operation of islanded MG and they use the voltage control concept of STATCOM controllers. Power output of batteries are controlled to keep DC link voltage constant.

As in current controlling mode, ZSI has two main controllers to operate as DC/DC converter to control MPP through D_{st} and DC/AC converter to control output voltage and frequency by controlling modulation index (M).

Same MPPT algorithm is used to achieve MPP in this mode by controlling Shoot though duty D_{st}.

Where, modulation index is controlled through closed loop feedback control system. However, in this mode, reference frequency, and reference voltage are not

fed from utility grid as it is not available in this state. Herein, reference frequency and voltage are set within pre-defined margins according to grid code.

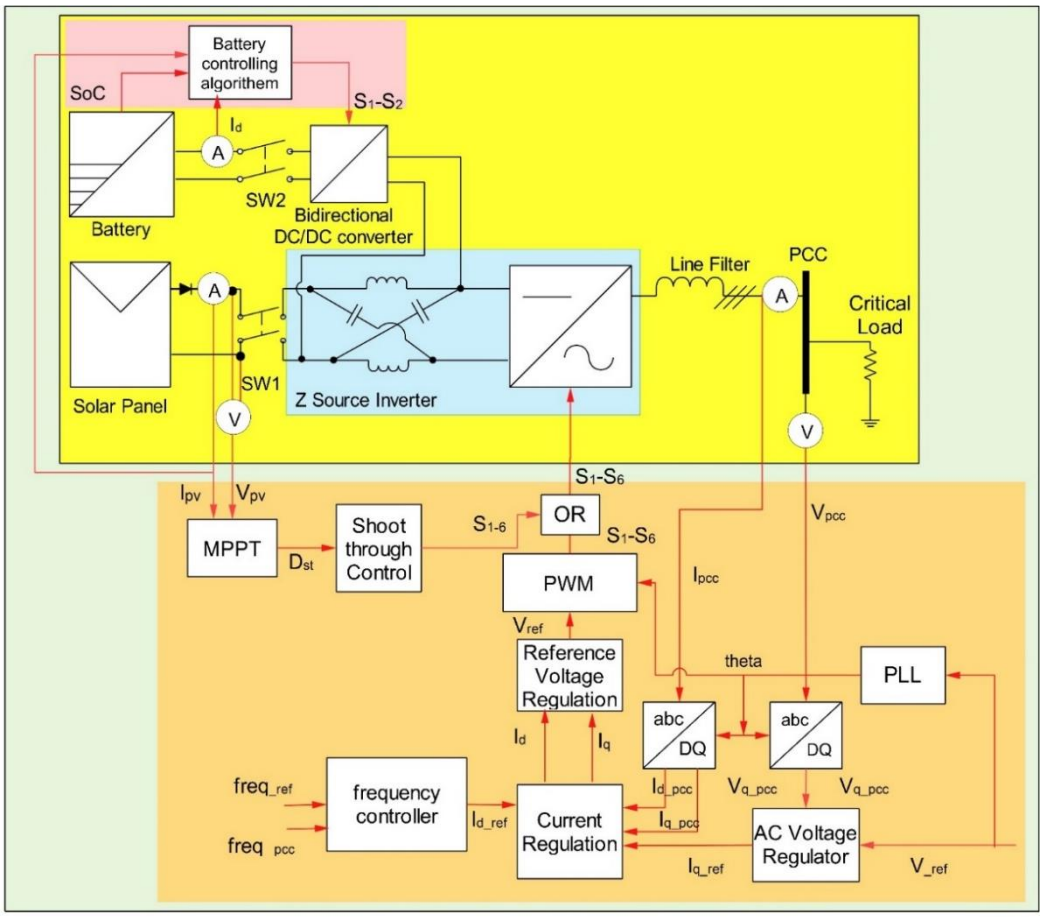

Figure 5.8 Z source inverter controller and battery controller for V-F control mode

The measured and reference frequency ($F_{ref} = 50\ Hz$) is compared and the error signal is sent to the PI controller to generates active current reference $\left(i_{d_{ref}}\right)$ while the measured and reference voltages (reference three phase signal is generated externally and the phase angle and the magnitude of this reference signal is followed through PLL block as used in current control method) at PCC compares and sends the error signal to PI controller to generates the reactive current reference $\left(i_{q_{ref}}\right)$. The sign of the error signal decides the injection and the absorption of the reactive power. PI controllers have tuned through trial-and-error method. The next inner voltage loop and current loops are same as current controlling mode to generate reference voltage signal for modulation. Then, simple boost control method is adopted for modulation as in current control mode.

6 SIMULATION RESULTS AND DISCUSSION

The proposed ZSI based reconfigurable architecture for SPV MG was developed in MATLAB\Simulink environment as separate sub systems for each mode of operations (Current controlling mode, V-F control mode and reactive power/ voltage control mode) and reconfigurable algorithm, to integrate each subsystem to perform as a reconfigurable system to verify the reality of each mode of operations.

6.1 Reconfiguration algorithm

The proposed reconfigurable algorithm as in Figure. 3.4, is developed in MATLAB/Simulink environment and the code is attached in Appendix A, and simulation results are in Figure. 6.1. External disturbances (PCC voltage (V_{PCC}), current (I_{PCC}) and frequency (F_{PCC}) deviations, DC link voltage variations (V_{DC}) and Solar PV generation variation (P_{pv}) were created to verify the output from the reconfiguration algorithm developed in MATLAB. Table 6.1 describes the time-based variations of each parameter and outcomes (M: status of Mode of operation, Sync; Synchronization command, Isl; Islanding command), from the developed reconfiguration algorithm.

Table 6.1 Reconfiguration algorithm input data and outcomes

Inputs						Outputs		
Time	V_{PCC}	I_{PCC}	F_{PCC}	V_{DC}	P_{pv}	M	Sync	Isl
0s -1s	230V	10A	50 Hz	800Vdc	10W	1	0	0
1s-2s	250V	10A	50 Hz	800Vdc	10W	3	0	0
2s-2.5s	230V	10A	50 Hz	800Vdc	10W	1	0	0
2.5s-3S	230V	10A	50 Hz	1500Vdc	10W	2	0	1 @2.5s
3S-3.5S	230V	10A	54.5Hz	1500Vdc	500W	2	0	0
3.5s -4s	250V	50A	54.5Hz	800Vdc	500W	2	0	0
4s -4.5s	230V	50A	54.5Hz	800Vdc	500W	2	0	0
4.5s-5s	230V	10A	50 Hz	800Vdc	500W	1	1 @4.5s	0
5s-6s	230V	10A	45.5 Hz	800Vdc	500W	2	0	1 @5s
6s-7s	230V	10A	50 Hz	800Vdc	10W	1	1 @6s	0
7s-8s	180V	10A	50 Hz	800Vdc	10W	2	0	1 @7s
8s-10s	230V	10A	50 Hz	800Vdc	10W	1	1 @8s	0
10s-11s	260V	10A	50 Hz	800Vdc	10W	2	0	1 @10s
11s-14s	230V	10A	50 Hz	800Vdc	10W	1	1 @11s	0
14s-15s	200V	10A	50 Hz	800Vdc	10W	3	0	0
15s-17s	230V	10A	50 Hz	800Vdc	10W	1	0	0
17s-20s	230V	10A	50 Hz	800Vdc	10W	1	0	0

Reactive power/Voltage control conditions V-F control conditions

M= 1 (current control), M=2 (V-F control), M=3 (V control), Sync=1(do synchronizing), Isl=1 (do islanding)

Over current conditions ($I_{\text{peak\_max}}$=30A) and DC over voltage conditions ($V_{\text{dc\_max}}$ =1000Vdc) were considered for islanding in addition to UOF and UOV protection conditions. When algorithm identifies a fault, it correctly checks the previous mode of operation and islanding signal is generated accordingly. Not only that, in current control mode it also checks previous mode of operation and generate synchronizing signal consequently. Voltage rise and dip conditions were created 1s to 2s and 14s to15s at low PV power generation. The simulated algorithm correctly selects right mode according to the pre described conditions and give islanding and synchronizing signal in each case accordingly.

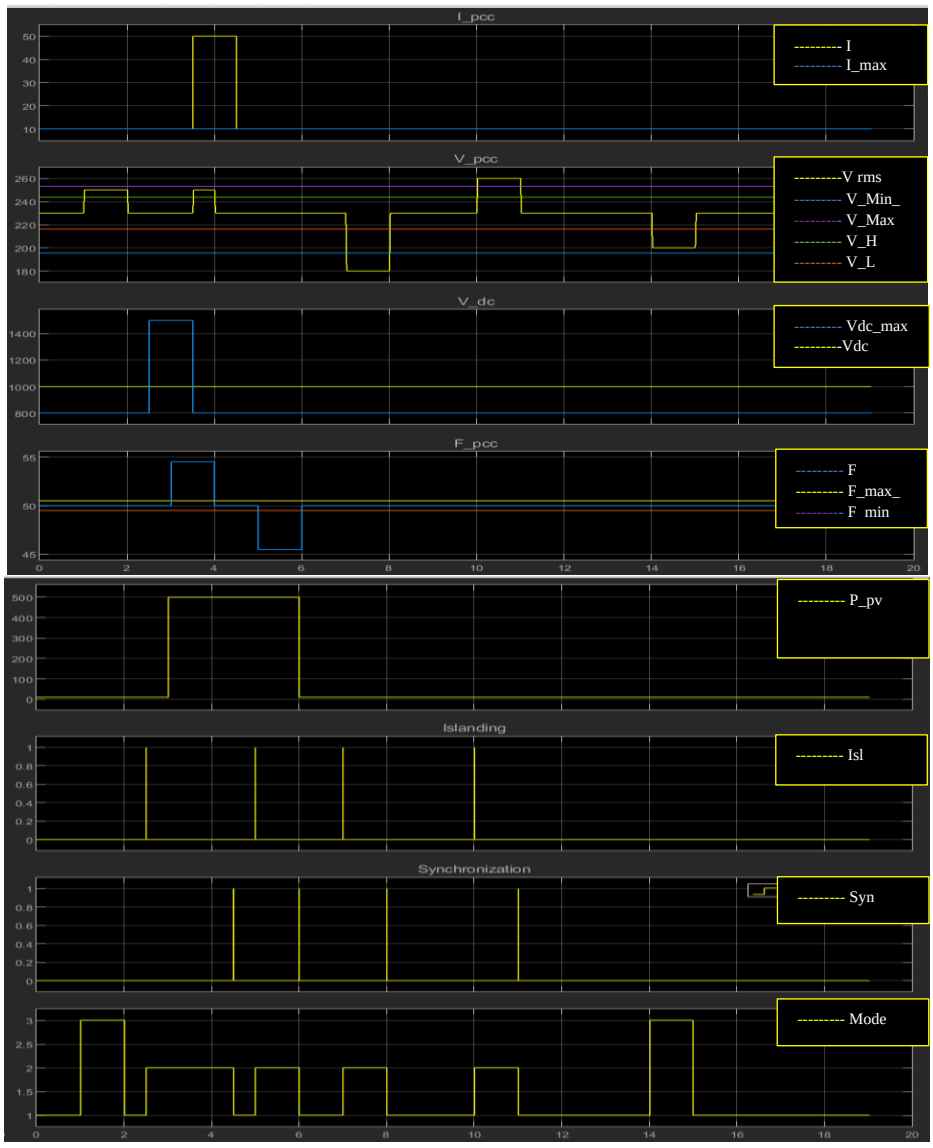

Figure 6.1 Simulation results of reconfiguration algorithm

6.2 Current controlling mode

All residential microgrid components and controller relevant to current control mode was simulated in MATLAB/Simulink environment as subsystem as in Figure. 6.2.

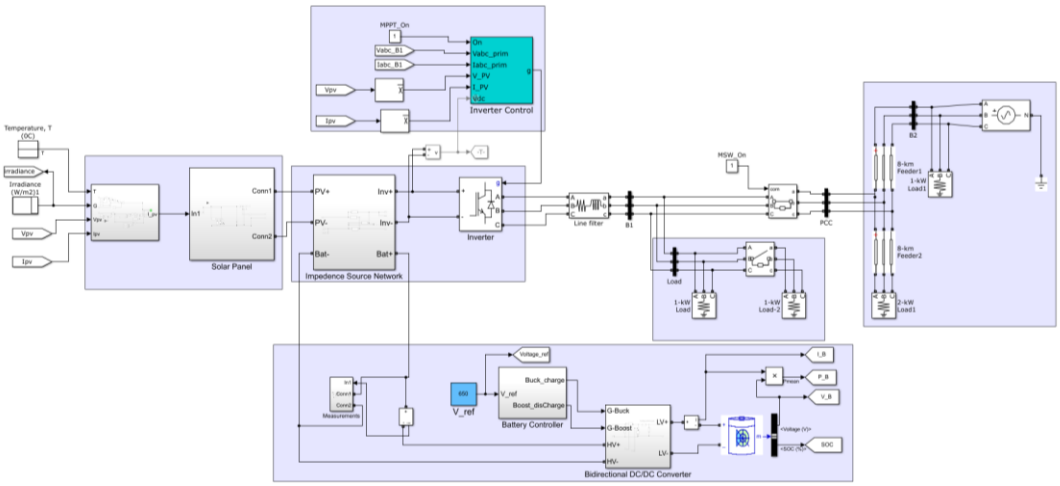

Figure 6.2 MATLAB/Simulink model for current controlling mode

The variations are adopted as to this mode in the given Table 6.2. The Solar irradiance and microgrid loads to check the performance of proposed ZSI based SPV microgrid and simulation results are given in Figure. 6.3.

Table 6.2 Variations of microgrid components and relevant outcomes – current control mode

Time	Solar irradiance	Microgrid Load	SPV power out
0s-0.2s	600 W/m2	1 kW	1000W
0.2s- 0.8s	1000 W/m2	1 kW	1600W
0.8s -2.2s	600 W/m2	1 kW	1000W
2.2s -3s	600 W/m2	2 kW	1000W

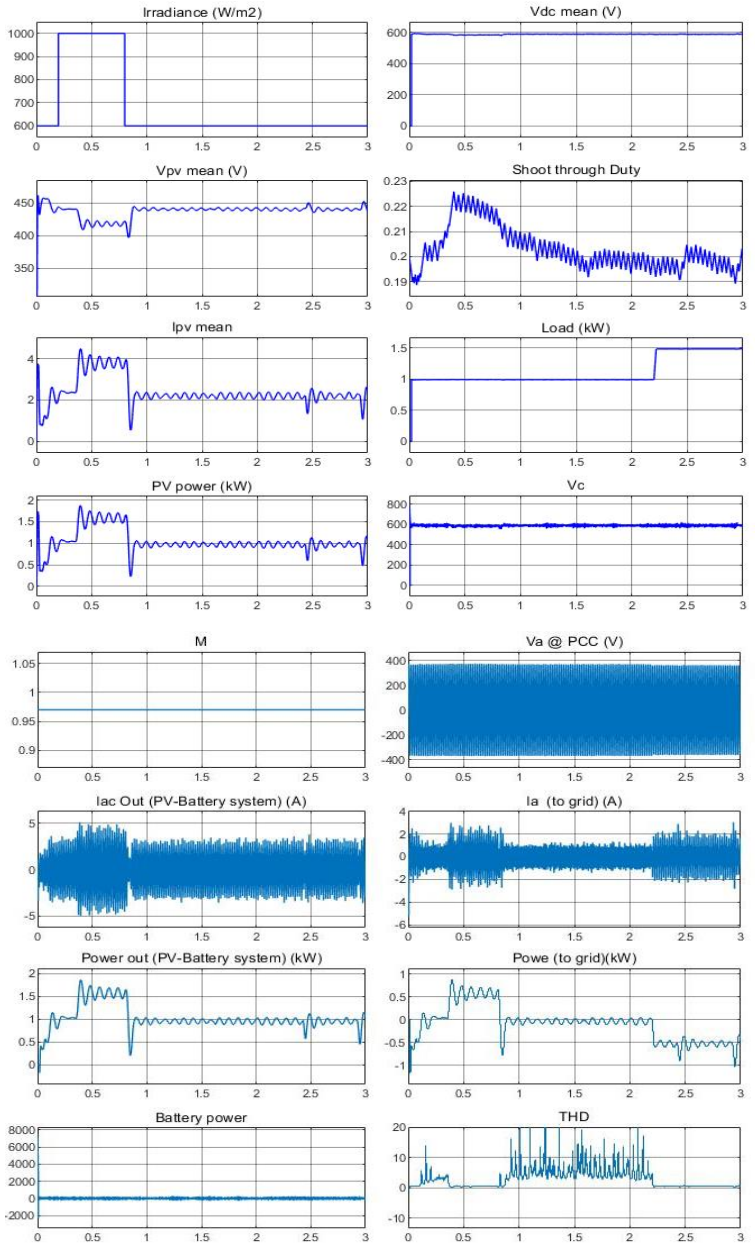

Figure 6.3 Simulation results of current control mode

At the start, solar irradiance is 600W/m2 up to 0.2s. The solar PV panels out 1000W which is almost closed to MPP power and it fulfills MG load demand. Therefore, no power exchange between utility and microgrid happens. During 0.2s to 0.8s irradiance increased to 1000W/m2 keeping load as 1kW. The SPV system generates 1600W which is delivered to the MG loads. The excess is delivered to the utility grid. With the connection of non-critical load at 2.2s until the end of simulation, the MG demand is increasing beyond the solar generation. Therefore, the MG draws power from utility grid during this time.

THD at PCC voltage is maintained around 0.5% when there is more than 50W of power transfer in between MG and Utility grid.

The simulation results are shown for MPPT performance at two different irradiance and MG response at two different power demand. Thus, the control objective was to obtain maximum power output from Solar PV system. This objective was clearly achieved according to simulation results as ZSI controller is converged nearly to the MPP all over the simulation period. The existing small oscillations are to be tuned in future by tuning PI controller.

6.3 Reactive power controlling mode

The proposed reactive power/voltage control mode was simulated in MATLAB/Simulink environment as given in Figure. 6.4. on following conditions and variations and simulation results are given in Figure. 6.5 and Figure. 6.6.

- Total simulation time: 1.65s
- PCC Voltage:
  - 0.0 s: V_{rms_PCC} =230V
  - 0.1 s: V_{rms_PCC}=263V
  - 1.6 s: V_{rms_PCC}=230V

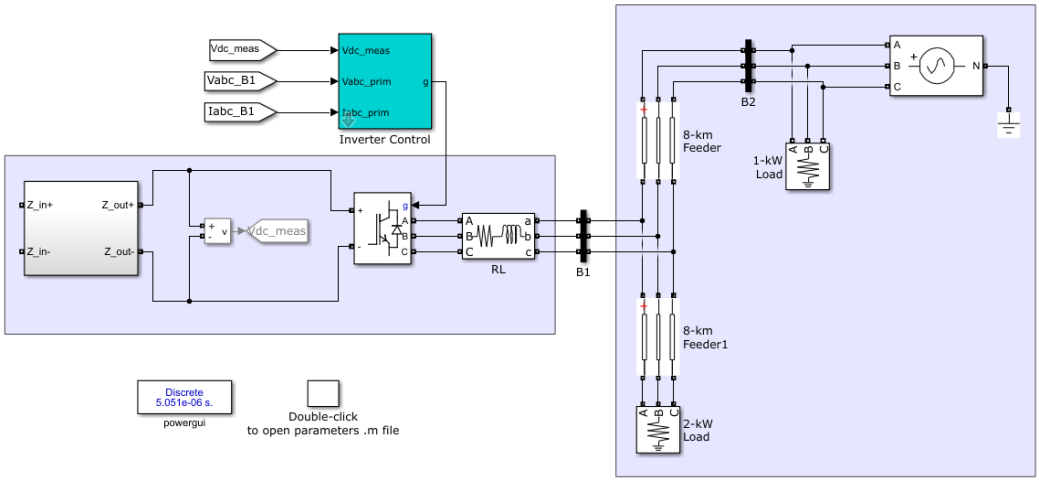

Figure 6.4 MATLAB/Simulink model for Reactive power/ voltage controlling mode

The PCC rms phase voltage is forced to change to 263V from 230v at 0.1s. in this controller. The MG experience voltage rises along 1.5s at PCC. Therefore, the microgrid consumes reactive power from utility grid. Voltage at PCC is controlled to set in voltage limits during voltage rise and rms voltage at PCC shows how it controlled within set limits while consuming reactive power by this MG working as a DSTATCOM. The controller needs further tuning for stable output voltage.

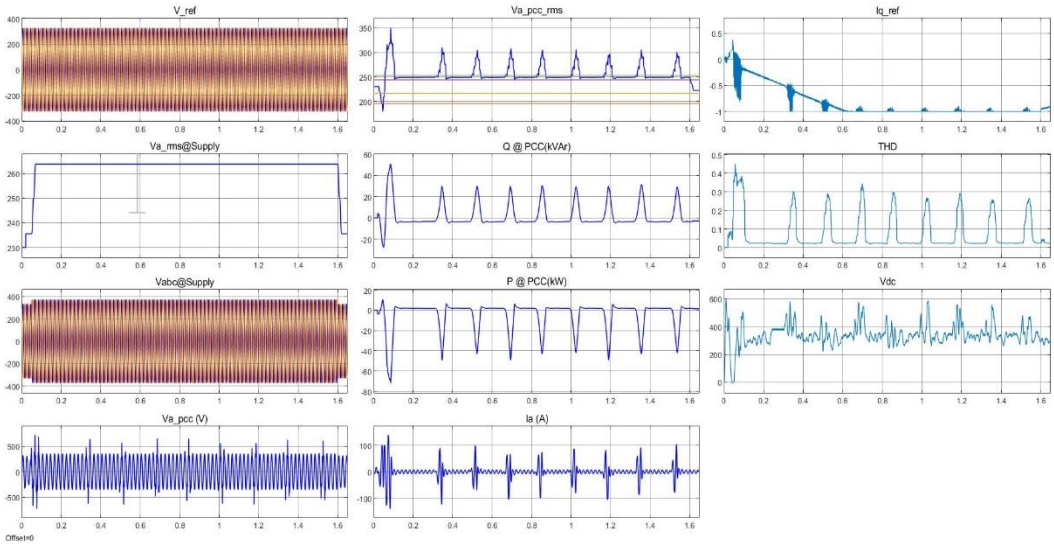

Figure 6.5 Simulation results of reactive power / voltage control mode

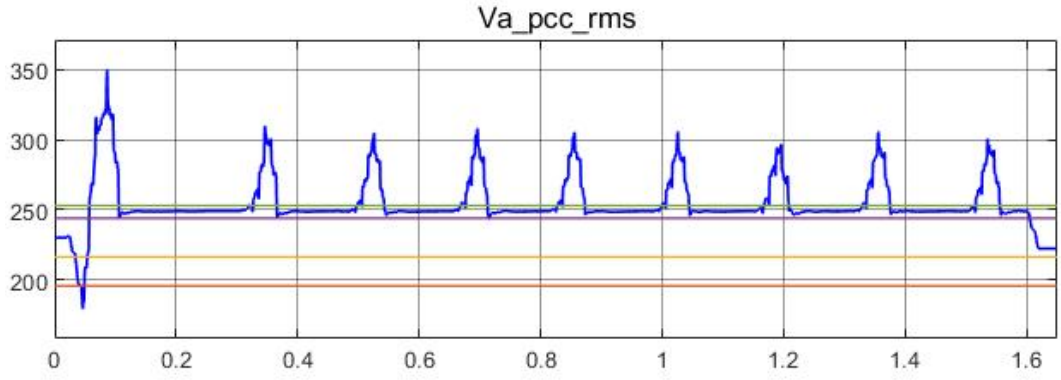

Figure 6.6 Simulation results of reactive power / voltage control mode - PCC voltage

6.4 V-F controlling mode

The proposed V-F control mode was simulated in MATLAB/Simulink environment as given in Figure. 6.7. The conditions and variations were used for the simulation are given as per Table 6.3 and simulation results are given in Figure. 6.8.

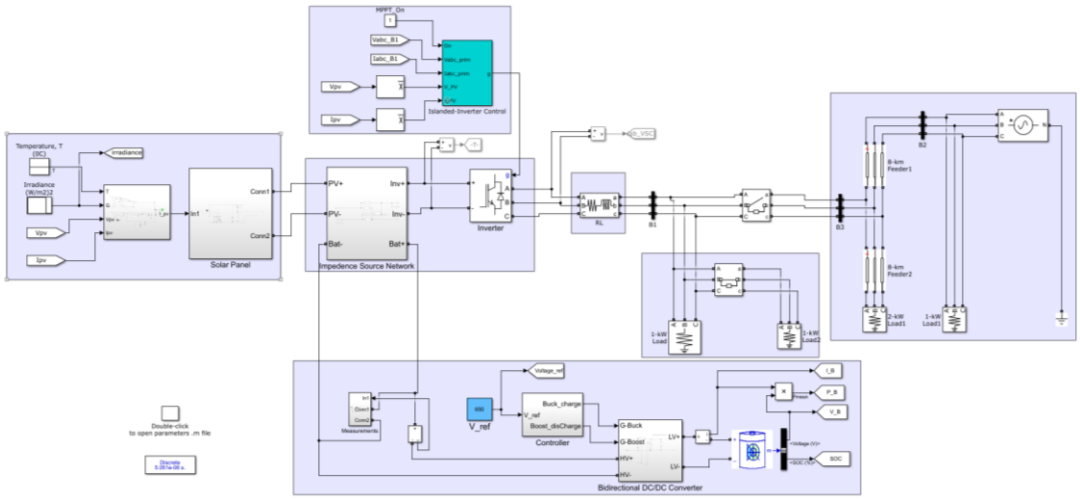

Figure 6.7 MATLAB/Simulink model of V-F control mode

Table 6.3 Variations of microgrid components and relevant outcomes – V-F control mode

Time	Solar irradiance	MG Load	SPV power out	Voltage	frequency	SOC%
0s-0.2s	600 W/m2	1.2 kW	600W	Within limits	Within limits	increasing
0.2s- 0.5s	1000 W/m2	1.2 kW	1600W	Within limits	Within limits	increasing
0.5s -0.8s	1000 W/m2	0.2 kW	600W	Within limits	Within limits	increasing
0.8s -1.2s	600 W/m2	0.2kW	700W	Within limits	Within limits	decreasing
1.2s – 3s	600 W/m2	1.2 kW	700W	Within limits	Within limits	decreasing

As in current control mode solar irradiance and load changes were created to monitor performance of the proposed MV microgrid architecture. Initially, MG load were set to 1.2kW while keeping solar irradiance 600W/m2 up to 0.2s. When the solar generation is not enough to supply loads. Then DC link voltage drops below it sets value then MPPT cannot successfully control PV voltage then maximum power cannot obtain at this time. However, battery is set to control DC link voltage then it takes control DC link voltage from both battery and solar power generation supply to load. Due to battery discharge to feed for load, SOC% drops in this period.

From 0.2s to 0.5s, solar irradiance increases up to 1000W/m2 keeping MG load

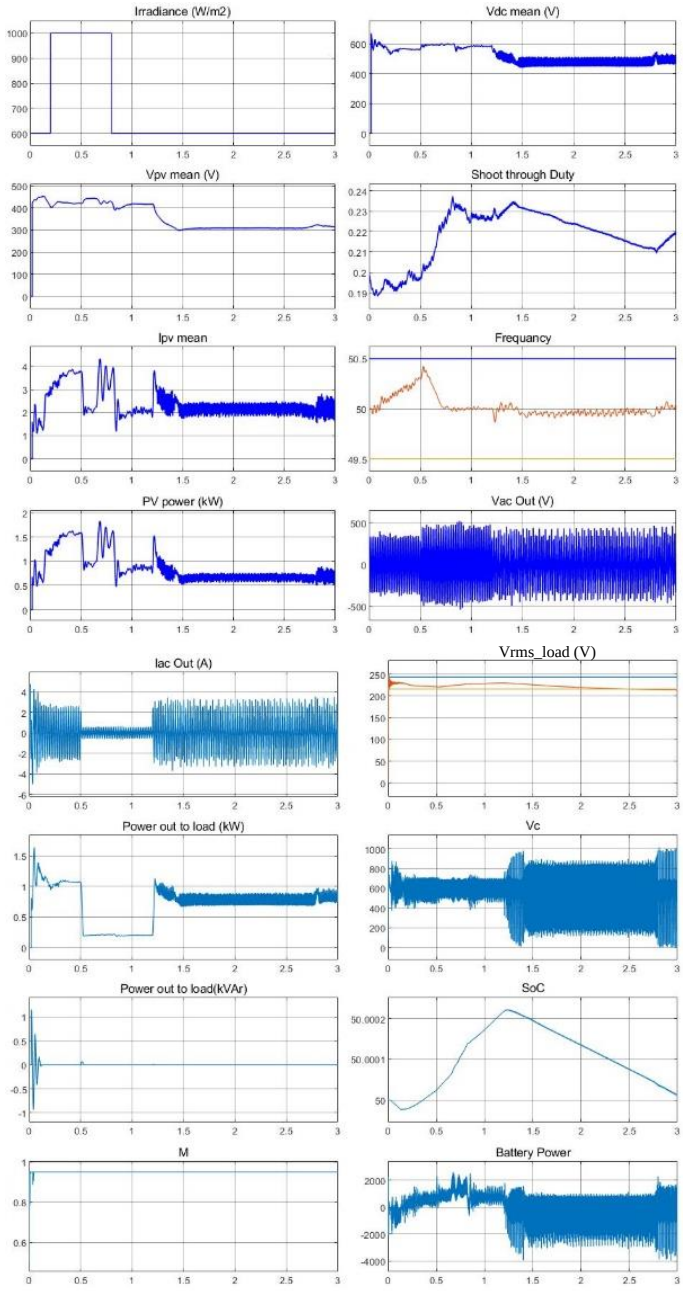

Figure 6.8 Simulation results of V-F control mode

1.2kW, then the MPP power at this irradiance is larger than connected load. Where MPPT is working properly. Where, generated solar power is larger than the loads and then excess power goes to battery charging. Then SOC% increases. From 0.5s to 0.8s, again the load is decreased to 0.2kW during solar irradiance 1000W/m2 which is also the same scenario. But excess generated power is greater than the previous case where battery charging rate is increased compared to previous time.

From 0.8 to 1.2s, irradiance is reduced to 600W/m2 keeping MG load to 0.2kW. The MG loads are lower than the generated solar power, but excess generated power is lower than previous time slot, then the rate of charging battery from excess power is lowered compared to previous case.

From 1.2s to end of the simulation, MG loads rise up to 1.2kW keeping 600W/m2 irradiance. As in the initial time slot, load is lower than generated power from solar, then battery is started to discharge. Then SOC% drops. During this simulation, voltage is successfully controlled within at set limits (230V*0.94 < V_{Load} < 230V*1.06) and Frequency is successfully controlled at set limits (50Hz*0.99 < F_{Load} < 50Hz*1.01) and supplied continues power to critical load. Therefore, the proposed V-F control mode is successfully simulated in MATLAB/Simulink environment by achieving its main objective to supply critical loads during utility grid outage or utility grid ground fault or intentional islanding of MG.

6.5 Future work

Here, each sub system is developed as a separate subsystem and each mode is validated as a separate sub system. But this research can be further developed up to the real-world practice to give the maximum benefit to the residential customers. Therefore, following improvements could be implemented for the existing work in future.

- All subsystems should be integrated to work as single system.
- The existing small oscillations are to be tuned in future by tuning PI controller in advanced method to get sharp and smooth performances.
- A current limiting circuit for reactive power / voltage control mode should be necessary to reduce spikes of current during capacitor charging states.
- Islanding method should be developed for hybrid islanding method or for a remote islanding method.
- Delay time/waiting time should be set for reconfiguration.
- Economic dispatch of solar battery system, economic benefit from peak shifting, demand control was not considered with existing tariff structure. It should be done in future through optimization techniques to get the maximum benefit from this architecture in future.

7 CONCLUSION

Microgrid architecture is vital to achieve above mentioned technical factors such as customer perception as many more features like power flow control, voltage regulation, and harmonic mitigation are expected from grid connected inverters while increasing utilization factor of the SPV system. Microgrid architecture are defined in two perspectives: control architecture and power architecture. In literature, different microgrid control architectures and microgrid power architectures have been proposed for residential microgrids. Where, reconfigurable control architecture and power architecture has proposed to utilize system components while reducing cost, size and weight and to increase the controllability and flexibility. In addition to that, reconfigurable systems allow the existing system to act in different configurations or as different systems to achieve different objectives by reducing system failures due to external problems and adopting dynamic changes of SPV generation and the utility grid. Since reconfigurable concept is adopted to this research.

The major controllable component of the SPV system is solar inverter and it will be the key component of the reconfigurable architecture. Hence, ZSI based solar inverter is selected inverter since it comparatively safe from short circuit operation by reducing inverter failures while reduces power losses by reducing power conversion stage (Single stage DC/AC power conversion with controllable buck boost operation with two control variables 1) Shoot through duty (Dst) and 2) Modulation Index (M) compared to conventional inverters. Not only that, but it also improves power quality by minimizing output voltage and current harmonics through reducing dead time.

The operation of ZSI based solar systems have been considered for MPPT dual mode operation and reactive power control as separate research work. The combined operation of grid connected mode and islanded mode while nighttime reactive power compensation is not proposed for a residential Solar PV systems. Hence, ZSI based reconfigurable architecture were the focus for this research to meet identified utility and consumer expectations: to obtain Maximum power generation from existing solar PV systems; to provide uninterrupted power supply to critical loads when utility

grid failure; to provide reactive power support to maintain power quality limits (Maintain voltage profile).

With the increase of expectations from both utilities and consumers, such as cost benefit operation, flexible operations, the solar PV system architecture expected to modify in future to absorb consumer and utility grid perceptions. Therefore, microgrid reconfiguration is initiate according to consumer and utility grid input.

As a summary, this research work proposes reconfigurable architecture with three configurations (1. Current control mode as a Current source, 2.V-F control mode as a Voltage source, 3). Reactive power control mode as a DSTATCOM) and enabling grid side control to select operating mode. The proposed SPV microgrid is successfully mathematically modeled. These 3 modes and reconfiguration algorithm simulated in MATLAB/Simulink environment accurately.

According to simulation results, during current control mode, maximum power from solar PV system was successfully extracted. Voltage at PCC has controlled during voltage rise successfully during reactive power control mode even though having several oscillations. Voltage and Frequency is controlled at set limits smoothly during V-F control mode successfully. Therefore, objective of this research was successfully achieved by the proposed reconfigurable architecture as explained in Table 7.1 and it can be fruitfully utilized for residential microgrids.

Table 7.1 Evaluation of research according to research objectives and outcomes

Objective	**Parameters considered for validation**	**Observations**
Z source inverter based Reconfigurable Architecture SPV microgrid	• Different configurations with different objectives and functions	MG architecture consisting with 3 configurations was proposed. • Current control mode as Current source • V-F control mode as voltage source • Reactive power/Voltage control mode as DSTATCOM The proposed reconfiguration algorithm is correctly identifying the mode of operations and sent islanding and synchronizing signal accordingly.

Obtain maximum power from solar generation	• Accuracy of MPPT	• MPP of the systems is accurately followed at different irradiation levels in current control mode
Provide uninterrupted power supply to the MG	• Resource Availability. • Maintain Power Quality limits • Capability to provide uninterrupted power supply for critical loads	• The power quality limits (rms voltage and frequency) are maintaining while suppling power for critical loads at V-F control mode
Provide reactive power requirement PCC	• Maintain voltage within designed voltage limits	• Maintain voltage within set limits during voltage rise at PCC, by MG working as DSTSTCOM in reactive power control mode

7.1 Limitations of this architecture

- V-f control mode
  - V-f control can be done in limited time having single ZSI for solar and Battery storage system. This can be omitted by sizing battery backup according to customer demand or adding another stable power source like diesel generator for this mode.

REFERENCES

A. Arulampalam, N. M. (2010). Micro-grid control of PV-Wind-Diesel hybrid system with islanded and grid connected operations. *2010 IEEE International Conference on Sustainable Energy Technologies (ICSET)* (pp. 1-6.). Kandy: IEEE.

A. Florescu, O. S. (2010). The advantages, limitations and disadvantages of Z-source inverter,. *CAS 2010 Proceedings (International Semiconductor Conference* (pp. 483-486). Sinaia: IEEE.

A. M. R. Lede, M. G. (2017). Microgrid architectures for distributed generation: A brief review . *2017 IEEE PES Innovative Smart Grid Technologies Conference - Latin America (ISGT Latin America),* (pp. 1-6.). Quito: IEEE.

A. Siddiqi and O. L. de Weck. (2008). Modeling Methods and Conceptual Design Principles for Reconfigurable Systems. *J. Mech. Des., 130*(10).

A. Siddiqi, .. L. (2008). Modeling Methods and Conceptual Design Principles for Reconfigurable Systems. *Journal of Mechanical Design*, 101-102.

A.Y. Hatata, E.-H. A.-R. (2016). A Review of Anti-islanding Protection Methods for Renewable Distributed Generation Systems. *Journal of Electrical Engineering*, 1-12.

Abdalla, I. A. (2013). *Integrated PV and multilevel converter system for maximum power generation under partial shading conditions.* UK: School of Electronic & Electrical Engineering (Leeds).

Ahmadi, S. S. (2017). Model predictive control of dual-mode operations Z-source inverter: Islanded and grid-connected. *2017 IEEE Energy Conversion Congress and Exposition (ECCE),* (pp. 4971-4977). Cincinnati, OH: IEEE.

Ahmed Saidi, B. C. (2017). Simulation and control of Solar Wind hybrid renewable power system. *2017 6th International Conference on Systems and Control (ICSC),* (pp. 51-56). Batna: IEEE.

Amit Kumer Podder, N. K. (2018). MPPT methods for solar PV systems: a critical review based on tracking nature. *IET Renewable Power Generation*, 18.

Andrii Chub, D. V. (2017). Wide Input Voltage Range Photovoltaic Micro converter with Reconfigurable Buck–Boost Switching Stage. *IEEE Transactions on Industrial Electronics* , 5974–5983.

Bello, E. R. (2017). *Design of a PV-system with batteries for a grid connected building* . Sweden: University of Gavle.

CEB. (n.d.). *SOURCE: DRAFT FINAL REPORT,FINDINGS OF COMMITTEE APPOINTED TO INVESTIGATE POWER SYSTEM FAILURE ON 27THSEPTEMBER 2015,*. MINISTRY OF POWER ENERGY AND RENEWABLE.

Chamana, I. M. (2014). Multi-mode operation of different PV/BESS architectures in a microgrid: Grid-tied and island mode,. *2014 IEEE PES T&D Conference and Exposition* (pp. 1-5). Chicago: IEEE.

Chapman., N. D. (2007). Boost Converter with a Reconfigurable Inductor. *Power Electronics Specialists Conference* (pp. 1695–1700). Orlando, FL, USA: IEEE.

Damiano La Manna, V. L. (2014). Reconfigurable electrical interconnection strategies for photovoltaic arrays: A review. *Renewable and Sustainable Energy Reviews*, 412-426.

Dmitri Vinnikov, A. C. (2016). Multi-Mode Quasi-Z-Source Series Resonant DC / DC Converter for Wide Input Voltage Range Applications. *2016 IEEE Applied Power Electronics Conference and Exposition (APEC)*, 2533-2539.

E Ghiani, S. M. (2005). Optimal Reconfiguration of Distribution Networks According to the Microgrid Paradigm. *2005 International Conference on Future Power Systems* (pp. 1–6). Amsterdam, Netherlands: IEEE.

E. Rodriguez-Diaz, E. J.-G.-M. (2017). Real-time Energy Management System for a hybrid AC/DC residential microgrid,, . *" 2017 IEEE Second International Conference on DC Microgrids (ICDCM)* (pp. 256-261.). Nuremburg,: IEEE.

Eiríksson, E. (2017). *Distribution grid capacity for reactive power support.* Sweden: KTH Royal Institute of Technology, School of Electrical Engineering.

Energy, D. o. (2015, September). Quadrennial Technology Review; An Assesment of Energy Technologies and Reserch Oppotunities. USA.

F. L. Paukner, C. N. (2015). Inductive filter design for three-phase grid connected power converters. *2015 IEEE 13th Brazilian Power Electronics Conference and 1st Southern Power Electronics Conference (COBEP/SPEC)* (pp. 1-5). Fortaleza, Brazil: IEEE.

Farid Katiraei, J. R. (2011, May-June). Solar PV Integration Challenges. *IEEE Power and Energy Magazine, 9*(3), 62-71.

Garrett Fitzgerald, J. M. (2015, OCTOBER). *THE ECONOMICS OF BATTERY ENERGY STORAGE HOW MULTI-USE, CUSTOMER-SITED BATTERIES DELIVER THE MOST SERVICES AND VALUE TO CUSTOMERS AND THE GRID.* Retrieved from 2020 Rocky Mountain Institute: https://rmi.org/wp-content/uploads/2017/03/RMI-TheEconomicsOfBatteryEnergyStorage-FullReport-FINAL.pdf

Gerald Cham Kpu, C. W. (2019). Islanding Detection in a Hybrid Renewable Energy System Microgrid by Utility Side Voltage and Current Measurements. *International Journal of Engineering Research and Technology. ,* 858-865.

Ghullam Mustafa Bhutto, C. B. (2017). Controlled Operation of the Islanded Portion of the International Council on Large Electric Systems (CIGRE) Low Voltage Distribution Network. *energies* . doi:10.3390/en10071021

Hansen, A., Sørensen, P. E., Hansen, L., & Bindner, H. W. (2001). Models for a Stand-Alone PV System. Denmark: DTU library.

Ho, Y. Z.-M. (2016). A review on Microgrid architectures and control methods. *2016 IEEE 8th International Power Electronics and Motion Control Conference (IPEMC-ECCE Asia)* (pp. 3149-3156). Hefei: IEEE.

Hongrae Kim, B. P. (2013). Reconfigurable Solar Converter: A Single-Stage Power Conversion PV-Battery System. *IEEE TRANSACTIONS ON POWER ELECTRONICS* , 3788–3797.

Iman Mazhari, M. C. (2014). Distributed PV-battery architectures with reconfigurable power conversion units. *2014 IEEE Applied Power Electronics Conference and Exposition (APEC)* (pp. 1-8). Fort Worth, TX, USA: IEEE.

J. M. Guerrero, M. C. (2013, April). Advanced Control Architectures for Intelligent Microgrids—Part I: Decentralized and Hierarchical Control. *IEEE Transactions on Industrial Electronics*, 1254-1262.

Jayasundara, D., Karunarathne, A., Edirisooriya, H., Jayasiri, L., Hemapala, K., Karunadasa, J., & K.A.H.Lakshika. (2018). Simulation Performance of Grid Connected Z-Source Solar Inverter with Incremental Conductance MPPT. *2018 2nd International Conference On Electrical Engineering (EECon)* (pp. 26-31). Colombo: IEEE.

K. A. H. Lakshika, M. K. (2020). Z-Source Inverter based reconfigurable architecture for solar photovoltaic microgrid. *2020 IEEE Region 10 Symposium (TENSYMP)* (pp. 1523-1546). Dhaka, Bangladesh: IEEE.

K. Kanchanee Navoda, A. S. (2017). Optimum Use of Solar Inverter by Feeding Reactive Power at the Night. *Annual Sessions of IESL, The Institution of Engineers, Sri Lanka*, 439 - 446.

K.A.Himali Lakshika, M. S. (2020). Reconfigurable solar photovoltaic systems: A review,. *Heliyon*, 1-18.

Kroposki, B. (Performer). (2016, August 24). *Prevention of Unintentional Islands in Power Systems with Distributed Resources.* Power Systems Engineering Center- National Renewable Energy Laboratory-NREL/PR-5D00-67185. Retrieved from National Renewable Energy Laboratory: https://www.nrel.gov/docs/fy16osti/67185.pdf

Leonard Mukwekwe, C. V. (2017). A review of the impacts and mitigation strategies of high PV penetration in low voltage networks. *2017 IEEE PES PowerAfrica* (pp. 274-279.). Accra: IEEE.

Leonics. (n.d.). *How to Design Solar PV System*. Retrieved from Leonics: http://www.leonics.com/support/article2_12j/articles2_12j_en.php

Low, H. W. (2013, June). *Control of Grid Connected Active Converter - Design of Control Strategies for Grid Synchronization.* Retrieved from semantic scholar: https://pdfs.semanticscholar.org/ba9d/e45b6b37f8d1f100bcdf906e187ebe1fcfb2.pdf

Lubna Mariam, M. B. (2013). A Review of Existing Microgrid Architectures. *Journal of Engineering* , 1-8.

M. Hanif, M. B. (2011). Understanding the operation of a Z-source inverter for photovoltaic application with a design example. *IET Power Electronics, 4* (3), p. 278,.

M. Malinowski, J. I.-R. (2017, Nov.). Solar Photovoltaic and Thermal Energy Systems: Current Technology and Future Trends. *Proceedings of the IEEE, vol. 105,* pp. 2132-2146.

Maknouninejad, A., Kutkut, N., Batarseh, I., & Qu, Z. (2011). Analysis and Control of PV Inverters Operating in VAR Mode at Night. *Innovative Smart Grid Technologies (ISGT) 2011* (pp. 1-5). Anaheim, CA, USA: IEEE.

Masoud Farhoodnea, A. M. (2012). Power quality impact of grid-connected photovoltaic generation system in distribution networks,. *2012 IEEE Student Conference on Research and Development (SCOReD)* (pp. 1-6). Pulau Pinang: IEEE.

Mehdi Hosseinzadeh, F. R. (2020). Islanding Fault Detection in Microgrids—A Survey. *Energies*, 1-28. doi:0.3390/en13133479

Ming-tang Chen, S.-h. L.-B.-Y. (2016). Implementing a Single- Phase Quasi-Z-Source Inverter with the Indirect Current Control Algorithm for a Reconfigurable PV System. *IEEE International Conference on Industrial TechnoTechnology (ICIT)* (pp. 323–328). Taipei, Taiwan: IEEE.

Min-Sung Kim, R. H.-J.-H.-Y. (2019). Comprehensive Review of Islanding Detection Methods for Distributed Generation Systems. *Energies*, 1-21.

Mohamed A. Eltawil, Z. Z. (2010). Grid-connected photovoltaic power systems: Technical and potential problems—A review. *Renewable and Sustainable Energy Reviews*, 112-129.

Most Nahida Akter, M. A. (2017). A hierarchicaltransactive energy management system for energy sharing in residentialmicrogrids. *Energies, 10*(12).

N. Solanki and J. Patel. (2016). 2016 IEEE 1st International Conference on Power Electronics Intelligent Control and Energy Systems (ICPEICES),. *Utilization of PV solar farm for Grid Voltage regulation during night; analysis & control* (pp. 1-5). Delhi, : IEEE.

Nikhil Sasidharan, J. G. (2017). A Novel Single-Stage Single-Phase Reconfigurable Inverter Topology for a Solar Powered Hybrid AC/DC Home. *IEEE Transactions on Industrial Electronics*, 2820–2828.

Orawan Poosri, C. C. (2016). Harmonics Impact of Rooftop Photovoltaic Penetration Level on Low Voltage Distribution System. *International Journal of Electronics and Electrical Engineering*, 221-225.

P. K. Peter, V. (2012). On the Input Resistance of a Reconfigurable Switched Capacitor DC–DC Converter-Based Maximum Power Point Tracker of a Photovoltaic Source. *IEEE Transactions on Power Electronics*, 4880-4893.

Paul Denholm, R. M. (2007). Evaluating the limits of solar photovoltaics (PV) in electric power systems utilizing energy storage and other enabling technologies. *Energy Policy*, 4424-4433.

Peng, F. Z. (2003). Z-source inverter. *IEEE Transactions on Industry Applications, 39*(2), 504-510. doi:10.1109/TIA.2003.808920

Phillip Oliver Kriett, M. S. (2012, June). Optimal control of a residential microgrid. *Energy, 42*(1), 321-330. Retrieved from https://doi.org/10.1016/j.energy.2012.03.049.

Pushkar Chaudhari, P. R. (2015). Design and Implementation of STATCOM for Reactive Power Compensation and Voltage Fluctuation Mitigation in Microgrid. *2015 IEEE International Conference on Signal Processing, Informatics, Communication and Energy Systems (SPICES)* (pp. 1-5). Kozhikode, India: IEEE.

R. Gharakhany, M. M. (2009). Reactive power compensation using Z-source based photovoltaic system. *2009 IEEE Power & Energy Society General Meeting* (pp. 1-7). Calgary, AB: IEEE.

R. K. Varma, S. S. (2011). "Novel application of a PV solar plant as STATCOM during night and day in a distribution utility network. *2011 IEEE/PES Power Systems Conference and Exposition*, (pp. 1-8). Phoenix, AZ, : IEEE.

R. Rizzo, I. S. (2015). A single input dual buck-boost output reconfigurable converter for distributed generation. *5th International Conference on Clean Electrical Power: Renewable Energy Resources Impact (ICCEP 2015)* (pp. 767–774). Taormina; Italy: IEEE.

Ravikumar, P. M. (2016). Refined Hybrid Microgrid Architecture for the Improvement of Voltage Profile. *Energy Procedia*, 645–654.

Ruban Preet Kaur, P. N. (2014). Performance Comparison of VSI Based DSTATCOM and ZSI Based DSTATCOM in A Distribution System Network. *IOSR Journal of Electrical and Electronics Engineering*, 30-35. doi:10.9790/1676-09633035

S. A. K. Mozafari Niapoor, S. D. (2010). PV power system based MPPT Z-source inverter to supply a sensorless BLDC motor. *2010 1st Power Electronic &*

Drive Systems & Technologies Conference (PEDSTC) (pp. 111-116). Tehran, Iran: IEEE.

S. Liu, W. Y. (2016). Multi-objective optimization dispatch of PV-MG considering demand response actions. *2016 35th Chinese Control Conference (CCC).* Chengdu.

Salehi, F. S. (2018). Robust Design of Microgrids With Reconfigurable Topology Under Severe Uncertainty. *IEEE Transactions on Sustainable Energy, 9*(2), 559-569.

Santiago Grijalva, M. U. (2011). Prosumer-based smart grid architecture enables a flat, sustainable electricity industry. *ISGT 2011* (pp. 1-6). Anaheim, CA, USA: IEEE. doi:0.1109/ISGT.2011.5759167

Shaw, P. (2015). Modeling and Control of a Battery Connected Standalone Photovoltaic System. In P. Shaw, *Modeling and Control of a Battery Connected Standalone Photovoltaic System* (p. 69). Odish: National Institute of Technology Rourkela .

Sicong Tan, J. X. (2012). Optimization of Distribution Network Incorporating Microgrid Using Vaccine-AIS H. *IECON 2012 - 38th Annual Conference on IEEE Industrial Electronics Society* (pp. 1381–1386). Montreal, QC, Canada: IEEE.

Singh, K. M. (2017). Multi-Objective Control Algorithm for Small Hydro and SPV Generation Based Dual Mode Reconfigurable System. *IEEE Transactions on Smart Grid*, 1–16.

Solar, W. (n.d.). *Off-Grid Battery Bank Sizing*. Retrieved from Wholesale Solar: https://www.wholesalesolar.com/solar-information/battery-bank-sizing

Sushil S. Thale, R. G. (2015). A Novel Reconfigurable Microgrid Architecture with Renewable Energy Sources and Storage. . *IEEE Transactions on Industry Applications*, 1805–1816.

T. Considine, W. C. (2012). "Understanding Microgrids as the Essential Architecture of Smart Energy. *Grid-Interop Forum*.

Ung, A. A. (2011). Design and Simulation of V2G Bidirectional Inverter and DC-DC Converter. San Luis Obispo : California Polytechnic State University.

Villalva, M. &. (2009). Modeling and circuit-based simulation of photovoltaic arrays. *Brazilian Power Electronics Conference, COBEP2009. 14*, pp. 1244-1254. Bonito-Mato Grosso do Sul, Brazil: IEEE. doi:10.1109/COBEP.2009.5347680

Weck., A. S. (2008). Modeling Methods and Conceptual Design Principles for Reconfigurable Systems,. *Journal of Mechanical Design*, 101-102,.

Wei Yee Teoh, C. W. (2011). An Overview of Islanding Detection Methods in Photovoltaic Systems . *International Journal of Electrical and Computer*

Engineering,World Academy of Science, Engineering and Technology, 1336 - 1344 .

Xiongfei Wang, J. M. (2010). Distributed Energy Resources in Grid Interactive AC Microgrids . *2010 2nd IEEE International Symposium on Power Electronics for Distributed Generation Systems* (pp. 806-812). Hefei, China: IEEE.

Yam P. Siwakoti, F. Z. (2015). Impedance-Source Networks for Electric Power Conversion Part II: Review of Control and Modulation Techniques. *IEEE TRANSACTIONS ON POWER ELECTRONICS*, 1887-1904.

Yi Huang, M. S. (2006). Z -Source Inverter for Residential Photovoltaic Systems. . *1776 IEEE TRANSACTIONS ON POWER ELECTRONICS*, 1776–1782.

Zhou Yang, C. N.-M. (2016). A Review on Microgrid Architectures and Control Methods. *International Power Electronics and Motion Control Conference (IPEMC-ECCE Asia)*. IEEE.

APPENDIX A: MATLAB/SIMULINK CODE FOR RECONFIGURATION ALGORITHM

```
function [M,Sync,Isl] = Reconfiguration(Vabc, Iabc, Vdc, fabc,
Ppv, Cus, M_uti )

% m= 1; current control m=2; V-F control; m=3; V control;
Sync=1; do synchronizing, Isl=1; do islanding

persistent Mpre;

if isempty(Mpre)
        Mpre=1;
End

if Cus==1;
      if Vabc <= 195.5 || Vabc >= 253 || fabc>= 50.5 || fabc
      <=49.5 || Iabc>=40 || Vdc >= 1000
          if Mpre==1 || Mpre==3
            M=2;
            Isl=1;
            Sync=0;
          else
            M=2;
            Sync=0;
            Isl=0;
          end
      else
          if ((Vabc <= 216.2 && Vabc >= 195.5) || (Vabc <= 253
      && Vabc >= 243.8)) && Ppv<20
                if Mpre==2
                 M=2;
                 Sync=0;
                 Isl=0;
                else
                 M=3;
                 Sync=0;
                 Isl=0;
                end
            else
              if Mpre==1 || Mpre==3
                 M=1;
                 Sync=0;
                 Isl=0;
              else
                 M=1;
                Sync=1;
                Isl=0;
               end
            end
      end
else
M = M_uti;
end
Mpre=M;
```